Quantum well polaritons: strong and weak coupling regimes

Celestino Creatore

UMI Number: U584897

All rights reserved

INFORMATION TO ALL USERS
The quality of this reproduction is dependent upon the quality of the copy submitted.

In the unlikely event that the author did not send a complete manuscript
and there are missing pages, these will be noted. Also, if material had to be removed,
a note will indicate the deletion.

UMI U584897
Published by ProQuest LLC 2013. Copyright in the Dissertation held by the Author.
Microform Edition © ProQuest LLC.
All rights reserved. This work is protected against
unauthorized copying under Title 17, United States Code.

ProQuest LLC
789 East Eisenhower Parkway
P.O. Box 1346
Ann Arbor, MI 48106-1346

ACKNOWLEDGEMENTS

First of all, I would like to thank my supervisor, Alex Ivanov, for all the teaching, guidance and support received during these years. I am also grateful for the useful collaboration with Igor Smolyarenko at Brunel University, London. I would also like to thank Prof. Kikuo Cho for his interesting lectures and discussions we had in Cardiff.

I would like to express my gratitude to Dr. Philp for his help in computing. Lots of thanks to Julie, Valentina, Pierpaolo and Andrew for their support and friendship. In particular, thanks to Leonidas and Lois, my office mates.

Many thanks to Francesca, Angelo piccolo, Angelo lungo and Rocco. Finally, I am indebted with my italian-dutch family. This thesis is dedicated to them.

ABSTRACT

The work described in this thesis is a theoretical investigation of the properties of exciton-polaritons in quantum wells (QWs). The polariton effect is first studied in the case of a completely coherent interaction between QW excitons and bulk photons, i.e. in the so called strong coupling limit. Then, an incoherent damping rate for the exciton states is included and the resulting modifications in the polariton dispersion are analyzed. A microscopic model which accounts for the scattering of QW excitons by random impurities is also proposed.

In the strong coupling limit, a definitive and correct description of the QW polariton dispersion, for both confined and radiative modes, is obtained when the exciton-photon coupling is treated non perturbatively. A self-consistent perturbation theory which qualitatively agrees with the obtained results is also formulated.

With increasing the incoherent damping, the orthogonality between radiative and confined polariton states is not affected, but a phase transition from the strong coupling regime to a weak coupling one occurs for both modes. The crossover between the two regimes is attributed to a topological change of the polariton dispersion curves when the damping rate reaches a critical value.

A microscopic approach dealing with scattering of excitons by random impurities is formulated in terms of a quadratic Hamiltonian for QW excitons, bulk photons and localised impurities. By analyzing the preliminary results based on the calculation of the relevant *eigenstates*, the mixing between radiative and confined modes is observed.

PUBLICATIONS

C Creatore and A L Ivanov. Weak and strong coupling limits for quantum well polaritons. *Phys. stat. sol. (c)*, **3**, 2444 (2006).

C Creatore and A L Ivanov. Strong and weak coupling regimes for quantum well polaritons. Submitted to *Phys. Rev. B.*

PRESENTATIONS

C Creatore and A L Ivanov. Long-range interaction of surface-deposited quantum dots via interface light. *Semiconductor and Integrated Optoelectronics Conference (SIOE)*, Cardiff (5-7 April 2004).

C Creatore and A L Ivanov. Collective interface-photon-mediated states of in-plane distributed quantum dots. *QEP-16 PHOTON 04*, Glasgow (6-9 September April 2004).

C Creatore and A L Ivanov. Weak and strong coupling limits for quantum well polaritons. *International Workshop on Nonlinear Optics and Excitation Kinetics in Semiconductors, NOEKS8*, Muenster, Germany (20-24 February 2006).

C Creatore and A L Ivanov. Weak and strong coupling limits for quantum well polaritons. *Condensed Matter and Materials Physics (CMMP 2006)*, Exeter (20-21 April 2006).

CONTENTS

List of Figures

1 INTRODUCTION

This thesis represents a theoretical investigation of the properties of exciton-polaritons in quantum wells (QWs). Polaritons are the mixed modes that arise from the interaction between material excitations (phonons, excitons...) and the retarded electromagnetic field. Polaritons have come out as a very prolific research field in solid-state physics and have been investigated both theoretically and experimentally for more than 40 years. Furthermore, the rapid and huge developments recently achieved in the nanostructure physics have stimulated new studies on excitons and polaritons in confined electronic and photonic structures.

In this research work, polaritons have been first studied in the case of a completely coherent "QW exciton - bulk photons" coupling and then by taking into account the effect of an incoherent damping for the exciton states. In the last case, a novel polariton effect has been found. A model which accounts for exciton scattering by random impurities has also been proposed.

1.1 OVERVIEW

In the first Chapter, background information that will be used throughout the thesis is provided. After a brief discussion about light-matter interaction, the theory of excitons in bulk and quantum well structures with regards to their coupling with the light field is briefly reviewed. In the second part the semi-classical and quantum theories for exciton polaritons are discussed. The last Section deals with the meaning of absorption and luminescence in the polariton picture.

In the second Chapter the polariton effect in quantum wells is investigated. Even though the polariton dispersion is a well established concept, some anomalies arise when the standard approach (described in the first part), based on the non-local response theory and on the perturbation theory, is applied. In order to get a complete and exact picture, in the second part the dispersion of QW polaritons is derived within a microscopic framework. The origin of the anomalies arising within the standard approach is then explained with a self-consistent perturbation theory. The last part of the Chapter deals with the description of the most relevant phenomena which affect the exciton-photon coupling.

The third Chapter is entitled 'Strong-weak coupling transition' and deals with the modifications which occur in the well developed QW-polariton dispersion when an incoherent damping rate for the QW-exciton states is introduced. The first part is devoted to the analysis of the confined QW polariton modes, while the second part focuses on the radiative states. Possible experimental verifications of the novel results reported here are also discussed.

In the fourth Chapter a microscopic model dealing with scattering of QW excitons by random impurities is introduced. Preliminary results show that, with increasing disorder, the radiative and confined polariton modes start to mix.

In the last Chapter, 'Conclusions', the main results are reviewed.

1.2 LIGHT-MATTER INTERACTION AND THE CONCEPT OF POLARITONS

The concept of polariton arises in a natural way after an accurate analysis of what is propagating when *light* travels through matter. In vacuum the solution is straightforward, since light in vacuum is a transverse electromagnetic wave and its quanta are known as photons. In matter, a more careful analysis is required.

The description of the interaction of light with matter can be endeavored at two levels [1]. One is the so called perturbative treatment, also known as the *weak coupling* case: in this case the electromagnetic field and the matter's excitations are considered independent variables. The exhaustive picture in this case is the following: a photon travels towards the matter, it is absorbed and matter goes from the ground state

to the excited. This approach, even though satisfactory in many cases, does not account for the whole physics behind this picture: the optically excited states of the matter are naturally associated with some polarization $\mathbf{P}$; if not, the transition would be optically forbidden since it would not couple to the electromagnetic field via the dipole operator. Also, every oscillating polarization will emit an electromagnetic wave that can act back onto the incident electromagnetic field. This interplay is what defines the strong coupling limit between light and matter and the concept of polaritons: the light travelling in a solid (for most of the spectral range) is always a mix of an electromagnetic wave (photons) and a "mechanical" polarization wave that can be quantized in form of quasiparticles with energy $\hbar\omega$ and momentum $\hbar\mathbf{k}$; this mixed wave can be itself quantized and its energy quanta are called polaritons.

1.3 EXCITONS

Excitons are the excited states of an insulating crystal which go beyond the one-electron approximation[1]: they are bound states of an electron in the conduction band and a hole in the valence band. Excitons can move through the crystal and transport energy, but do not transport charge as they are electrically neutral. Excitons are unstable because the electron and hole eventually recombine.

In direct band-gap semiconductors, excitons can be created either (i) by absorption of a photon having energy less than the band-gap energy E_g (also the minimum energy needed to create a free electron-hole pair), but sufficient to excite an electron to the excitonic bound state, or (ii) by absorption of a photon having energy equal to or larger than the band-gap energy, which generates a free electron and a free hole which then relax in energy (typically by emission of phonons) until they eventually form a bound state.

In semiconductors excitons are usually weakly bound (Wannier-Mott excitons), the attraction between the electron and hole being small in comparison with the band-gap energy E_g and their radius much larger than the interatomic spacing. Hence, their motion can be described by a two-particle effective mass equation [2, 3]. Frenkel excitons, mainly found in molecular crystals, represent the other limiting case, i.e,

[1] In this approximation the interaction with the transverse electromagnetic field accounts only for inter- and intraband transitions, whereas two-particle (excitonic) states are needed in order to explain polariton effects.

when the electron-hole pair is tightly bound and it is associated with a single atom. Figure 1.1 shows a schematic diagram of both kind of excitons.

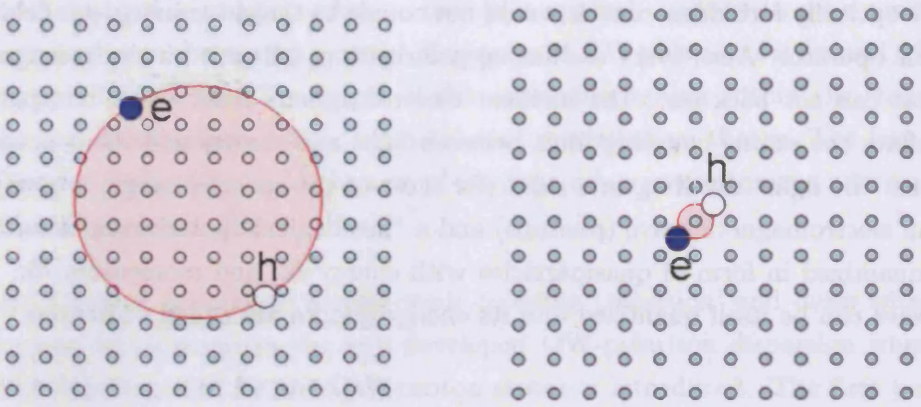

(a) Wannier-Mott exciton. (b) Frenkel exciton.

Figure 1.1: Schematic diagram of a free (or Wannier-Mott) exciton and a tightly bound (or Frenkel) exciton (not to scale). The cyan dots represent the atoms in the crystal, and the blue and white circles represent the electron and hole respectively.

In order to define and derive some relevant physical quantities that will be used and referred to throughout the rest of this thesis, the starting point is the N-electron Hamiltonian of the semiconductor crystal. Within the the Hartree-Fock approximation the crystal ground state $|i\rangle$ is given by the Slater determinant where the electrons (at position $\mathbf{r_i}$ and with wavevectors $\mathbf{k}_i$, $i = 1, ..., N$) occupy all the Bloch states $\psi_{\mathbf{vk_v}}$ in the valence band:

$$|i\rangle = \Psi_0 = A\{\psi_{\mathbf{vk_1}}(\mathbf{r_1}), \psi_{\mathbf{vk_2}}(\mathbf{r_2}), ..., \psi_{\mathbf{vk_N}}(\mathbf{r_N})\}, \tag{1.1}$$

where A is the antisymmetrizing operator. The one-electron excited state $|f\rangle$ is then written as

$$|f\rangle = \Psi_{\mathbf{ck_c},\mathbf{vk_v}} = A\{\psi_{\mathbf{vk_1}}(\mathbf{r_1}), ..., \widehat{\psi_{\mathbf{vk_v}}}(\mathbf{r_i}), \psi_{\mathbf{ck_c}}(\mathbf{r_i}), ..., \psi_{\mathbf{vk_N}}(\mathbf{r_N})\}, \tag{1.2}$$

where the valence Bloch function $\psi_{\mathbf{vk_v}}$ has been replaced by the conduction Bloch function $\psi_{\mathbf{ck_c}}$. By working only in the subspace of states of the form (1.2) (so, only

one pair of bands is considered), the exciton wavefunction $\Psi_{\rm exc}$ can be written as:

$$\Psi_{\rm exc} = \sum_{\mathbf{k_c},\mathbf{k_v}} A(\mathbf{k_c},\mathbf{k_v})\Psi_{\mathbf{ck_c},\mathbf{vk_v}}\,, \tag{1.3}$$

where $A(\mathbf{k_c},\mathbf{k_v})$ is a k-space envelope function and the exciton wavevector $\mathbf{k_x} = \mathbf{k_c} - \mathbf{k_v}$ is a good (conserved) quantum number whose existence results from the translational symmetry of the crystal. Wannier-Mott excitons are studied more easily [4] in terms of the real-space envelope function defined as

$$F(\mathbf{r_e},\mathbf{r_h}) = \frac{1}{\sqrt{V}} \sum_{\mathbf{k_c},\mathbf{k_v}} A(\mathbf{k_c},\mathbf{k_v}) e^{i(\mathbf{k_c}\cdot\mathbf{r_e} - \mathbf{k_v}\cdot\mathbf{r_h})}\,, \tag{1.4}$$

where V is the crystal volume and $\mathbf{r_e}$ and $\mathbf{r_h}$ refer to the electron and hole positions respectively. A Schrödinger equation for excitons can be written in terms of the real-space exciton wavefunction:

$$\left[E_{\rm c}(-i\nabla_{\rm e}) - E_{\rm v}(-i\nabla_{\rm h}) - \frac{e^2}{\varepsilon_{\rm b}|\mathbf{r_e}-\mathbf{r_h}|} + J_{\rm cv}\delta(\mathbf{r_e}-\mathbf{r_h}) - E\right] F(\mathbf{r_e},\mathbf{r_h}) = 0\,, \tag{1.5}$$

where $E_{\rm c}(\mathbf{k})$, $E_{\rm v}(\mathbf{k})$ are the conduction and valence band dispersions respectively, $\varepsilon_{\rm b}$ is the background dielectric constant screening the electron-hole Coulomb attraction and $J_{\rm cv}$ is the electron-hole exchange interaction.

An exciton related to a pair of parabolic bands has the following energy dispersion:

$$E_n(\mathbf{k_x}) = E_{\rm g} - \frac{R^*}{n^2} + \frac{\hbar^2 k^2}{2M_{\rm x}}\,, \quad n = 1, 2, \ldots\,, \tag{1.6}$$

where n is the principal quantum number and

$$R^* = \frac{\mu e^4}{2\varepsilon_{\rm b}^2\hbar^2} = \frac{\hbar^2}{2\mu(a_{\rm B})^2} \tag{1.7}$$

is the effective Rydberg (binding) energy, $\mu = (1/m_{\rm e}^* + 1/m_{\rm h}^*)^{-1}$ is the reduced electron-hole effective mass ($m_{\rm e}^*$ and $m_{\rm h}^*$ are the electron and hole effective masses respectively), $M_{\rm x} = m_{\rm e}^* + m_{\rm h}^*$ is the total effective mass, $k = |\mathbf{k_x}|$ and $a_{\rm B}$ is the exciton Bohr radius. This latter is given by $a_{\rm B} = \hbar^2\varepsilon_{\rm b}/(\mu e^2)$ and is typically much larger than the hydrogenic Bohr radius, as semiconductors are characterized by large dielectric constants and small effective masses. In Eq. (1.6), the electron-hole exchange interaction has been neglected; it just leads to extra shifts and splittings of the exciton states and, in particular, as $\mathbf{k_x} \to 0$, it includes a non-analytical part

which is responsible for the (instantaneous) longitudinal-transverse (LT) splitting in the polariton dispersion.

EXCITON OSCILLATOR STRENGTH

In general, in time-dependent perturbation theory, the oscillator strength $f_{\hat{\epsilon}}$ for a transition from a state $|i\rangle$ (with energy E_i) to a state $|f\rangle$ (with energy E_f) is a dimensionless quantity defined by

$$f_{\hat{\epsilon}} = \frac{2}{m_0\hbar\omega}|\langle f|\hat{\epsilon}\cdot\sum_i \mathbf{p}_i|i\rangle|^2 , \tag{1.8}$$

where $\hbar\omega = E_f - E_i$, $\mathbf{p}_i$ are the momentum operators of the electrons, $\hat{\epsilon}$ is the polarization vector related to the plane wave of frequency ω inducing the transition and m_0 is the free electron mass. Accordingly, the exciton oscillator strength, i.e, the oscillator strength of the transition from the crystal ground state to the exciton state, is defined as

$$f_{\hat{\epsilon}} = \frac{2}{m_0\hbar\omega}\left|\langle\Psi_{\rm exc}|\hat{\epsilon}\cdot\sum_i \mathbf{p}_i|\Psi_0\rangle\right|^2 , \tag{1.9}$$

where $\hbar\omega = E_{\rm exc} - E_0$ is the transition energy. For Wannier-Mott excitons, either free or bound, and in the effective mass approximation, the above relation reads

$$\begin{aligned} f_{\hat{\epsilon}} &= \frac{2|\hat{\epsilon}\cdot\mathbf{p}_{\rm cv}|^2}{m_0\hbar\omega}\left|\int F(\mathbf{r}_{\rm e},\mathbf{r}_{\rm h})\delta(\mathbf{r}_{\rm e}-\mathbf{r}_{\rm h})d\mathbf{r}_{\rm e}d\mathbf{r}_{\rm h}\right|^2 \\ &= \frac{2|\hat{\epsilon}\cdot\mathbf{p}_{\rm cv}|^2}{m_0\hbar\omega}\left|\int F(\mathbf{r}=0,\mathbf{R})d\mathbf{R}\right|^2 , \end{aligned} \tag{1.10}$$

where $\mathbf{p}_{\rm cv}$ is the interband momentum matrix element and, in the second line, the real-space envelope function has been expressed in terms of the relative and center-of-mass exciton variables $(\mathbf{r},\mathbf{R})$. The exciton oscillator strength is thus dependent on the envelope function evaluated at zero electron-hole separation. For free excitons in bulk semiconductors, as a result of the conservation of the exciton wavevector $\mathbf{k}_{\rm x}$, $F(\mathbf{r},\mathbf{R}) = e^{i\mathbf{k}_{\rm x}\cdot\mathbf{R}}F(\mathbf{r})$ and Eq. (1.10) can be arranged as

$$f_{\hat{\epsilon}} = g\frac{2|\hat{\epsilon}\cdot\mathbf{p}_{\rm cv}|^2}{m_0\hbar\omega}V|F_n(0)|^2\delta_{\mathbf{k}_{\rm x},0} , \tag{1.11}$$

where g is a spin-orbit factor taking into account the spin (singlet) component of the exciton state. Hence, the dimensionless exciton oscillator strength is proportional

to the crystal volume V – this is a consequence of the exciton center-of-mass wavefunction that extends over the whole crystal – and the meaningful quantity is the oscillator strength per unit volume f/V.

When the light-matter coupling is studied only within perturbation theory, the oscillator strength per unit volume of an isolated resonance can be associated to the absorption coefficient $\alpha(\omega)$ integrated over the absorption peak according to the following relation:

$$\int \alpha(\omega)\mathrm{d}\omega = \frac{2\pi^2 e^2}{n m_0 c}\frac{f}{V}. \tag{1.12}$$

Thus, absorption measurements can be performed in order to evaluate the exciton oscillator strength and also to trace the border between the *excitonic* regime, in which the effect of the radiation field on the electronic states of a crystal can be studied by time-dependent perturbation theory, and a regime where such a description of a *weak* light-matter coupling is not valid. In this last case Eq. (1.12) does not hold anymore and the behavior of the integrated absorption can be fully explained only within the polariton picture, i.e. in the strong light-matter coupling, as it will be detailed in Section 1.5.

1.4 QUANTUM WELL EXCITONS

When the motion of a particle is confined in one direction and the confinement becomes of the order of the particle's de Broglie wavelength, quantum effects begin to dominate its behavior: the particle's momentum and energy becomes quantized in that direction, while the motion in the other two dimensions is not affected.

The simplest structure in which this effect can be observed for excitons is a quantum well. This structure consists of a very thin ($\sim$ 10 nm) layer of semiconductor surrounded by thick layers of another semiconductor having a larger band-gap. Due to the alignment of the bulk band structures, a band discontinuity (band offset) between the conduction (and valence) band edges appears. This variation of the band edge from one material to the other determines quantum confinement effects. For the purposes of this thesis, only I-type structures, i.e, structures in which electrons and holes are confined in the same material, will be considered.

Figure 1.2 shows the energy levels of both electrons and holes in a single quantum

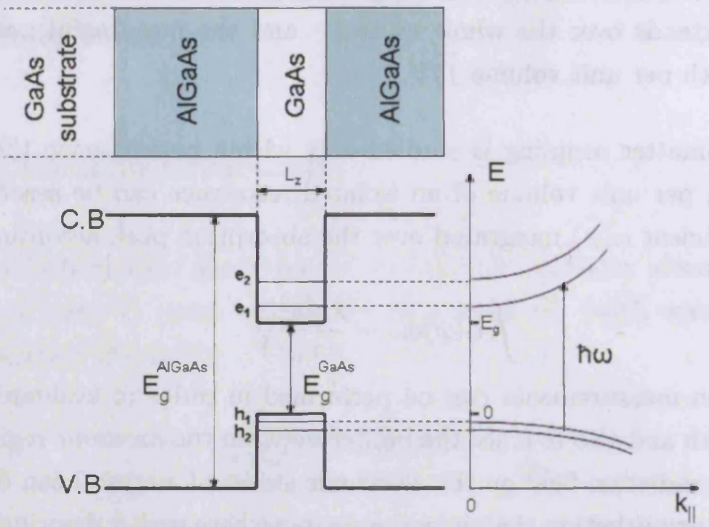

Figure 1.2: Energy band diagram of a single quantum well structure with electron and hole energy levels depicted. L_z is the width of the QW.

well: one of the effects of the reduced dimensionality is the splitting of the valence-band states from which the splitting into light- and heavy-hole excitons results. As a consequence, in order to describe the exciton states, one needs more quantum numbers apart from the principal one.

In heterostructures like quantum wells, electronic states can be studied in a phenomenological but accurate way with the envelope function method [5, 6]: electrons and holes are expressed by an effective mass equation with a confinement potential due to the band offset. In a quantum well, the square-well potential leads to the quantum-mechanical problem of a particle-in-a-box: the motion along the growth direction (here taken as the z-direction) is quantized, and the energy levels, called *subbands*, have a two-dimensional dispersion $E_n(\mathbf{k}_\parallel)$ as a function of the in-plane wavevector $\mathbf{k}_\parallel$.

Excitons in quantum wells are described by the following Hamiltonian:

$$H = E_\mathrm{g} - \frac{\hbar^2\nabla_\mathrm{e}^2}{2m_\mathrm{e}^*} - \frac{\hbar^2\nabla_\mathrm{h}^2}{2m_\mathrm{h}^*} + V_\mathrm{e}(z_\mathrm{e}) + V_\mathrm{h}(z_\mathrm{h}) - \frac{e^2}{\varepsilon_\mathrm{b}|\mathbf{r}_e - \mathbf{r}_h|}, \tag{1.13}$$

where $V_\mathrm{e}(z_\mathrm{e})$, $V_\mathrm{h}(z_\mathrm{h})$ are the square-well confining potentials for electrons (at position

z_e) and holes (at position z_h), respectively, and E_g is the band-gap of the well material.

In general, due to the confinement-induced decrease of the electron-hole separation, the binding energy E_b of a quantum well exciton is larger than the bulk value, and this leads to more stable exciton states and to enhanced effects for what concerns absorption and photoluminescence. In the ideal two-dimensional limit, i.e. vanishing well width and infinite barrier height, the exciton dispersion is given by

$$E_n(\mathbf{k}_\parallel) = E_g - \frac{R^*}{(n-1/2)^2} + \frac{\hbar^2 k_\parallel^2}{2M_x}. \tag{1.14}$$

The binding energy of the ground state (1S) exciton is thus $4R^*$ and the effective Bohr radius is half its bulk value. Starting from a very wide quantum well and decreasing its width L, the binding energy monotonically increases from the bulk value R^* to the 2D value $4R^*$ [7, 8]. This holds only for the ideal case: when a realistic (finite) band offset is taken into account, the carriers' wavefunctions leak into the barrier material for small well widths, and, as a consequence, the binding energy shows a maximum and then decreases towards the bulk value when the well width goes to zero [9]. However, when the QW is surrounded by a material with a smaller dielectric constant, enhancement of the binding energy beyond the value $4R^*$ can be achieved, as it has been experimentally demonstrated in Ref. [10].

As in bulk semiconductors, the oscillator strength is defined by Eq. (1.8). Since now only the conservation of the in-plane exciton wavevector $\mathbf{k}_x$ (now playing the role of the only *good* quantum number) holds, the real-space envelope function describing the exciton wavefunction is factorized as $F(\mathbf{r}_e, \mathbf{r}_h) = e^{i\mathbf{k}_x \cdot \mathbf{R}_\parallel} F(\rho, z_e, z_h)$, where $(\rho, \mathbf{R}_\parallel)$ are the in-plane relative and center-of-mass exciton variables. The expression for the oscillator strength per unit area[2] S is then

$$\frac{f_{\hat{\epsilon}}}{S} = g \frac{2|\hat{\epsilon} \cdot \mathbf{p}_{cv}|^2}{m_0 \hbar \omega} \left| \int F(\rho = 0, z, z) \mathrm{d}z \right|^2, \tag{1.15}$$

where, as in Eq. (1.11), g is the spin-orbit factor.

[2]This is the only meaningful physical quantity since the oscillator strength of a quantum well exciton is proportional to the sample surface S.

to the top of the potential well. In this case, it is more convenient to treat [11] the electronic states in the barrier as the unperturbed states, whereas the "quantum well" acts as a localized, δ-like attractive potential. The localization energy $E_{\rm loc}$ is defined by writing the energy of electron levels as $E_{\rm g}^{\rm b} - E_{\rm loc}$, where $E_{\rm g}^{\rm b}$ is now the barrier band-gap. Similarly as in wide quantum wells, two different physical regimes can described.

When the localizations energies $E_{\rm loc,e}$ and $E_{\rm loc,h}$ of electrons and holes in the well are larger than the excitonic binding energy, electrons and holes are both separately localized and each pair of electron-hole levels defines an excitonic series whose energy spectrum is $E_{\rm g}^{\rm b} = E_{\rm g}^{\rm b} - E_{\rm loc,e} - E_{\rm loc,h} - E_{\rm b}$. This is the *strong* (or electron-hole) *localization* regime. When on the contrary the localization energy is smaller than the binding energy, the Coulomb attraction becomes dominant and the center of mass of the exciton is localized as a whole. The energy spectrum in this regime of *weak* (or center-of-mass) *localization* is given by $E_{\rm exc} = E_{\rm g}^{\rm b} - R^{*} - E_{\rm loc,exc}$.

In narrow quantum wells the oscillator strength behaves similarly as in wide quantum wells. In the strong localization regime, the oscillator strength decreases for decreasing well widths: the carrier wavefunctions in fact are more delocalized in the barriers. Also, the in-plane exciton radius reaches the 3D value. In the localized center-of-mass regime, the oscillator strength is proportional to the localization length. The latter increases with decreasing well widths and so does the oscillator strength. Hence, the oscillator strength in narrow quantum wells again exhibits a minimum moving from the strong to the weak localization regime.

Figure 1.3 shows the behavior of the oscillator strength calculated [14] as a function of the well width: the two minima which occur first at the strong-weak confinement transition and then at the strong-weak localization transition are clearly spotted.

1.5 POLARITONS IN BULK SEMICONDUCTORS

In semiconductors excitons are strongly coupled to the radiation field and most of the optical properties can be fully understood only within the strong-coupling picture, i.e. the polariton picture. One relevant example, in this sense, is represented [1] by the refractive index $n(\omega)$ associated with a photon $\hbar\omega$ propagating in a semiconductor crystal away from the resonance. In this case, up to the second order perturbation

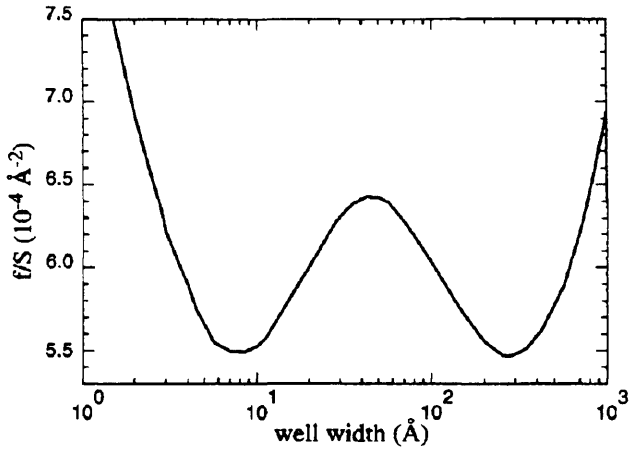

Figure 1.3: Oscillator strength per unit area as a function of the quantum well width. The excitonic transition refers to the lowest heavy-hole state in a $GaAs/Al_{0.15}Ga_{0.85}As$ quantum well. From Ref. [14].

theory, the refractive index is given by

$$n(\omega) - 1 \propto \left| \sum_z \frac{\langle i|H_D|z\rangle\langle z|H_D|i\rangle}{E_z - E_i - \hbar\omega} \right|^2 . \tag{1.16}$$

Equation (1.16) means that a photon $\hbar\omega$ excites a virtual state $|z\rangle$ which, after a time Δt given by the uncertainty principle, emits a photon identical to the incident one, putting back the system to the initial state $|i\rangle$. This picture clearly fails when ω gets close to the resonance energy $E_z - E_i$, since $\Delta E = E_z - E_i - \hbar\omega = 0$ and $n(\omega)$ diverges.

In the polariton picture this problem does not occur, since the mixed state of electromagnetic radiation and matter excitation is quantized as a whole. In Section 2.2 a similar problem related to the radiative modes of QW polaritons will be faced.

Figure 1.4 shows a diagrammatic representation of an exciton-polariton. In this picture an incident photon generates an electron-hole pair which in turn recombines generating a photon and so on. The Coulomb interaction necessary to form a bound electron-hole pair, i.e. the exciton, is represented by the vertical lines between the electron and hole lines.

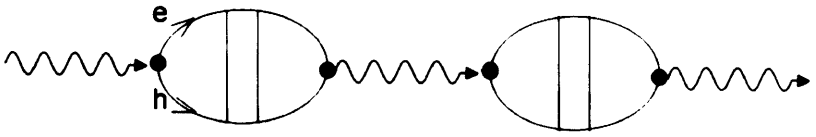

Figure 1.4: Schematic of an exciton-polariton according to the diagram technique.

The concept of exciton-polariton can be introduced also as the solution of an apparent paradox [4]. Due to the electron - hole exchange interaction, the dispersion of optically active excitons splits between longitudinal and transverse modes [2]: this means that for $\mathbf{k_x} \rightarrow 0$ the state of the matter is twofold degenerate, while, in cubic crystals, due to symmetry considerations [3], a threefold degeneracy is required at $\mathbf{k_x} = 0$. Such a paradox is solved if one takes into account that excitons with wavevectors of the order of the wavevector of the light in the sample - $k_x < k_0$ ($k_0 = n\omega/c$) - are strongly coupled to the transverse electromagnetic field and give rise to exciton-polaritons. As it will be shown, the polariton dispersion is characterized by two modes (an upper mode and a lower one) that at $\mathbf{k_x} = 0$ are degenerate with the longitudinal exciton; hence, the threefold degeneracy required by the cubic symmetry is recovered.

A semiclassical theory of polaritons was first developed during the fifties by Huang [15] and Born and Huang [16], analyzing the long-wavelength lattice vibrations in ionic crystals. The quantum-mechanical theory was then introduced by Fano [17], Hopfield [18] and Agranovich [19]. Exciton-polaritons are also discussed in many textbooks of Semiconductor Optics [1, 20] and a more detailed analysis can be found in many review papers [4, 21–27]. It is worth to notice that excitons-polaritons are just an example of the strong-coupling between light and matter. In metallic photonic crystal slabs, for example, the strong coupling between localized particle plasmons and optical waveguide modes results in the formation of a new quasi-particle called waveguide-plasmon polariton [28].

In the following part of this Chapter the semiclassical and quantum theories for exciton-polaritons in bulk semiconductors will be reviewed.

SEMICLASSICAL THEORY

As previously mentioned, a semiclassical theory for polaritons in bulk systems was first proposed and developed by Huang [15, 16], in order to describe the infrared absorption of light below the Reststrahl frequency due to phonon resonances.

The solution of Maxwell equations and the constitutive relation $\mathbf{D} = \varepsilon(\omega)\mathbf{E}$, yield the following dispersion relations:

$$\frac{c^2k^2}{\omega^2} = \varepsilon(\omega)\,, \tag{1.17}$$

for transverse modes (characterized by $\nabla \cdot \mathbf{D} = \nabla\varepsilon_0\varepsilon(\omega)\mathbf{E} = 0$), and

$$\varepsilon(\omega) = 0\,, \tag{1.18}$$

for longitudinal modes. The former is also known as the *polariton equation.* Moreover, according to Lorentz's model of light-matter coupling, in the vicinity of a single dipole-active resonance of frequency ω_0, the dielectric function reads:

$$\varepsilon(\omega) = \varepsilon_\mathrm{b} + \frac{4\pi\beta\omega_0^2}{\omega_0^2 - \omega^2 - i\gamma\omega}\,, \tag{1.19}$$

where ε_b is the so called background dielectric constant where all the constant contributions from higher resonances $\omega_{0j} \gg \omega_0$ are summarized in, γ is a phenomenological damping constant, and β is the polarizability.
Combining the polariton equation (1.17) with the dielectric function Eq. (1.19) results in the polariton dispersion relation (here written for $\gamma = 0$):

$$\omega^4 - \omega^2\left(\omega_0^2 + \frac{4\pi\beta\omega_0^2}{\varepsilon_\mathrm{b}} + \frac{c^2k^2}{\varepsilon_\mathrm{b}}\right) + \frac{c^2k^2\omega_0^2}{\varepsilon_\mathrm{b}} = 0\,. \tag{1.20}$$

The polariton dispersion can also be obtained by solving the following set of two coupled equations:

$$\begin{cases} \varepsilon_\mathrm{b}\ddot{\mathbf{E}} - c^2\nabla^2\mathbf{E} = -4\pi\ddot{\mathbf{P}}\,, \\ \ddot{\mathbf{P}} + \omega_0^2\mathbf{P} = \omega_0^2\beta\mathbf{E}\,. \end{cases} \tag{1.21}$$

The first is the Maxwell equation for the transverse part of the electromagnetic field ($c^2\nabla^2\mathbf{E} = \partial^2\mathbf{D}/\partial t^2$) with $\mathbf{D} = \varepsilon_\mathrm{b}\mathbf{E} + 4\pi\mathbf{P}$, where $\mathbf{P}$ is the contribution to the electric polarization of the matter from a particular oscillator with its own resonance-frequency ω_0; the second one is the equation of motion for the polarization $\mathbf{P}$ coupled

to the electric field through the polarizability β (at ω_0).
Plane wave solutions of the system (1.21) satisfy:

$$\begin{bmatrix} -\omega^2+\omega_0^2 & -\beta\omega_0^2 \\ -4\pi\omega^2 & -\varepsilon_b\omega^2+c^2k^2 \end{bmatrix} \begin{bmatrix} P \\ E \end{bmatrix} = 0\,. \tag{1.22}$$

By equating the determinant of the coefficients to zero, one obtains the eigenfrequencies ω of the $\mathbf{P}-\mathbf{E}$ coupled modes as functions of the wavevector k, i.e. the polariton dispersion (1.20).

The meaning of the above relations can be reviewed as follows: the electromagnetic wave propagating through the matter with the dielectric dispersion given by Eq. (1.19), has a dispersion $\omega = \omega(k)$ given by Eq. (1.20) and the quantum of this coupled wave is the *polariton*. It is worth to notice that it is not essential to know whether the electromagnetic field of the polariton comes from an external source or not, since the polarization $\mathbf{P}$ always comes with the electric field $\mathbf{E}$ and vice versa, through the coupled equations (1.21).

In particular, when dealing with excitons, the generic dipole-active resonance ω_0 must be replaced by the exciton dispersion, $\omega_k = \omega_0 + (\hbar k^2/2M_x)$, where $\mathbf{k}$ is the exciton wavevector, $k = |\mathbf{k}|$ and $M_x = m_e^* + m_h^*$ is the reduced effective mass of the exciton; the related exciton-polariton dispersion $\omega = \omega(k)$ is sketched in Fig. 1.5.

The transverse modes are described by a lower and an upper branch, anticrossing close to the wavevector of the light in the sample and both twofold degenerate. In the limit of no retardation (the so called instantaneous or electrostatic limit, obtained by letting $c \to \infty$) the transverse solution has a frequency $\omega_T = \omega_0$; the longitudinal solution is a pure electrostatic one and has a frequency

$$\omega_L = \omega_0 \left(1 + \frac{4\pi\beta}{\varepsilon_b}\right)^{1/2}. \tag{1.23}$$

For any kind of matter-excitation (either excitons or phonons) in interaction with the light field, the polariton dispersion is characterized mainly by two parameters:

- The longitudinal-transverse splitting. It is the electrostatic shift of the longitudinal mode, given by $\omega_{LT} = \omega_L - \omega_T \simeq (2\pi\beta/\varepsilon_b)\omega_0$; this quantity is a measure of the instantaneous ($c \to \infty$), long-range Coulomb interaction. In the case of phonon-polaritons it corresponds to the splitting between LO and TO optical

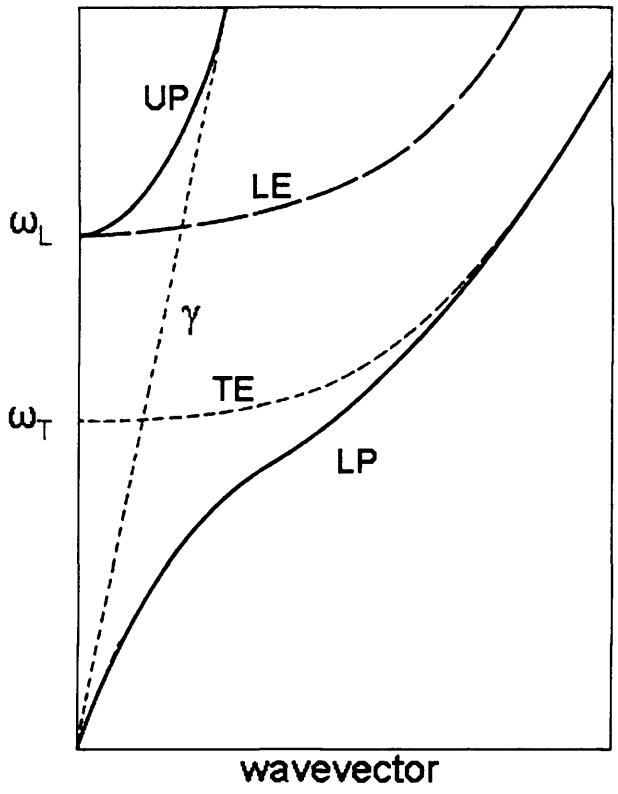

Figure 1.5: Exciton-polariton dispersion: the upper (UP) and lower (LP) polariton modes together with the longitudinal exciton (LE) (solid lines); the dispersions of the independent photon (γ) and transverse exciton (TE) dispersions are also shown (dashed lines).

phonons, while for exciton-polaritons it coincides with the non analytical part of the electron-hole exchange interaction[3].

- The polariton splitting. It is the splitting between the upper and lower polariton modes at the crossing point between the bare photon dispersion and free polarization (see Fig. 1.5). It is given by the following expression:

$$2\omega_C = (2\omega_0\omega_{LT})^{1/2}, \tag{1.24}$$

and it represents a measure of the strength of the interaction between the dipole active excitation and the retarded electromagnetic field.

[3]As a consequence, the LT splitting cannot be considered as a true polaritonic effect

For what concerns exciton-polaritons, due to the motion of the exciton's center of mass (i.e. the spatial dispersion), their dispersion turns upwards at large wavevectors as it is shown in Fig. 1.5. Hence, for frequencies greater than the longitudinal one (see the frequency range $\omega > \omega_{\mathrm{L}}$ in Fig. 1.5) there are two propagating modes at the same energy, as first pointed out by Pekar [29]. Having more than one mode means that the two boundary conditions that can be deduced from Maxwell's equations are no longer sufficient in order to specify their relative amplitudes: for a given incident wave on a semi-infinite crystal, the amplitudes of one reflected and one transmitted wave can be deduced, but, if there are two (or even more) states at the same frequency coupling to the incident light field, one (or more) additional boundary conditions (ABC) are needed. Even if it is not object of investigation of this research work, it is worth to mention that a vast literature is devoted to the ABC problem [24, 27, 29–31] and that recently it has been re-analyzed and it is a controversial issue [32, 33].

QUANTUM THEORY OF POLARITONS

In a quantum-mechanical framework, polaritons are the solutions of a second-quantized Hamiltonian describing excitons, photons and their mutual interaction. Here, the quantization procedure obtained within a microscopic approach [18, 19] is briefly described.

The Lagrangian density for the system "excitons-photons" is given [34] by

$$\mathcal{L} = \frac{1}{8\pi v^2}\left(\frac{\partial \mathbf{A}}{\partial t}\right)^2 - \frac{1}{8\pi}(\nabla \times \mathbf{A})^2 + \frac{1}{2\beta\omega_0^2}\left(\frac{\partial \mathbf{P}}{\partial t}\right)^2 - \frac{1}{2\beta}\mathbf{P}^2 + \frac{1}{c}\mathbf{A}\cdot\frac{\partial \mathbf{P}}{\partial t}, \qquad (1.25)$$

where ω_0 is the exciton frequency, $v = c/\sqrt{\varepsilon_{\mathrm{b}}}$ and $\mathbf{A}$ and $\mathbf{P}$ are the potential vector field and the density of polarization (due to excitons) respectively. From Eq. (1.25) the Maxwell equations and the constitutive relation given in Eq. (1.21) can be derived. From the Lagrangian density one receives the Hamiltonian density $\mathcal{H}$ as

$$\mathcal{H} = \vec{\rho}_{\mathbf{A}}\frac{\partial \mathbf{A}}{\partial t} + \vec{\rho}_{\mathbf{P}}\frac{\partial \mathbf{P}}{\partial t} - \mathcal{L} = \qquad (1.26)$$

$$= 2\pi v^2 \vec{\rho}_{\mathbf{A}}^2 + \frac{1}{8\pi}(\nabla \times \mathbf{A})^2 + \frac{1}{2\beta}\mathbf{P}^2 + \frac{\omega_0^2\beta}{2}\vec{\rho}_{\mathbf{P}}^2 - \frac{\omega_0^2\beta}{c}\vec{\rho}_{\mathbf{P}}\cdot\mathbf{A} + \frac{\omega_0^2\beta}{2c^2}\mathbf{A}^2, \qquad (1.27)$$

where $\vec{\rho}_{\mathbf{A}}$ and $\vec{\rho}_{\mathbf{P}}$ are the conjugate momenta of the the potential vector field $\mathbf{A}$ and the density of polarization $\mathbf{P}$ (i.e. the classical canonical variables) respectively. The

(operator) Hamiltonian is then obtained by integrating Eq. (1.26) over the quantization volume V in which the fields **A** and **P** are expanded (with periodic boundary conditions) as

$$\begin{aligned}\mathbf{P} &= \sum_k \left(\frac{\hbar\beta\omega_0}{2V}\right)^{1/2} \hat{\epsilon}_k e^{i\mathbf{k}\cdot\mathbf{r}}(b_k + b_{-k}^\dagger)\,,\\ \mathbf{A} &= \sum_k \left(\frac{2\pi\hbar v}{V|\mathbf{k}|}\right)^{1/2} \hat{\epsilon}_k e^{i\mathbf{k}\cdot\mathbf{r}}(a_k - a_{-k}^\dagger)\,,\end{aligned} \tag{1.28}$$

where k includes the wavevector $\mathbf{k}$ and the polarization vector λ of the plane wave $[k = (\mathbf{k}, \lambda);\ -k = (-\mathbf{k}, \lambda)]$ and $\hat{\epsilon}_k$ is a unit vector perpendicular to $\mathbf{k}$; $a_k^\dagger, a_k$ $(b_k^\dagger, b_k)$ are the Bose operators for photons (excitons).

The resulting Hamiltonian [18, 35, 36] is:

$$\begin{aligned}H &= \sum_k \left[\hbar v k \left(a_k^\dagger a_k + \frac{1}{2}\right) + \hbar\omega_k \left(b_k^\dagger b_k + \frac{1}{2}\right) + \right.\\ &+ \left. iC_k \left(a_k^\dagger + a_{-k}\right)\left(b_k - b_{-k}^\dagger\right) + D_k \left(a_k^\dagger + a_{-k}\right)\left(a_k + a_{-k}^\dagger\right)\right]\,,\end{aligned} \tag{1.29}$$

where $\hbar\omega_k = \hbar\omega_0 + (\hbar^2 k^2)/(2M_x)$ is the exciton dispersion, and the prefactors C_k and D_k are defined as

$$C_k = \hbar\omega_0 \left(\frac{\pi\beta\omega_k}{vk\varepsilon_b}\right)^{1/2} \quad ; \quad D_k = \hbar\omega_0 \frac{\pi\beta\omega_k}{vk\varepsilon_b}\,. \tag{1.30}$$

The quadratic form (1.29) can be diagonalized by a canonical transformation [37]

$$\begin{aligned}\hat{S} : a_k &\rightarrow \hat{S} a_k \hat{S}^\dagger\,,\\ b_k &\rightarrow \hat{S} b_k \hat{S}^\dagger\,,\end{aligned} \tag{1.31}$$

where $\hat{S}\hat{S}^\dagger = \hat{I}$. The four-parametric canonical transformation $\hat{S}$ is [37]:

$$\begin{aligned}\hat{S} &= \hat{S}_4 \hat{S}_3 \hat{S}_2 \hat{S}_1\,,\\ \hat{S}_1 &= \exp\left[\zeta_k \left(a_k^\dagger a_{-k}^\dagger - a_k a_{-k}\right)\right]\,,\\ \hat{S}_2 &= \exp\left[i\delta_{\mathbf{k}} \left(a_k^\dagger b_k + a_k b_k^\dagger + a_{-k}^\dagger b_{-k} + a_{-k} b_{-k}^\dagger\right)\right]\,,\\ \hat{S}_3 &= \exp\left[i\Delta_p \left(a_{-p} b_k + a_{-k}^\dagger b_k^\dagger + a_k b_{-k} + a_k^\dagger b_{-k}^\dagger\right)\right]\,,\\ \hat{S}_4 &= \exp\left[\eta_k \left(a_k^\dagger a_{-k}^\dagger - a_k a_{-k}\right) + (\zeta_k + \eta_k)\left(b_k^\dagger b_{-k}^\dagger - b_k b_{-k}\right)\right]\,,\end{aligned} \tag{1.32}$$

where ζ_k, δ_k, Δ_k, and η_k are the four real parameters. The photon and exciton operators (a_k and b_k) are expressed through the polariton operators $\xi_k^{(s=+,-)}$ (lower and upper branch polariton) by the Hopfield's matrix [18] (R):

$$\begin{pmatrix} a_k \\ b_k \\ a_{-k}^\dagger \\ b_{-k}^\dagger \end{pmatrix} = \begin{pmatrix} R_1 & iR_2 & R_3 & -iR_4 \\ iR_2 & R_1 & -iR_4 & R_3 \\ R_3 & iR_4 & R_1 & -iR_2 \\ iR_4 & R_3 & -iR_2 & R_1 \end{pmatrix} \begin{pmatrix} \xi_k^{(-)} \\ \xi_k^{(+)} \\ \xi_{-k}^{(-)\dagger} \\ \xi_{-k}^{(+)\dagger} \end{pmatrix} , \tag{1.33}$$

where

$$\begin{aligned} R_1 &= \cos\delta_k \cosh\Delta_k \cosh(\eta_k + \zeta_k) + \sin\delta_k \sinh\Delta_k \sinh(\eta_k + \zeta_k) , \\ R_2 &= \cos\delta_k \sinh\Delta_k \sinh\eta_k - \sin\delta_k \cosh\Delta_k \cosh\eta_k , \\ R_3 &= -\sin\delta_k \sinh\Delta_k \cosh(\eta_k + \zeta_k) - \cos\delta_k \cosh\Delta_k \sinh(\eta_k + \zeta_k) , \\ R_4 &= \cos\delta_k \sinh\Delta_k \cosh\eta_k - \sin\delta_k \cosh\Delta_k \sinh\eta_k . \end{aligned} \tag{1.34}$$

According to eq. (1.33), a polariton eigenstate involves modes k and $-k$. However, these polariton modes decouple in the resonant approximation of the exciton-photon interaction. The inverse polariton transformation is given by

$$(R)^{-1} = \begin{pmatrix} R_1 & -iR_2 & -R_3 & iR_4 \\ -iR_2 & R_1 & iR_4 & -R_3 \\ -R_3 & -iR_4 & R_1 & iR_2 \\ -iR_4 & -R_3 & iR_2 & R_1 \end{pmatrix} . \tag{1.35}$$

The four independent elements $R_{i=1,2,3,4}$ of matrix (R) can be found from diagonalization of the transformed Hamiltonian (1.29). They are expressed through the parameters of the initial polariton Hamiltonian, e.g. in Ref. [18].
Since $\xi_k^{(-)\dagger}$ and $\xi_k^{(+)\dagger}$ are identified with the creation operators for the lower and upper polariton respectively, it is required that that they satisfy the Bose commutation rules

$$\left[\xi_k^{(s)}, \xi_{k'}^{(s')\dagger}\right] = \delta_{k\,k'}\delta_{s,s'} ; \quad \left[\xi_k^{(s)}, \xi_{k'}^{(s)}\right] = \left[\xi_k^{(s)\dagger}, \xi_{k'}^{(s')\dagger}\right] = 0 , \tag{1.36}$$

and that the Hamiltonian is diagonal in $\xi_k^{(s)\dagger}$, $\xi_k^{(s)}$, i.e.

$$\left[\xi_k^{(s)}, H\right] = \hbar\Omega^{(s)}(k)\xi_k^{(s)} . \tag{1.37}$$

Applying the conditions (1.36,1.37) leads to an eigenvalue problem, whose secular

equation is:

$$\Omega_k^4 - \left(v^2k^2 + \omega_k^2 + \frac{4\pi\beta}{\varepsilon_b}\omega_0^2\right)\Omega_k^2 + v^2k^2\omega_k^2 = 0\,. \tag{1.38}$$

The polarizability β is related to the oscillator strength per unit volume f by $\beta = e^2 f/(m_0\omega_0^2 V)$ (m_0 is the free electron mass) and the LT splitting and the exciton-photon coupling given in the previous paragraph can be accordingly rewritten as

$$\omega_{LT} = \frac{2\pi}{\varepsilon_b}\frac{e^2}{m_0\omega_0}\frac{f}{V}\,, \tag{1.39}$$

and

$$\omega_C = \left(\frac{\pi e^2}{\varepsilon_b m_0}\frac{f}{V}\right)^{1/2}\,. \tag{1.40}$$

The dispersion (1.38) is identical to the classical dispersion relation (1.20) and it is an expected result, since the commutator algebra used is formally equivalent to the classical algebra of the Poisson's brackets. Furthermore, this result means that polaritons are the real elementary excitations (eigenstates) of the crystal. Since their energy and momentum is conserved indefinitely, with the exception of their interaction with surfaces or vibrational states which gives rise to a finite lifetime, polaritons are stationary states.

In the resonant exciton-photon interaction, i.e. $ck/\sqrt{\varepsilon_b} \simeq \omega_0$, the interaction part of the Hamiltonian (1.29) reduces to $iC_k\sum_k\left(a_k^\dagger b_k - b_k^\dagger a_k\right)$ and the total Hamiltonian is diagonalized using a canonical transformation $\hat{S} = \exp\left[i\phi_k\left(a_k^\dagger b_k + a_k b_k^\dagger\right)\right]$:

$$\begin{pmatrix} a_k \\ b_k \end{pmatrix} = \begin{pmatrix} iv_k & u_k \\ u_k & iv_k \end{pmatrix}\begin{pmatrix} \xi_k^{(-)} \\ \xi_k^{(+)} \end{pmatrix}\,, \tag{1.41}$$

where $u_k = \cos\phi_k$ and $v_k = \sin\phi_k$. The corresponding inverse transformation is

$$\begin{aligned} \xi_p^{(-)} &= -iv_k a_k + u_k b_k\,, \\ \xi_k^{(+)} &= u_k a_k - iv_k b_k\,. \end{aligned} \tag{1.42}$$

Eq. (1.42) shows that a polariton is a composite quasi-particle consisting of the exciton and photon components. The functions u_k^2 and v_k^2 yield the relative contributions and the sum rule "$u_k^2 + v_k^2 = 1$" holds. In Section 3.2 the photon component of the confined polariton mode in quantum wells will be derived.

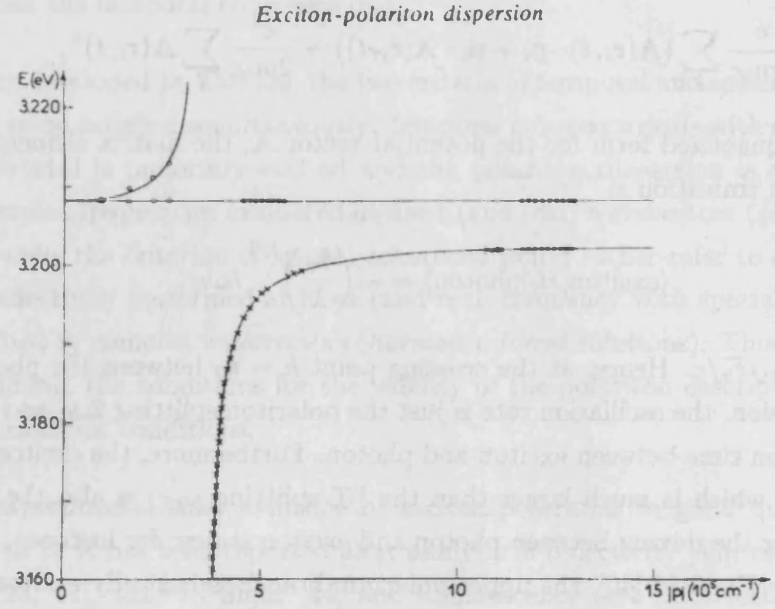

Figure 1.6: Polariton dispersion for the Z_3 exciton in CuCl. Circles by two-photon absorption [38]; dots and crossed by Hyper-Raman scattering [25].

MEANING AND RELEVANCE OF THE POLARITON CONCEPT

From what has been stated in the previous paragraph, it is the polariton dispersion (and not the bare exciton's one) that is measurable in high-quality crystals and at low temperatures and huge experimental evidence has been reported in the last three decades (see for example the review by Bassani [26]). As an example, Fig. 1.6 shows the upper and lower branches together with the dispersion of the longitudinal exciton in CuCl obtained by nonlinear optical spectroscopy.

The question under which conditions polaritons and not excitons will be observed has not a general and straightforward answer and, even if a possible reply rests on the experiment to perform, two main criteria can be set down, namely *temporal coherence* and *spatial coherence* [11, 39].

Temporal coherence involves the exciton-photon coupling and requires all dephasing processes to be slower than the oscillation rate between excitons and photons in the polariton state. Using the interaction Hamiltonian H_i for the interaction between

radiation and matter given by

$$H_i = \frac{e}{2m_0c}\sum_i \left(\mathbf{A}(\mathbf{r}_i,t)\cdot\mathbf{p}_i + \mathbf{p}_i\cdot\mathbf{A}(\mathbf{r}_i,t)\right) + \frac{e^2}{2m_0c}\sum_i \mathbf{A}(\mathbf{r}_i,t)^2\,, \tag{1.43}$$

and a second-quantized form for the potential vector $\mathbf{A}$, the matrix element for the photon-exciton transition is

$$\langle \text{exciton}|H_i|\text{photon}\rangle = -\left(\frac{k_0}{k}\right)^{1/2}\hbar\omega_C\,, \tag{1.44}$$

where $k_0 = \omega_0\sqrt{\varepsilon_b}/c$. Hence, at the crossing point $k = k_0$ between the photon and exciton dispersion, the oscillation rate is just the polariton splitting $2\omega_C$ and $(2\omega_C)^{-1}$ is the oscillation time between exciton and photon. Furthermore, the exciton-photon coupling $\hbar\omega_C$, which is much larger than the LT splitting ω_{LT}, is also the relevant energy scale for the mixing between photon and exciton states: for instance, as it has been shown by Hopfield [40], the upper polariton branch is basically exciton-like for energies $\mid \omega - \omega_0 \mid < \omega_C$.

In GaAs ($\hbar\omega_0 = 1.515$ eV and $\hbar\omega_{LT} = 0.08$ meV [41]) the coupling energy $\hbar\omega_C = 7.8$ meV and the oscillation time $(2\omega_C)^{-1} = 0.04$ ps. Such exciton-photon oscillation rate is much faster than other characteristic times. For instance, in 190 nm thick GaAs layers, the measured dephasing time is $T_2 = 7.0 \pm 0.5$ ps $\gg (2\omega_C)^{-1}$. Hence, polaritons are *very stable* particles from the point of view of their temporal behavior.

The criterion of spatial coherence applied to the exciton-photon coupling requires the coherence length l_c of the exciton wavefunction to be much larger than the wavelength of light, otherwise the dipole matrix element between exciton and photon is reduced. As originally pointed out by Tait [39], the requirement of spatial coherence can be expressed in terms of marginal value γ_c [39, 42] for the homogeneous broadening (here denoted by γ) of the exciton:

$$\gamma < \gamma_c = \left(\frac{8\omega_{LT}}{M_x c^2}\right)^{1/2}\omega_0\,. \tag{1.45}$$

The above criterion follows from the relation $l_c > \lambda$, where λ is the light wavelength and the coherence length l_c of the exciton wavefunction is identified with the exciton mean free path, $l_c = \gamma^{-1}v_g$, $v_g = d\omega_k/dk$ being the exciton group velocity evaluated at the longitudinal frequency[4]. It means that scattering processes must not occur

[4]It is worth to notice that in this criterion it is not fully clear i) if the coherence length l_c

within a light wavelength. In general the criterion of spatial coherence is much more stringent than the temporal coherence one.

In the theory developed by Tait [39] the two criteria of temporal and spatial coherence do not have to be satisfied simultaneously: temporal coherence deals with experiments where the crystal is uniformly excited and the polariton dispersion is described in terms of complex frequencies evaluated at fixed (and real) wavevectors (*quasi-particle* solutions), while the criterion of spatial coherence would rather refer to experiments of optical reflectivity performed at fixed (and real) frequency with spatially decaying fields described by complex wavevectors (*harmonic-forced* solutions). Thus, as written at the beginning, the conditions for the validity of the polariton description depend on the experimental conditions.

From the experimental side, evidence of exciton-polaritons in good quality GaAs crystals up to 20 K has been reported after analysis of reflectivity [43], resonant light scattering [23, 41], time of flight [44] and luminescence (see next section) experiments [43, 45, 46].

ABSORPTION AND LUMINESCENCE

Previously, through a microscopic analysis of the exciton-photon interaction, it has been shown that polaritons are the eigenstates of an infinite crystal and, in the absence of dissipative processes, they are stationary states. As a consequence, within the exciton-polariton picture, optical absorption cannot be due to coupling of light to the exciton alone, but it must follow from the presence of dissipative processes like exciton-phonon coupling and/or interaction with crystal defects [18]. The physical picture is the following: an incoming photon creates an excitonic transition and then it is re-emitted with the same wavevector and so forth, unless scattering events destroy the translational symmetry and transfer energy to the crystal lattice.

Absorption measurements performed on CdS [47], Cu_2O [48, 49] GaSe [50], ZnSe [51] and GaAs [52] crystals clearly show that, by decreasing the temperature T, the integrated absorption $K(T) = \int \alpha(\omega)d\omega$, $\alpha(\omega)$ being the absorption coefficient, is constant only above a critical temperature T^* and then decreases to smaller values for $T < T^*$. The temperature T^* is then the crossover between the excitonic ($T > T^*$)

can always be identified with the mean free path, ii) the reason why the group velocity should be evaluated at the longitudinal frequency.

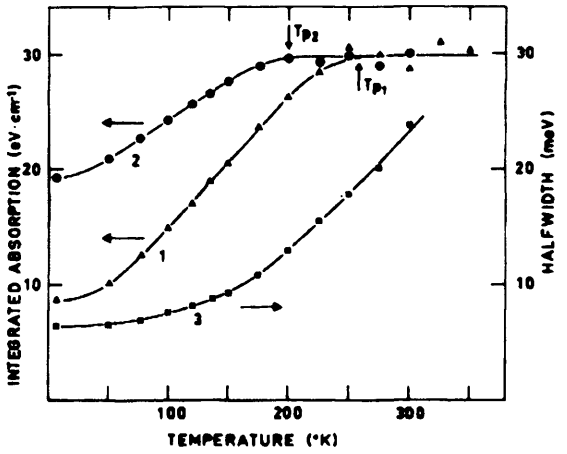

Figure 1.7: Temperature dependence of the integrated absorption for GaSe samples of thickness 97 μm (curve 1) and 26 μm (curve 2). The crossover temperatures T_{p_1} and T_{p_2} between the excitonic and the polaritonic regime are clearly shown. From Ref. [50].

and the polaritonic ($T < T^*$) regime and only in the former case the exciton-radiation coupling can be treated within the perturbation theory, disregarding the oscillatory exchange of energy between exciton and photon, i.e, the polariton effect. In particular, it has been shown that, if the exciton has no spatial dispersion, the integrated absorption is constant and temperature independent [53]. In Section 3.1 it will be shown that the same sum rule holds for non-radiative polariton modes in quantum wells. Figure 1.7 shows such crossover in GaSe samples [50].

The exciton-photon interaction alone cannot describe the radiative decay of excitons in an infinite crystal and the reason lies again in the translational invariance: due to the conservation of crystal momentum, an exciton with a given wavevector and polarization can interact with only one photon having the same wavevector and polarization. Hence, there is no density of states for radiative decay and only stationary polariton states (due to the coupling between two discrete states) can be created. Within the polariton framework, the radiative decay of free excitons can occur only through conversion of polaritons into photons at the surface of the crystal sample: a polariton with a given wavevector propagates up to the crystal surface and there it gets a finite probability to be transmitted. Hence, the *radiative decay rate* Γ of a

polariton with a well-defined wavevector can be expressed as

$$\Gamma \sim (1-R)\frac{v_g}{L}, \tag{1.46}$$

where R is the reflection coefficient at the surface and v_g is the polariton group velocity; the lifetime increases with the crystal size L and it can be thought as the confinement time of the polariton in the sample.

Polariton luminescence is indeed a very complex phenomenon since it is the result of the interplay between polariton propagation, damping and thermalization processes. The most relevant microscopic process responsible for the relaxation of exciton-polaritons is the exciton-phonon interaction, i.e. scattering of an exciton with wavevector $\mathbf{k}$ from the state $|\mathbf{k}\rangle$ to the state $|\mathbf{k} \mp \mathbf{q}\rangle$ with emission or absorption of a phonon with wavevector $\mathbf{q}$. The scattering rate γ_k of an exciton with wavevector $\mathbf{k}$ corresponds to the phenomenological damping constant γ introduced in Eq. (1.19).

At low temperatures, when $k_B T \ll \omega_{LT}$, polaritons are mostly distributed in the lower branch (that extends down to the photon-like region). Since the exciton energy $\hbar\omega_k$ is much larger than the lattice temperature $k_B T$, they are likely to cascade down this branch by emission (rather than absorption) of phonons (thermalization). However, polaritons can occasionally reach the surface and be reflected back and the probability of coming out as photons increases for decreasing k since the photon character (along the lower branch) increases. As a result, polaritons are mostly distributed in the so called *bottleneck* region [54]: a rather restricted region in k-space above which polaritons are in a quasi-thermal equilibrium, and below which, since the density of states decreases and the group velocity increases, the radiative lifetime dominates over thermal relaxation and polaritons are converted into outgoing photons.
In the case of nonresonant excitation, the observed luminescence spectra show two peaks related to luminescence from lower and the upper polariton branch as it has been observed in CdS [55, 56], GaAs [43, 46] and in GaN [57]. The lifetime of the luminescence is calculated to be in the ns range [45, 58], but it is very sensitive on the sample's size and shape and on the excitation conditions as well.

Even though the luminescence lineshape and the radiative lifetime are determined by the specific experimental conditions, the widely reported evidence clearly indicates that, for a complete interpretation of low-temperature luminescence experiments in pure semiconductor crystals, the polariton picture is the relevant one.

1.6 SUMMARY

In this Chapter the polariton effects, defined as those arising from the interaction between excitons and the transverse electromagnetic field, have been investigated. Excitons and their relevant properties in both bulk and quantum well structures have been briefly described, with particular attention to the oscillator strength, which characterizes the interaction between excitons and the electromagnetic field. The polariton dispersion can be derived either in a classical framework, or within a quantum-mechanical approach based on the second quantization of the exciton and photon fields. In an infinite crystal polaritons are stationary states and what is detected as radiative lifetime is actually the confinement time of polaritons in a finite size sample. Two criteria for the observability of polariton effects can be formulated: spatial coherence that applies when the frequency is real and the (polariton) distribution is non-uniform and temporal coherence, dealing with experiments in which polaritons are created with a well-defined wavevector and a uniform distribution.

2 Quantum Well Polaritons

This Chapter deals with the modifications (with respect to the bulk case) of the polariton concept which take place in quantum wells. This is a broad field that was started in the late sixties by Agranovich [59] and then developed during the years also in connection with the study of other confined structures like multiple quantum wells, superlattices and microcavities.

In quantum wells the breaking of the translational symmetry – the only good quantum number is now the in-plane wavevector $\mathbf{k}_{\parallel}$ – along the growth direction gives rise to two kind of polaritons: non-radiative (or confined) and radiative modes.

In the first two Sections, the concept of QW-polariton is introduced and the dispersion of both modes is obtained within a standard approach based on the non-local response theory and the standard perturbation theory. A microscopic theory which treats the "QW exciton - bulk photons" interaction non perturbatively is then developed. In the last part of the Chapter a self-consistent perturbation theory is formulated.

2.1 Non-radiative and radiative modes

As it has been explained in the previous Chapter, polariton effects result from the interaction between excitons and the retarded (transverse) part of the electromagnetic field. There is a major difference between polariton effects in bulk and in confined systems (see Fig. 2.1). In bulk crystals, due to the strict conservation of crystal momentum, an exciton with a given wavevector $\mathbf{k}_x$ can interact with only one photon

with the same wavevector and polarization. Hence, polaritons in bulk semiconductors are stationary states since there is no density of states for the radiative decay.

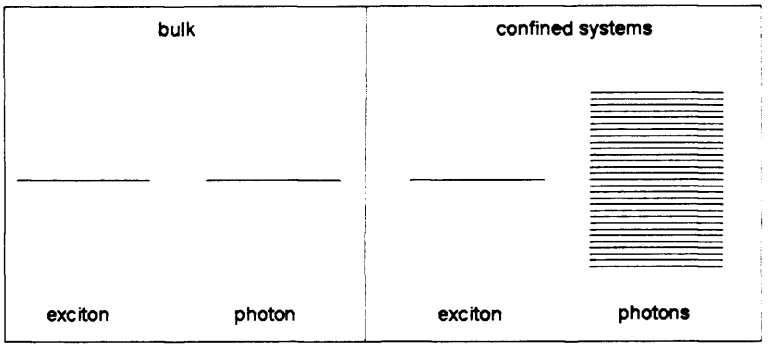

Figure 2.1: Schematic picture (see Ref. [4]) of the exciton-photon interaction. In bulk (left), the interaction of the exciton with a single photon mode leads to stationary polariton states and to a splitting of the eigenmodes. In quantum wells and in general in all low-dimensional systems, an exciton interacts with a continuum of photon modes, giving rise to the radiative decay of the exciton itself.

In quasi-two-dimensional systems[1], since the translational invariance is broken along the growth direction, an exciton with an in-plane wavevector $\mathbf{k}_x = \mathbf{k}_{||}$ can interact with photons having the same in-plane wavevector, but with all possible values of k_z, i.e. the growth-direction component of the the three-dimensional bulk photon wavevector (see Fig. 2.1). Hence, there is a finite density of states for radiative decay. This is given by

$$\begin{aligned} \rho\left(\mathbf{k}_{||}, \omega = \omega^{x}_{\mathbf{k}_{||}}\right) &= \sum_{k_z} \delta\left(\hbar\omega^{x}_{\mathbf{k}_{||}} - \frac{\hbar c}{\sqrt{\varepsilon_b}}\sqrt{k_{||}^2 + k_z^2}\right) = \\ &= \frac{V}{2\pi S}\left(\frac{\sqrt{\varepsilon_b}}{\hbar c}\right)^2 \frac{\hbar\omega^{x}_{\mathbf{k}_{||}}}{\sqrt{k_0^2 - k_{||}^2}}\theta\left(k_0 - k_{||}\right) . \end{aligned} \tag{2.1}$$

where $\omega^{x}_{\mathbf{k}_{||}} = \omega_0 + (\hbar k_{||}^2)/(2M_x)$ is the QW exciton dispersion (M_x is the in-plane translational mass), $k_0 = k_0(\omega) = \sqrt{\varepsilon_b}\omega/c$ and $\omega^{\gamma}_{\mathbf{k}} = (c/\varepsilon_b)\sqrt{k_{||}^2 + k_z^2}$ are the wavevector $[\mathbf{k} = (\mathbf{k}_{||}, k_z), k_{||} = |\mathbf{k}_{||}|]$ and frequency of the light in the sample [described by the background dielectric constant ε_b and volume (area) V (S)] respectively, and $\Theta(x)$ is the Heaviside function [$\Theta(x)$=1 for x > 0, $\Theta(x)$=0 for x < 0]. From the density

[1]The term 'quasi' is used here to distinguish from exact 2D systems in which the wave function is completely confined to a plane, i.e. has no extension outside the plane.

of states (2.1) it can thus be inferred that only excitons with $k_{\|} < k_0$, i.e excitons lying within the photon cone, decay radiatively and that, in general, the interaction between QW excitons and the radiation field gives rise to two kind of states [59]:

1. States with $k_{\|} > k_0$. These states cannot decay radiatively and can be thought as the counterpart of bulk polaritons in quantum wells. They (analogously to surface modes) lie on the right of the photon cone, in the $(k_{\|}, \omega)$ plane, and do not couple to incident light propagating along the growth direction. These modes are trapped in the sense that they are guided by the quantum well and accompanied by an evanescent light-field in the growth direction and are called *confined* or *non-radiative polaritons*. Although invisible in standard optical experiments, these states considerably contribute to the total optical response associated with QW excitons in a "hidden" way: QW excitonic molecules for instance, can dissociate into outgoing confined QW-polaritons or an LA-phonon-assisted Umklapp processes between the radiative and confined modes can occur [60, 61].

2. States with $k_{\|} < k_0$. These states have a finite radiative lifetime, lie on the left of the photon line in the $(k_{\|}, \omega)$ plane and their electric field has an oscillatory behavior far from the well. These modes are the observable ones in standard optical experiments and can be called *radiative polaritons*.

2.2 SEMICLASSICAL THEORY

As in bulk semiconductors, a semiclassical theory for QW-polaritons is based on the solutions of Maxwell equations together with a constitutive relation which accounts for the excitonic resonance. In this case the formalism to be used, i.e. the dielectric response of the system, is intrinsically nonlocal since now the translational invariance is broken along the growth direction. The approach described here is semiclassical in the sense that classical Maxwell equations are used to find the electromagnetic modes, but the microscopic quantum-mechanical theory is used for the response function.

The theory reported here is valid in the limit $L \sim a_B$, i.e. the *strong confinement* regime (see Section 1.4), also called the *quantum well* regime.

The starting point is the constitutive relation [4]

$$\mathbf{D}(z) = \varepsilon_{\mathrm{b}}\mathbf{E}(z) + 4\pi \int \chi(z,z')\mathbf{E}(z')\mathrm{d}z' , \tag{2.2}$$

where the integral in the r.h.s. term is the polarization $\mathbf{P}(z)$ (the linear response) of the material and $\chi(z,z')$ is the nonlocal susceptibility as given in the linear response theory [62–64] by

$$\chi(z,z') = \sum_{\lambda} \chi_{\lambda}(\omega,\mathbf{k}_{\parallel})\rho_{\lambda}(z)\rho_{\lambda}(z') . \tag{2.3}$$

In the above definition λ are quantum numbers related to the excited states of the crystal and only one pair of subbands has been considered: the quantity $\rho_{\lambda}(z) = F_{\mathrm{QW}}(\rho = 0)c(z)v(z)$ [where $F_{\mathrm{QW}}(\rho)$ is the exciton envelope function in the relative coordinate system and $c(z)$, $v(z)$ are the conduction and valence band confinement functions respectively] and $\chi_{\lambda}(\omega,\mathbf{k}_{\parallel})$ is given (see Refs. [4, 65]) by

$$\chi_{\lambda}(\omega,\mathbf{k}_{\parallel}) = \frac{\mu_{cv}^2}{\hbar(\omega^{\mathrm{x}}_{\mathbf{k}_{\parallel}} - \omega - i\gamma)} , \tag{2.4}$$

where $\mu_{cv} = \langle u_{\mathrm{c}}|e\mathbf{r}|u_{\mathrm{v}}\rangle$ is the dipole moment between conduction and valence bands of the bulk [u_{c} (u_{v}) are the Bloch functions at the bottom (top) of the conduction (valence) bands] and $\hbar\omega^{\mathrm{x}}_{\mathbf{k}_{\parallel}}$ is the energy of the exciton level taken in consideration.

By assuming that the quantum well lies in the (x,y) plane (z is the growth direction), and the exciton wavevector $\mathbf{k}_{\mathrm{x}} = \mathbf{k}_{\parallel}$ is placed along the x-axis, i.e. $\mathbf{k}_{\parallel} = k_{\parallel}\hat{x}$, three modes can be distinguished according to the polarization vector $\hat{\epsilon}$: L-modes have $\hat{\epsilon} \parallel \hat{x}$, T-modes have $\hat{\epsilon} \parallel \hat{y}$, while Z-modes have $\hat{\epsilon} \parallel \hat{z}$ (the Z-mode exists only for the light-hole exciton).

NON-RADIATIVE MODES

The nonlocal formalism is applied to get the dispersion of these modes by taking only one resonant term (i.e. only one excitonic resonance, typically the n=1 s-like exciton) in the nonlocal susceptibility (2.4) [65–68]. Within this scheme, the QW is enclosed in a large box of width d, such that the response function is essentially zero for $|z|, |z'| > d/2$, and the electric field is assumed to decay exponentially far from the well:

$$E(|z| > d/2) = Ae^{-\kappa(|z|-d/2)}e^{i(k_{\mathrm{x}}x-\omega t)} , \tag{2.5}$$

where the decay constant is given by

$$\kappa = \sqrt{k_{\|}^2 - \varepsilon_b \frac{\omega^2}{c^2}} \,. \tag{2.6}$$

Such a decay constant is the consequence of the phase matching at the boundaries between the solutions inside the well and free electromagnetic waves in the barrier [65]: by introducing a k_z wavevector component describing the propagation of free waves in the barrier and from the identity of the in-plane wavevector $\mathbf{k}_{\|}$ in the barrier and in the well, the following equation holds:

$$k_z^2 = k_0^2 - k_{\|}^2 \,, \tag{2.7}$$

where the wavevector of the light in the sample k_0 ($=\sqrt{\varepsilon_b}\omega/c$) corresponds to the total vector modulus in the barrier. Hence, for $k_{\|} > k_0$ (non-radiative polaritons), k_z becomes pure imaginary - $k_z = i\kappa$ - and the solution is an evanescent wave in the z-direction having κ as decay constant.

For T-modes (also referred to as TE- or s-polarization modes), the electric and magnetic fields are:

$$\begin{aligned} \mathbf{E} &= \hat{y} E_y \,, \\ \mathbf{B} &= \frac{c}{\omega}(-\hat{x} k_z + \hat{z} k_{\|}) E_y \,. \end{aligned} \tag{2.8}$$

Maxwell equations imply

$$\nabla \nabla \cdot \mathbf{E} - \nabla^2 \mathbf{E} = \frac{\omega^2}{c^2} \mathbf{D} \,. \tag{2.9}$$

Since then for TE-modes $\nabla \cdot \mathbf{E} = 0$, the above equation can be re-written, for $|z| < d/2$ as

$$\left(\frac{\partial^2}{\partial z^2} - \kappa^2 \right) E_y = -4\pi \frac{\omega^2}{c^2} \chi(\omega, \mathbf{k}_{\|}) \rho(z) \int \rho(z') E_y(z') \mathrm{d}z' \,. \tag{2.10}$$

It can be shown [4, 65], that a solution of Eq. (2.10) satisfying the Maxwell boundary conditions (continuity of $E_{\|}$, $B_{\|}$ at the interface well-barrier $z = d/2$) is of the form

$$E_y = \int \rho(z') e^{-\kappa |z - z'|} \mathrm{d}z' \,. \tag{2.11}$$

By substituting in Eq. (2.10), the dispersion relation of T-mode polaritons is given as

$$T: \quad \frac{2\pi\omega^2}{\kappa c^2} |F_{QW}(0)|^2 \chi(\omega, \mathbf{k}_{\|}) P(\kappa) = 1 \,, \tag{2.12}$$

where $P(\kappa)$ is defined by

$$P(\kappa) = \int\int c^*(z)v(z)v^*(z')c(z')e^{-\kappa|z-z'|}\mathrm{d}z\mathrm{d}z' . \tag{2.13}$$

The dispersion relations of $L-$ and $Z-$mode polaritons can be found in a similar way and are given by (see Ref. [4]):

$$L: \quad \frac{2\pi}{\varepsilon_\mathrm{b}} |F_\mathrm{QW}(0)|^2 \chi(\omega, \mathbf{k}_\parallel)\kappa P(\kappa) = -1 , \tag{2.14}$$

$$Z: \quad \frac{2\pi}{\varepsilon_\mathrm{b}} |F_\mathrm{QW}(0)|^2 \chi(\omega, \mathbf{k}_\parallel) \left(\frac{\mathbf{k}_\parallel^2}{\kappa} P(\kappa) - 2\mathcal{I} \right) = 1 , \tag{2.15}$$

where $\mathcal{I}$ is defined by

$$\mathcal{I} = \int |c(z)|^2 |v(z)|^2 \mathrm{d}z . \tag{2.16}$$

In more complicated confined structures, the confined eigenstates may be also found using the *embedding* method (see Refs. [69, 70] for details)

RADIATIVE MODES

The dispersion of radiative polaritons can be found as the solution of Eq. (2.10) for $k_\parallel < k_0$, in terms of a scattering problem of barrier waves by the well [65], by defining appropriate Breit-Wigner scattering coefficients for the three optically active modes L, T and Z. A brief explanation of the method (see Ref. [65] for details) in the case of transverse modes is here reported.

By imposing (as already explained in the previous paragraph for non-radiative modes) the Maxwell boundary conditions on the solutions inside the well and in the barrier, a scattering amplitude coefficient S, defined as the ratio between the outgoing (E^out) and the incoming (E^inc) field, can be computed in terms of the field itself (E_y for T-modes) in the well and its derivative:

$$S = \frac{E_\mathrm{y}^\mathrm{out}}{E_\mathrm{y}^\mathrm{inc}} = \frac{E_\mathrm{y} - \frac{1}{ik_z}\partial_z E_\mathrm{y}}{E_\mathrm{y} + \frac{1}{ik_z}\partial_z E_\mathrm{y}}|_{z=d/2^-} , \tag{2.17}$$

where the wavevector k_z is now real and equal to $\sqrt{k_0^2 - k_\parallel^2}$, and the superscript - means that the well surface is approached from the inside. Substituting an appropriate

solution of Eq. (2.10) in the amplitude given above, yields:

$$S = \exp[ik_z d]\frac{\omega - \overline{\omega}(\mathbf{k}_\parallel) - i\Gamma(\mathbf{k}_\parallel)}{\omega - \overline{\omega}(\mathbf{k}_\parallel) + i\Gamma(\mathbf{k}_\parallel)}\,, \tag{2.18}$$

with

$$\overline{\omega}_{\rm T}(\mathbf{k}_\parallel) = \omega^{\rm x}_{\mathbf{k}_\parallel} + 4\pi\frac{\mu_{cv}^2\,|F_{\rm QW}(0)|^2}{\varepsilon_{\rm b}\hbar}k_0^2 P(k_z)\,, \tag{2.19}$$

$$\Gamma_{\rm T}(\mathbf{k}_\parallel) = \frac{2\pi\mu_{cv}^2\,|F_{\rm QW}(0)|^2\,Q(k_z)^2}{\varepsilon_{\rm b}\hbar}\frac{k_0^2}{k_z}\,, \tag{2.20}$$

where $P(k_z)$, $Q(k_z)$ are quantities related to the confinement functions $v(z)$ and $c(z)$ similarly as in Eqs. (2.13) and (2.16). Expressions of the form (2.18) for the scattering amplitude generate Breit-Wigner resonances and this occurs when

$$\overline{\omega}_{\rm T}(\mathbf{k}_\parallel) = \omega\,. \tag{2.21}$$

The above equation [when Eq. (2.19) is used] gives the resonant frequency at each $\mathbf{k}_\parallel$, i.e. the dispersion of the radiative polaritons (i.e. the radiative corrections to the exciton frequency $\omega^{\rm x}_{\mathbf{k}_\parallel}$) and, for every resonance, the corresponding lifetime broadening $\Gamma_{\rm T}(\mathbf{k}_\parallel)$ is given by Eq. (2.20). By a similar procedure, solutions for the other two optically active modes can be found [26, 65].

The lifetime broadenings $\Gamma_{\rm T}(\mathbf{k}_\parallel)$, just obtained as a natural property of the Breit-Wigner resonance, can also be found by using the standard perturbation theory applied to a free exciton in an isolated QW, always under the assumption that the in-plane wavevector $\mathbf{k}_\parallel = k_\parallel\hat{x}$ is conserved. In this way (see for instance Refs. [71–74]), the radiative widths are straightforwardly expressed in terms of the exciton oscillator strength per unit area f_ℓ/S. Within this framework, the Fermi Golden Rule[2] with the interaction Hamiltonian given in Eq. (1.43) is used to calculate the transition rate between the initial state $|{\rm i}\rangle$ consisting of an exciton state with polarization vector $\hat{e}$ and zero photons, and the final state $|{\rm f}\rangle$ describing the crystal ground state $|0\rangle$ plus a photon having a 3D wavevector $\mathbf{k} = (\mathbf{k}_\parallel, k_z)$ and polarization λ. With a second quantization form for the vector potential field, the matrix element is given by

$$\langle {\rm i}|\mathcal{L}|{\rm f}\rangle = -\frac{e}{m_0 c}\left(\frac{2\pi\hbar c}{\sqrt{\varepsilon_{\rm b}}kV}\right)^{1/2}\langle {\rm exciton}|\hat{\epsilon}^{(\lambda)}_{\mathbf{k}}\cdot\sum_{\rm i}\mathbf{p}_{\rm i}|0\rangle\,. \tag{2.22}$$

[2]To the lowest order of the time-dependent perturbation theory, the transition probability per unit time from an initial state $|{\rm i}\rangle$ to a final state $|{\rm f}\rangle$ induced by an harmonic perturbation $H_{\rm I} = \mathcal{L}e^{\mp i\omega t}$ is given by $\mathcal{P}_{{\rm i}\to{\rm i}} = \frac{2\pi}{\hbar}|\langle {\rm i}|\mathcal{L}|{\rm f}\rangle|^2\delta(E_{\rm f} - E_{\rm i} \mp \hbar\omega)$, where -(+) stands for absorption (emission).

By expressing the sum over the photon polarizations of the squared matrix element in terms of the exciton oscillator strength $f_{\hat{\epsilon}}$ (see Refs. [3, 4] for details), i.e. $\sum_\lambda |\langle i|\mathcal{L}|f\rangle|^2 = \frac{\pi e^2\hbar^2}{\varepsilon_b moV}\sum_\lambda f_{\hat{\epsilon}}|\hat{e}\cdot\hat{\epsilon}^{(\lambda)}|^2$, the Golden Rule reads

$$\Gamma(\mathbf{k}_\parallel) = \frac{2\pi^2}{\varepsilon_b}\frac{e^2\hbar^2}{moV}\sum_{k_z}\sum_\lambda |\hat{e}\cdot\hat{\epsilon}^{(\lambda)}|^2\delta\left(\hbar\omega^{\mathrm{x}}_{\mathbf{k}_\parallel} - \frac{\hbar c}{\sqrt{\varepsilon_b}}\sqrt{k_\parallel^2+k_z^2}\right). \tag{2.23}$$

In the equation above the sum over k_z of the energy conservation δ-function is the one-dimensional density of states already introduced in Eq. (2.1) and its evaluation gives the decay rate in terms of the oscillator strength per unit area $f_{\hat{\epsilon}}/S$ as

$$\Gamma(\mathbf{k}_\parallel) = \frac{2\pi}{\varepsilon_b}\frac{e^2}{moc}\frac{k_0}{k_z}\sum\lambda\frac{f_{\hat{\epsilon}}}{S}|\hat{e}\cdot\hat{\epsilon}^{(\lambda)}|^2\Theta(k_0-k_\parallel), \tag{2.24}$$

where, once again, $k_z = \sqrt{k_0^2-k_\parallel^2}$.

The three modes (T, L and Z) are then defined according to the relative orientation between the exciton polarization vector $\hat{e}$ and the photon polarization vectors $\hat{\epsilon}^{(\lambda)}$. Given $\mathbf{k}_\parallel = k_\parallel\hat{x}$, the two orthogonal photon polarization vectors can be taken as $\hat{\epsilon}^{(1)} = \hat{y}$ and $\hat{\epsilon}^{(2)} = (k_z\hat{x} - k_x\hat{z})/k_0$.

Hence, for T-excitons, $\sum_\lambda f_{\hat{\epsilon}}|\hat{e}\cdot\hat{\epsilon}^{(\lambda)}|^2 = f_{xy}$, where f_{xy} is the oscillator strength for in-plane polarization. For L-excitons, $\sum_\lambda f_{\hat{\epsilon}}|\hat{e}\cdot\hat{\epsilon}^{(\lambda)}|^2 = f_{xy}(k_z/k_0)^2$, and for Z-excitons, $\sum_\lambda f_{\hat{\epsilon}}|\hat{e}\cdot\hat{\epsilon}^{(\lambda)}|^2 = f_z(k_\parallel/k_0)^2$, where f_z is the oscillator strength for the z-polarized light-hole exciton (for light polarized along the growth direction only light-hole transitions are allowed). The radiative widths (2.24) can then be expressed as follows:

$$\Gamma_{\mathrm{T}}(\mathbf{k}_\parallel) = \frac{2\pi}{\sqrt{\varepsilon_b}}\frac{e^2}{m_0c}\frac{f_{xy}}{S}\frac{k_0}{\sqrt{k_0^2-k_\parallel^2}} = \Gamma_0\frac{k_0}{\sqrt{k_0^2-k_\parallel^2}}, \tag{2.25}$$

$$\Gamma_{\mathrm{L}}(\mathbf{k}_\parallel) = \frac{2\pi}{\sqrt{\varepsilon_b}}\frac{e^2}{m_0c}\frac{f_{xy}}{S}\frac{\sqrt{k_0^2-k_\parallel^2}}{k_0} = \Gamma_0\frac{\sqrt{k_0^2-k_\parallel^2}}{k_0}, \tag{2.26}$$

$$\Gamma_{\mathrm{Z}}(\mathbf{k}_\parallel) = \frac{2\pi}{\sqrt{\varepsilon_b}}\frac{e^2}{m_0c}\frac{f_z}{S}\frac{k_\parallel^2}{k_0\sqrt{k_0^2-k_\parallel^2}}. \tag{2.27}$$

From Eq. (2.25), it can be noticed that at $\mathbf{k}_\parallel = 0$ ($k_z = k_0$) both L- and T-modes have the same decay rate $\Gamma_0 \equiv (2\pi e^2/(\sqrt{\varepsilon_b}m_0c))(f_{xy}/S)$ (called intrinsic radiative rate); the decay time of the exciton state is $\tau_0 = 1/\Gamma_0$ (called intrinsic radiative lifetime). Using an oscillator strength $f_{xy}/S = 50\cdot 10^{-5}\,\mathring{A}^{-2}$, a correct value for a heavy-hole exciton in GaAs/Al_xGa_{1-x}As quantum well 100 $\mathring{A}$ thick [75], one finds $\hbar\Gamma_0 = 0.026$ meV and τ_0=12 ps.

Figure 2.2 shows the polariton dispersion for a CuCl quantum well (radiative shifts) for both radiative and non-radiative modes as calculated in Ref. [65], according to the expressions previously written. One of the first features to be noticed is that a radiative shift of exciton energies (due to the interaction with the retarded electromagnetic field) occurs for both modes, but it is actually very small, except in the very proximity of the light line. It is also very peculiar that the transverse mode (as well as the Z-mode) shows a strong discontinuity when $k_{\|} = k_0$. This behavior is related to the dispersion $\Gamma_T(\mathbf{k}_{\|})$ of the radiative widths (depicted in Fig. 2.2) that is characterized by steep divergences of the transverse (and Z-) modes as $k_{\|}$ approaches k_0. In Ref. [65] the authors conclude that, in the case of transverse modes, no solutions are possible at $k_{\|} = k_0$, since Γ_T becomes infinite [see Eq. (2.25)] and thus, the meaning of the dispersion curve in Fig. 2.2 (a) is that the mode with $k_{\|} = k_0$ is excluded from the crystal by the symmetry breaking.

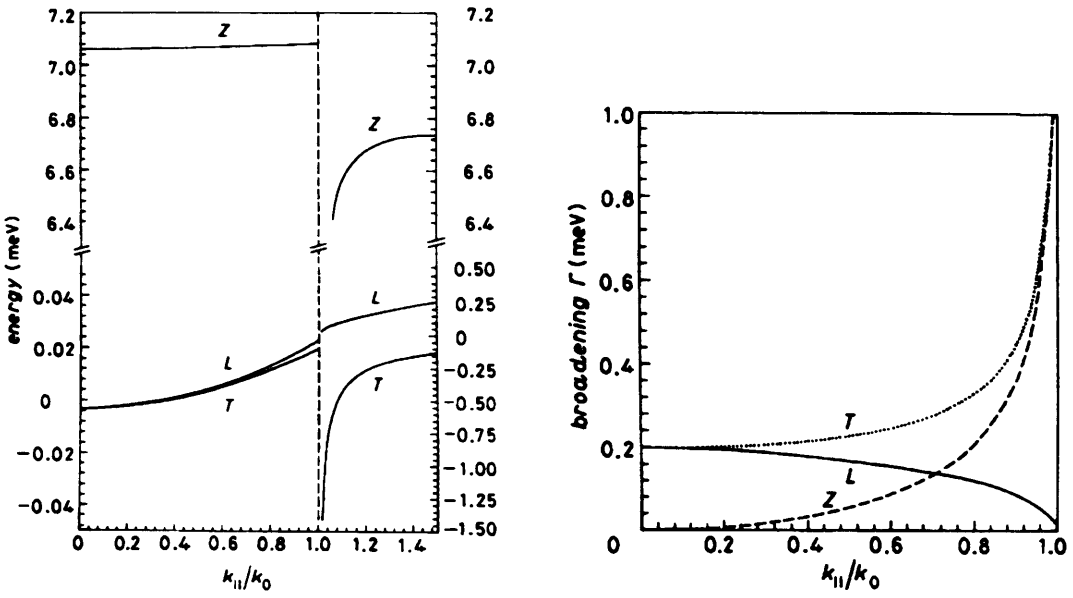

(a) (b)

Figure 2.2: (a) Dispersion of radiative (left) and non-radiative (right) polaritons; (b) lifetime broadening of radiative polaritons. Both (a) and (b) refer to a 20 $\AA$ wide CuCl QW; $k_{\|}$ is given in units of $k_0 = k_0(\omega_0)$. The radiative widths $\Gamma(\mathbf{k}_{\|})$ [in (b) given in meV] for T- and $Z-$mode polaritons diverge as $1/\sqrt{1-(k_{\|}/k_0)^2}$ near $k_{\|} = k_0$. From Ref. [65].

Actually, the divergence in the radiative lifetime of $T-$mode[3] polaritons has no physical explanation and should be regarded as an artifact of the perturbation theory; the authors themselves are aware about this problem as they briefly report (without providing yet a solution) about it in later works [4, 11, 72].

Hence, in order to provide a precise description of the QW polariton problem (in terms of both radiative corrections and radiative widths) it is necessary to go beyond the perturbation theory and work within a fully microscopic approach for the interaction between QW excitons and bulk photons. In the next Section, by setting up a second-quantized form for the Hamiltonian describing the system "bulk photons - QW excitons" in the presence of dipole interaction between them, a dispersion relation $\omega = \omega(k_{\|})$ describing both conjugate modes (non-radiative and radiative polaritons) is derived and numerically solved. The dispersion of the transverse radiative widths $\Gamma_{\mathrm{T}} = \Gamma_{\mathrm{T}}(k_{\|})$ does not show any divergence at point $k_{\|} = k_0$ in this case. Physical arguments in support of this last result are given by a "self-consistent" perturbation theory for the joint density of states for the optical decay of QW excitons as detailed in Section 2.4.

2.3 MICROSCOPIC APPROACH

The Hamiltonian of a system "bulk photons – QW excitons", in the presence of dipole interaction between the two species (see Appendix A), is given by

$$H = H_{\gamma} + H_x + H_i^{\mathrm{I}} + H_i^{\mathrm{II}}\,, \tag{2.28}$$

with

$$\begin{aligned}
H_{\gamma} &= \sum_{\mathbf{k}} \hbar\omega_{\mathbf{k}}^{\gamma} \alpha_{\mathbf{k}}^{\dagger}\alpha_{\mathbf{k}}\,, \\
H_x &= \sum_{\mathbf{k}_{\|}} \hbar\omega_{\mathbf{k}_{\|}}^{\mathrm{x}} b_{\mathbf{k}_{\|}}^{\dagger} b_{\mathbf{k}_{\|}}\,, \\
H_i^{\mathrm{I}} &= i\sum_{\mathbf{k}_{\|}}\sum_{k_z} C_{\mathbf{k}_{\|},k_z}(\alpha_{\mathbf{k}_{\|},k_z} + \alpha^{\dagger}_{-\mathbf{k}_{\|},-k_z})(b_{-\mathbf{k}_{\|}} - b^{\dagger}_{\mathbf{k}_{\|}})\,, \\
H_i^{\mathrm{II}} &= \frac{1}{\hbar\omega^{\mathrm{x}}_{\mathbf{k}_{\|}}}\sum_{\mathbf{k}_{\|}}\sum_{k_z,k_z'} C_{\mathbf{k}_{\|},k_z} C_{\mathbf{k}_{\|},k_z'}(\alpha_{\mathbf{k}_{\|},k_z} + \alpha^{\dagger}_{-\mathbf{k}_{\|},-k_z})(\alpha_{-\mathbf{k}_{\|},-k_z'} + \alpha^{\dagger}_{\mathbf{k}_{\|},k_z'})\,,
\end{aligned} \tag{2.29}$$

[3]From now on, only transverse modes will be analyzed.

where $b_{\mathbf{k}_\parallel}$ ($b^\dagger_{\mathbf{k}_\parallel}$) and $\alpha_{\mathbf{k}}$ ($\alpha^\dagger_{\mathbf{k}}$) are the QW exciton and bulk photon annihilation (creation) operators, respectively, $\omega^{\mathrm{x}}_{\mathbf{k}_\parallel} = \omega_0 + (\hbar k^2_\parallel)/(2M_{\mathrm{x}})$ and $\omega^{\gamma}_{\mathbf{k}} = (ck)/\sqrt{\varepsilon_{\mathrm{b}}}$ are the exciton and photon dispersions, respectively [$k = |\mathbf{k}|$, $\mathbf{k} = (\mathbf{k}_\parallel, k_z)$], and M_{x} is the in-plane translational mass of a QW exciton.
The coupling constant $C_{\mathbf{k}_\parallel, k_z}$ is given by

$$C_{\mathbf{k}_\parallel, k_z} = \sqrt{\frac{R_{\mathrm{QW}}\omega_0}{2L\omega^{\gamma}_{\mathbf{k}}}}\,, \tag{2.30}$$

where L is the z-direction quantization length of the light field ($L \to \infty$) and R_{QW} is the dimensional oscillator strength of exciton-photon interaction per QW unit area (having dimensions of [eV^2 Å]) defined in terms of the oscillator strength for in plane polarization f_{xy} by

$$R_{\mathrm{QW}} = \frac{2\pi e^2\hbar^2}{\varepsilon_{\mathrm{b}} m_0}\frac{f_{xy}}{S}\,. \tag{2.31}$$

Hence, the Hamiltonian (2.28) is relevant to the optics of transverse (T-mode) QW excitons which interact with the in-plane TE-polarized light field. The photon-mediated long-range exchange interaction and non-resonant terms of "QW exciton – bulk photon" coupling are also included in the description.

The quadratic Hamiltonian (2.28) is exactly solvable and it gives rise to the quasi-2D polariton (non-radiative) and radiative states of QW excitons. This case deals only with the coherent interaction between the particles [H^{I}_i and H^{II}_i terms in Eqs. (2.28)-(2.29)] and therefore inherently refers to the strong coupling between QW excitons and bulk photons. Alternatively, the (quasi-) eigenenergies of QW excitons can be found from Eq. (2.28) by using the standard diagram technique [73, 76–78]. This latter approach is useful to include the particle rate γ_{x} of incoherent scattering of QW exciton, i.e. the homogeneous broadening.
The Dyson equation [79] for QW excitons is

$$G_{\mathbf{k}_\parallel}(\omega) = G^{(0)}_{\mathbf{k}_\parallel}(\omega) + G^{(0)}_{\mathbf{k}_\parallel}(\omega)\Sigma_{\mathbf{k}_\parallel}(\omega)G_{\mathbf{k}_\parallel}(\omega)\,, \tag{2.32}$$

where $G_{\mathbf{k}_\parallel}$, $G^{(0)}_{\mathbf{k}_\parallel}$ are the propagators of optically-dressed and optically-non-interacting excitons, respectively, the latter given by

$$G^{(0)}_{\mathbf{k}_\parallel} = \frac{2\omega^{\mathrm{x}}_{\mathbf{k}_\parallel}}{\omega^2 - (\omega^{\mathrm{x}}_{\mathbf{k}_\parallel} - i\gamma_{\mathrm{x}}/2)^2}\,, \tag{2.33}$$

and $\Sigma_{\mathbf{k}_\parallel}$ is the photon-mediated self-energy given by

$$\Sigma_{\mathbf{k}_\parallel}(\omega) = \frac{2\omega^2}{\hbar^2(\omega^{\mathrm{x}}_{\mathbf{k}_\parallel})^2} \sum_{k_z} \frac{\mid C_{\mathbf{k}_\parallel,k_z} \mid^2 \omega^{\gamma}_{\mathbf{k}}}{(\omega^{\gamma}_{\mathbf{k}})^2 - \omega^2} . \tag{2.34}$$

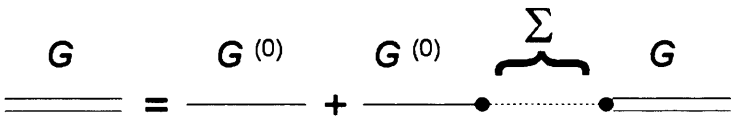

Figure 2.3: Diagrammatic representation of the Dyson equation.

Figure 2.3 shows diagrammatically the conversion of an optically dressed QW exciton into a non-interacting exciton and non-interacting exciton that couples with the light field through the photon-mediated self-energy.

By using Eqs. (2.32)-(2.34), the final expression for the propagator $G(\mathbf{k}_\parallel)$ is given by

$$G_{\mathbf{k}_\parallel}(\omega) = \frac{2\omega^{\gamma}_{\mathbf{k}}}{\omega^2(\omega^{\gamma}_{\mathbf{k}} - i\gamma_{\mathrm{x}}/2)^2 - 2\omega^{\gamma}_{\mathbf{k}}\Sigma_{\mathbf{k}_\parallel}(\omega)} . \tag{2.35}$$

Straightforward calculation of the poles of $G(\mathbf{k}_\parallel)$ yields the spectrum of optically-dressed QW excitons:

$$\omega^2 - (\omega^{\mathrm{x}}_{\mathbf{k}_\parallel} - i\gamma_{\mathrm{x}}/2)^2 + \frac{\varepsilon_{\mathrm{b}} R_{\mathrm{QW}} \omega^2}{c^2\hbar^2\sqrt{k_\parallel^2 - k_0^2(\omega)}} = 0 . \tag{2.36}$$

For $\gamma_{\mathrm{x}} = 0$, when no decoherence of exciton-photon interaction occurs, the dispersion Eq. (2.36) can also be derived by solving (see for example Ref. [71] and Appendix A for a complete and independent derivation) the Hamiltonian (2.28).

Both the confined (non-radiative) and radiative states are nonperturbatively described by the *same* dispersion relation (2.36) as its *conjugated* solutions [$\omega = \mathrm{Re}[\omega] + i\,\mathrm{Im}[\omega] = \mathrm{Re}[\omega] - i\,\Gamma_{\mathrm{T}}/2$], a property not completely realized in literature.

The confined QW polariton modes, guided by the quantum well and always accompanied by an evanescent light field ($E(z) = E(0)e^{-\kappa|z|}$) in the growth direction, are

characterized by

$$\begin{aligned} \mathrm{Re}[\kappa] &> 0; \quad \kappa = \sqrt{k_{\|}^2 - k_0^2(\omega)}, \\ \mathrm{Im}[\omega] &\leq 0. \end{aligned}$$

The first criterion ensures that the light field associated with QW polaritons has an evanescent envelope in the z-direction, $E(z) = E(0)\exp(-\kappa|z|)$, while the second one stems from the casuality principle. These states refer to the physical sheet of the two-fold Riemann energy plane, while the radiative polariton modes with

$$\begin{aligned} \mathrm{Im}[\omega] &\leq 0, \\ \mathrm{Re}[\kappa] &< 0, \end{aligned}$$

are located on the unphysical sheet of the energy plane. This latter result is a signature of the metastable states decaying in outgoing waves [80]. Thus, in order to find the energy spectrum of the radiative states, one has to use $-\kappa$ with $\mathrm{Re}[\kappa] > 0$ for $\sqrt{k_{\|}^2 - k_0^2(\omega)}$ when solving Eq. (2.36). This can also be justified by analyzing the Dyson equation (2.32) for the radiative states in terms of the advanced, rather than retarded, Green functions. The initial three-dimensional Hamiltonian (2.28) maps on to a non-Hermitian two-dimensional Hamiltonian which has the quasi-spectrum given by Eq. (2.36) and describes the localized states, which are split-off from the continuum (confined polaritons), and the metastable states (radiative polaritons).

Before moving to the analysis of the numerical solutions of the dispersion relation (2.36), it is worth to stress its meaning and importance. The dispersion of the confined QW polariton modes, as derived in the first paragraph of the previous Section, has been widely discussed in the last two decades for the case $\gamma_x = 0$ [65–68, 76–78, 81], while, the radiative states of QW excitons have been mainly considered in terms of the perturbation theory [71–74] as it has been described in the last paragraph of the previous Section. By solving Eq. (2.36), the radiative states are treated non-perturbatively, and this is particularly important in the vicinity of the resonant crossover between the dispersions of bulk photons and QW excitons, i.e. at the *dangerous* point $k_{\|} \to k_0 = k_0(\omega_0)$.

The radiative half-width $\Gamma/2 = \Gamma_T/2 = -\mathrm{Im}[\omega(k_{\|})]$ and radiative (Lamb) shift (radiative correction) $\Delta = \Delta_T = \mathrm{Re}[\omega(k_{\|})] - \omega_0$, calculated with Eq. (2.36) for the radiative and confined states (the radiative width of these latter modes being zero, since they are *trapped* states, i.e. described by an infinite lifetime $1/\Gamma_T$) of QW excitons in

the strong coupling limit ($\gamma_x = 0$), are plotted in Figs. 2.4 and 2.5, respectively (see the solid lines). For comparison, in Fig. 2.4 the half-width $\Gamma/2$ calculated with the perturbation theory is also shown by a thin solid line. In this latter case the radiative width is given by Eq. (2.25). In contrast to the perturbative approach of Eq. (2.25), the exact radiative width of QW excitons described with the Hamiltonian (2.28) does not diverge at $k_\parallel = k_0$ and even persists beyond the photon cone (see the dispersions in the interval $[C, B]$ in both Figs. 2.4,2.5). This result has already been realized[4] numerically [76, 78, 82], but no physical grounds have been given to support the numerical solutions.

In the rest of this Section the characteristic points (A and B in Figs. 2.4, 2.5) are quantified.

The point A, where the maximum value of $\Gamma = \Gamma_T^{max}$ occurs, is specified (see Appendix C) by

$$\begin{aligned} k_\parallel &= k_\parallel^{(A)} = k_0(\omega_0)\,, \\ \Gamma_T^{(A)} &= \Gamma_T^{max} = \frac{\sqrt{3}}{2}\left(\Gamma_0^2\omega_0\right)^{1/3}, \\ \Delta_T^{(A)} &= \frac{1}{4}\left(\Gamma_0^2\omega_0\right)^{1/3}, \end{aligned} \tag{2.37}$$

where Γ_0, the radiative width (expressed in eV) at $\mathbf{k}_\parallel = 0$ is now given in terms of the dimensional oscillator strength R_{QW} as

$$\Gamma_0 = \Gamma_T(\mathbf{k}_\parallel = 0) = \frac{\sqrt{\varepsilon_b} R_{QW}}{\hbar c}\,. \tag{2.38}$$

According to Eqs. (2.37), Γ_T^{max} is much larger than Γ_0. The terminal point B, where the radiative width Γ_T becomes equal to zero and the Lamb shift reaches its maximum value $\Delta = \Delta_T^{max}$, lies outside the photon cone, $k_\parallel^{(B)} > k_0 = k_0(\omega_0)$, and is characterized (see Appendix C) by

$$\begin{aligned} k_\parallel &= k_\parallel^{(B)} = k_0(\omega_0)\left[1 + \frac{3}{2}\left(\frac{\Gamma_0}{2\omega_0}\right)^{2/3}\right] = k_0 + \frac{3}{2\sqrt[3]{4}}\,\frac{\sqrt{\varepsilon_b}}{\hbar c}\left(\Gamma_0^2\omega_0\right)^{1/3}, \\ \Gamma_T^B &= 0\,, \\ \Delta_T^{(B)} &= \Delta_T^{max} = \frac{1}{\sqrt[3]{4}}\left(\Gamma_0^2\omega_0\right)^{1/3}. \end{aligned} \tag{2.39}$$

[4] In particular, in Ref. [76], Orrit and coworkers state that the dispersion of the radiative states beyond the photon line (point C in Figs. 2.4 and 2.5) has to be considered unphysical.

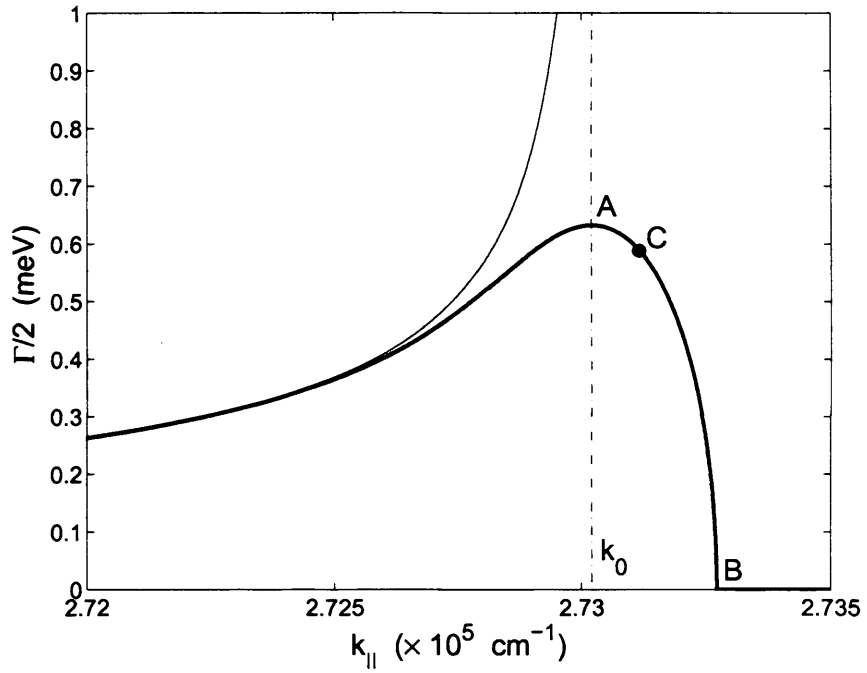

Figure 2.4: The radiative half-width $\Gamma/2 = \Gamma_T/2$ of T-mode QW polaritons as function of the in-plane wavevector $k_{||}$, evaluated with the standard perturbative approach given by Eq. (2.25) (thin solid line) and by the exact diagonalization of the Hamiltonian (2.28), i.e. by solving Eq. (2.36) (solid line). The dashed-dotted vertical line indicates $k_0 = k_0(\omega_0) = (\sqrt{\epsilon_b}\omega_0)/(\hbar c)$. In numerical calculations $R_{QW} = 0.025\,\mathrm{eV}^2\text{Å}$ and $\omega_0 = 1.5\,\mathrm{eV}$, so that $\Gamma_0 = 45.5\,\mu\mathrm{eV}$ and the intrinsic radiative lifetime of QW excitons is given by $\tau_R = \hbar/\Gamma_0 = 14.5\,\mathrm{ps}$.

In close vicinity of the critical point B, the radiative width Γ_T decreases proportionally to the square root of $k_{||}^{(B)} - k_{||}$ (see Fig. 1) and is approximated by

$$\Gamma_T(\mathbf{k}_{||} \to \mathbf{k}_{||}^{(B)}) = \frac{6\sqrt[6]{2}}{\sqrt{5}} \left(\Gamma_0^2\omega_0\right)^{1/3} \frac{1}{\sqrt{k_0}} \sqrt{k_{||}^{(B)} - k_{||}}\,. \tag{2.40}$$

For $\gamma_x = 0$, the case considered in this Section, there are no roots of Eq. (2.36) relevant to the radiative modes for $k_{||} > k_{||}^{(B)}$.

In the next Section, in order to understand the removal of $(k_0^2 - k_{||}^2)^{-1/2}$ divergence which appears in the perturbative approach given by Eq. (2.25), the joint density of states (JDS), $\rho(\mathbf{k}_{||}, \omega)$, for the resonant optical decay of QW excitons in the bulk photon modes is examined.

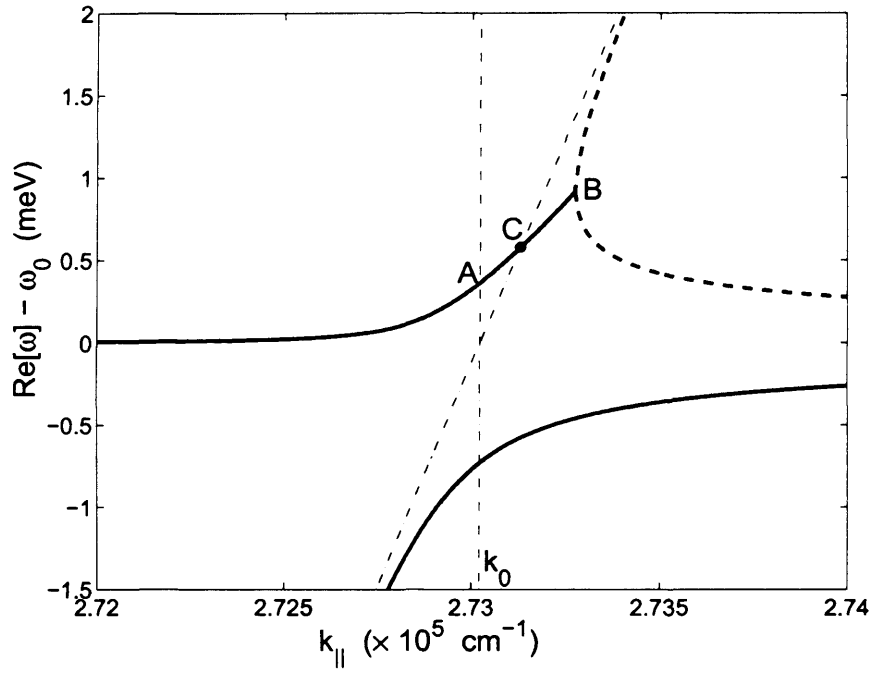

Figure 2.5: The polariton dispersion $\mathrm{Re}[\omega] - \omega_0$, i.e., the Lamb shift $\Delta = \Delta_T$ of optically-dressed T-mode QW excitons as function of the in-plane wavevector $k_{\|}$. The numerical calculations have been performed solving the dispersion Eq. (2.36), the upper (lower) solid line refers to the radiative (confined) polariton states. The dash-dotted line shows the dispersion of bulk photons, $(\hbar c k_{\|}/\sqrt{\varepsilon_b}) - \omega_0$. The dashed two-branch dispersion curve beyond the terminal, bifurcation point B is relevant to the radiative states and has no physical meaning for $\gamma_x = 0$ (see Section. 3.3).

2.4 THE NON-PERTURBATIVE CORRECTIONS TO THE RADIATIVE STATES OF QW EXCITONS

When the total scattering rate of QW excitons due to incoherent sources (γ_x) and to the coherent optical decay itself (Γ) is taken into account, the JDS $\rho(\mathbf{k}_{\|}, \omega)$ for the resonant optical decay of the excitons into bulk photon modes can be written in the form

$$\rho\left(\mathbf{k}_{\|}, \omega = \omega^{x}_{\mathbf{k}_{\|}}\right) \propto \frac{1}{\pi} \int_{-\infty}^{+\infty} dk_z \, \frac{\gamma}{\gamma^2 + \left(\omega^{x}_{\mathbf{k}_{\|}} - \omega^{\gamma}_{\mathbf{k}}\right)^2}, \tag{2.41}$$

where $2\gamma = \gamma_x + \Gamma$ is the total scattering rate which includes incoherent damping (γ_x) and the coherent radiative decay (Γ).

The meaning of Eq. (2.41) is that, due to the scattering-induced relaxation of the

energy conservation law, $\omega^{x}_{\mathbf{k}_\parallel} (\simeq \omega_0) = \omega^{\gamma}_{\mathbf{k}} \left(= c/\sqrt{\varepsilon_b}\sqrt{k_\parallel^2 + k_z^2}\right)$ the profile of the integrand function in the JDS changes from a δ-function as given in Eq. (2.1), to a Lorentzian one.

When $\partial\omega^{\gamma}_{\mathbf{k}}(k_\parallel, k_z)/\partial k_z \neq 0$ at k_z given by the energy conservation law $\omega^{x}_{\mathbf{k}_\parallel}(k_\parallel) = \omega^{\gamma}_{\mathbf{k}}(k_\parallel, k_z)$, the integrand function on the r.h.s of Eq. (2.41) preserves its Lorentzian shape even in terms of k_z. In this case $\rho(k_\parallel)$ does not depend on γ, and the standard perturbative approach of Eq. (2.25) is valid.

The situation is different when $k_\parallel \to k_0$: the solution of the energy conservation equation $\omega^{x}_{\mathbf{k}_\parallel}(k_\parallel) = \omega^{\gamma}_{\mathbf{k}}(k_\parallel = k_0, k_z)$ is $k_z = 0$, and $\partial\omega^{\gamma}_{\mathbf{k}}(k_\parallel = k_0, k_z)/\partial k_z = 0$, indicating a 1D van Hove singularity in the joint density of states. In this case the JDS $\rho(k_\parallel, \omega = \omega^{x}_{\mathbf{k}_\parallel})$ is strongly affected by γ in the close vicinity of $k_\parallel = k_0$.

By using the standard perturbation theory in connection with the JDS determined by Eq. (2.41), one can derive (see the detailed derivation in Appendix B) the following expression for the optical decay of QW excitons:

$$\Gamma_T(k_\parallel) = \frac{(\sqrt{2}k_0^2 k_\parallel \tilde{\gamma})\Gamma_0}{\left[(k_0^2 - k_\parallel^2)^2 + 4\tilde{\gamma}^2 k_0^2 k_\parallel^2\right]^{1/2}\left[\left[(k_0^2 - k_\parallel^2)^2 + 4\tilde{\gamma}^2 k_0^2 k_\parallel^2\right]^{1/2} - (k_0^2 - k_\parallel^2)\right]^{1/2}}, \tag{2.42}$$

where $\tilde{\gamma} = \gamma/\omega_0$.

The regular perturbative solution [see the T-mode line in Fig. 2.2 (b) and the thin solid line in Fig. 2.4] refers to $k_\parallel \lesssim k_0 - \tilde{\gamma}k_0$, with the dimensionless parameter $\tilde{\gamma} = \gamma/\omega_0 \sim 10^{-4} - 10^{-3}$. In this case, the JDS is given by

$$\rho = \frac{\varepsilon_b \omega_0}{\pi c^2 \hbar^2} \frac{1}{\sqrt{k_0^2 - k_\parallel^2}}, \tag{2.43}$$

and Eq. (2.42) reduces to the standard case Eq. (2.25).

In contrast, for the narrow wavevector band $|k_\parallel - k_0| \lesssim \tilde{\gamma}k_0$, the 1D van Hove singularity strongly affects the radiative corrections. In particular, for $k_\parallel = k_0$ Eqs. (2.41) and (2.42) yield

$$\begin{aligned} \rho(k_\parallel = k_0) &= \frac{\sqrt{\varepsilon_b}}{2\pi\hbar c}\frac{1}{\sqrt{\tilde{\gamma}}}, \\ \Gamma_T(k_\parallel = k_0) &= \frac{\Gamma_0}{2\sqrt{\tilde{\gamma}}}. \end{aligned} \tag{2.44}$$

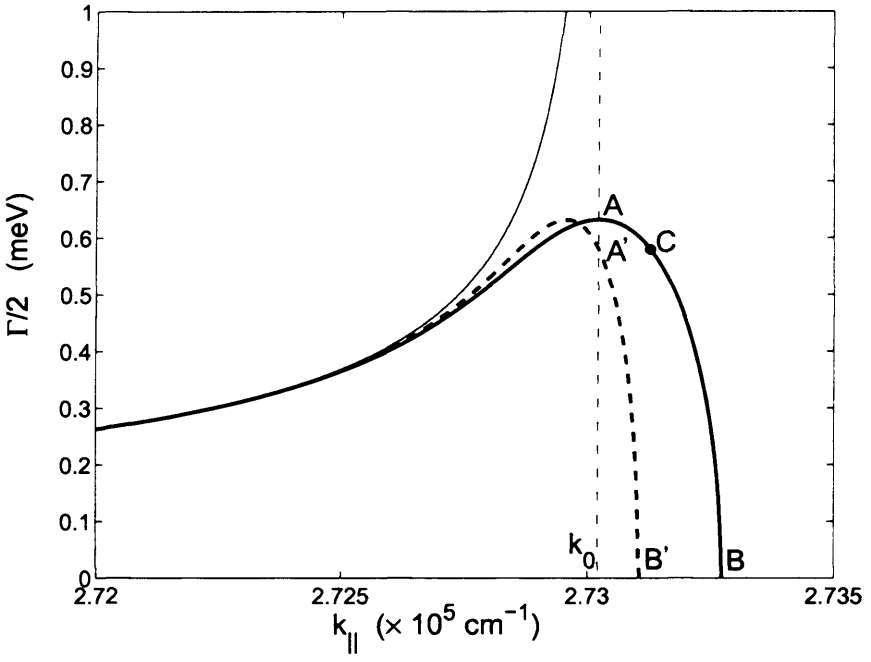

Figure 2.6: The radiative half-width $\Gamma/2 = \Gamma_T/2$ of T-mode QW polaritons evaluated with the self-consistent perturbation Eq. (2.42) (dashed line) and by the exact diagonalization of the Hamiltonian (2.28). It is shown also the result of the standard perturbative approach given by Eq. (2.25) (thin solid line). The dashed-dotted vertical line indicates $k_0 = k_0(\omega_0) = (\sqrt{\varepsilon_b}\omega_0)/(\hbar c)$.

Equations (2.44) clearly show that the scattering processes relax the 1D van Hove singularity at $k_\parallel = k_0$ by removing the divergence and giving rise to a final value of $\Gamma_T(k_\parallel = k_0) \propto 1/\gamma^{1/2}$.

In the case of a completely coherent interaction of QW excitons with bulk photons, i.e. when the incoherent scattering rate $\gamma_x = 0$, Eq. (2.42) can also be used to formulate a "self-consistent" perturbation theory. In this case, one substitutes $\tilde{\gamma} = \Gamma_T/(2\omega_0)$ and, for the narrow band $|k_\parallel - k_0| \lesssim \tilde{\gamma}k_0$, i.e. even beyond the critical point $k_\parallel = k_0$, Eq. (2.42) can be written as

$$x^2(x+\varepsilon) = \frac{\Gamma_0^2}{16\omega_0^2}, \quad x = \sqrt{\varepsilon^2 + \Gamma_T^2/(4\omega_0^2)}\ ;\ \varepsilon = \frac{k_\parallel - k_0}{k_0}\ (|\varepsilon| \lesssim \tilde{\gamma})\,. \tag{2.45}$$

Hence, the radiative width $\Gamma_T = \Gamma_T(k_\parallel)$ can be found as a real root of the cubic equation (2.42) with the r.h.s. explicitly dependent on Γ_T. Figure 2.6 shows the

radiative widths $\Gamma_T = \Gamma_T(k_\parallel)$ numerically evaluated with the self-consistent perturbation theory (dashed line). It can be clearly seen that the self-consistent perturbation theory reproduces qualitatively the exact solution for the radiative states (solid line in Fig. 2.6). In particular, for $k_\parallel = k_0$ the self-consistent perturbative Eqs. (2.44) with $\tilde{\gamma} = \Gamma_T/(2\omega_0)$ yield $\Gamma_T(k_\parallel = k_0) = (1/\sqrt[3]{2})\left(\Gamma_0^2\omega_0\right)^{1/3}$, a value by only 8% smaller than the exact one, $\Gamma_T^{(A)}$, given by Eqs. (2.37) (see points A and A' in Fig.2.6).

Within this "self-consistent" perturbative approach, the appearance of the radiative states beyond the photon cone, i.e. beyond the point C in Figs. 2.4 and 2.5 is thus clarified as due to the scattering-induced relaxation of the energy conservation law, $\omega^x_{\mathbf{k}_\parallel} \simeq \omega_0 = (c/\sqrt{\varepsilon_b})\sqrt{k_\parallel^2 + k_z^2}$, in the resonant conversion "QW exciton $\leftrightarrow$ bulk photon". This is true even for $\gamma_x = 0$, since the coherent optical decay itself relaxes the energy conservation law, putting the quasi-eigenenergies of the radiative states in the complex plane. Of course, the energy is exactly conserved in the incoming and outgoing channels of the scattering process "incoming bulk photon $\rightarrow$ QW exciton $\rightarrow$ outgoing bulk photon"). Moreover, a straightforward analysis of Eq. (2.41) shows the existence of the JDS relevant to the resonant coupling of QW excitons and bulk photons even beyond the photon cone, if γ is nonzero, and qualitatively justifies the asymptotic $\Gamma_T \propto \sqrt{k_\parallel^{(B)} - k_\parallel}$ [see Eq. (2.40)] which is valid for $k_0 < k_\parallel \leq k_\parallel^{(B)}$.

It is worth to notice that, for this strong coupling limit of QW excitons and bulk photons ($\gamma_x = 0$), the width Γ_T and Lamb shift Δ_T of the radiative states at $k_\parallel \simeq k_0$ are uniquely scaled by the control parameter $\left(\Gamma_0^2\omega_0\right)^{1/3}$ [see Eqs. (2.37)-(2.39)]. Furthermore, the maximum radiative width $\Gamma_T^{max} = \Gamma_T^{(A)}$ cannot screen completely the maximum radiative blue shift $\Delta_T^{max} = \Delta_T^{(B)}$, because the shift – half-width ratio $2\Delta_T^{max}/\Gamma_T^{max} = (2\sqrt[3]{2})/\sqrt{3} \simeq 1.5$, according to Eqs. (2.37)-(2.39). The radiative corrections can be seen experimentally for high-quality GaAs quantum wells even with a relatively small oscillator strength of QW excitons. For example, for the parameters used in these evaluations, one estimates $\left(\Gamma_0^2\omega_0\right)^{1/3} \simeq 1.46\,\text{meV}$, $\Gamma_T^{max}/2 \simeq 0.63\,\text{meV}$, and $\Delta_T^{max} \simeq 0.92\,\text{meV}$.

2.5 THERMALIZATION, DEPHASING AND DISORDER EFFECTS

With the parameters used to numerically *simulate* a standard GaAs/Al_xGa_{1-x} quantum well of about 100 $\AA$ width, the decay time τ_0 ($= \hbar/\Gamma_0$ when Γ_0 is expressed in eV) of an exciton state at $k_{||} = 0$ is about 14 ps. Such short lifetimes have been measured with time-resolved luminescence experiments under resonant excitation [83–86], in order to excite directly the $k_{||} = 0$ exciton state and avoid thermalization processes. The radiative width Γ_0 can also be evaluated from a calculation of the QW reflectivity within the non-local susceptibility scheme (see for example Refs. [4, 81]) and in this case the theory is compared with the radiative linewidth measured from reflectivity experiments [87].

In general, several effects can change the simple picture described so far. For instance, the intrinsic radiative decay of free excitons has been derived here under the assumption of the conservation of the in-plane wavevector $\mathbf{k}_{||}$, thereby neglecting the role of interface roughness and acoustic phonon scattering. The wavevector conservation is a good assumption only when the coherence length of the exciton is longer than the wavelength of the light (as it has been discussed in Section 1.5 for bulk polaritons); as a result, the short intrinsic lifetimes reported in the references previously cited, have been observed only in carefully selected samples and at low temperature. Moreover, even at low temperatures, the exciton can be bound at impurities or interface defects and the interface roughness affects the exciton motion acting as a disordered potential. In this latter case a *mobility edge* within the inhomogeneously broadened exciton line is produced [88]: below the mobility edge the exciton is localized by the disorder and above it the exciton is mobile and the roughness works as a dephasing mechanism reducing the exciton coherence length. Finally, at finite temperature, the scattering with acoustic phonons (thermalization) has to be taken into account.
In the following paragraphs, some relevant phenomena which affect the ideal exciton-photon coupling picture will be outlined.

THERMALIZATION

Thermalization processes are due to inelastic scattering with acoustic phonons [89]: the exciton wavevector changes, but the total exciton population does not. To understand the importance of this effect, one needs to compare the scattering rate with the radiative lifetime: the scattering rate by acoustic phonons has been measured to be linear with the temperature T with a coefficient $\gamma_{ap} = 5\,\mu eV/K$ for a standard QW $135\,\mathring{A}$ thick [89]. In general, thermalization processes are faster than the radiative recombination: while decaying radiatively, excitons are always thermally distributed. With this assumption, the decay rate of the luminescence is given by the thermal average of the decay rate Eq. (2.25). In this effect the two relevant characteristic energies are (i) the thermal energy $k_B T$ and (ii) the kinetic energy of the exciton that decay radiatively, $E_1 = (\hbar^2 k_0^2)/(2M_x)$, M_x being the exciton mass. With $M_x = 0.25\,m_0$, $E_1 \approx 1.1\ K$ and so, for temperatures $T \gg 1\ K$, only a tiny fraction of excitons occupy the states $k_{||} < k_0$, which radiatively decay.
By averaging the radiative widths over the Boltzmann distribution, the decay rate of the luminescence $\tau(T)$ (in the case of heavy hole excitons) is found [72] to be linearly dependent on the temperature according to

$$\tau(T) = \frac{3}{2}\frac{M_x k_B T}{\hbar^2 k_0^2}\tau_0\,, \tag{2.46}$$

where τ_0 is the radiative lifetime at $\mathbf{k}_{||} = 0$. The predicted linear increasing of the effective radiative lifetime (2.46) with temperature, much longer than the *bare* radiative lifetime at $\mathbf{k}_{||} = 0$, has been observed experimentally [90–92], even if the values can vary in a wide range according to the samples used due to the exciton localization at interface defects [74]. The case of $k_B T < E_1$ and $k_B T_0$ (T_0 is the degeneracy temperature of QW-excitons) has been analyzed in Ref. [93].

DISORDER: *dephasing* AND *scattering*

From a microscopic point of view, the origin of disorder is most commonly due to interface roughness or alloying. Phenomena related to disorder can be classified in two main classes: either they are viewed as effects of partial breakdown of temporal coherence, i.e. *dephasing*, or they account for the breakdown of spatial coherence, i.e. *scattering*.

Typical effects related to dephasing are the inhomogeneous broadening of exciton lines [94] and the induced changes of the exciton optical properties [95], the modifications of the exciton radiative lifetime [73, 74, 96]. Examples of momentum broadening due to scattering phenomena are the resonant Rayleigh scattering [88, 97, 98] and the finite risetime [85, 99–102] in the time-resolved behavior of secondary radiation.

If phenomena related to the breakdown of spatial coherence (like resonant Rayleigh scattering) are not taken into account, disorder should be thought as a static perturbation which does not induce any dephasing by itself: what disorder does produce is a (partial) exciton localization resulting in an inhomogeneous distribution (inhomogeneous broadening) of exciton energies which is responsible for interference effects in the emitted radiation after excitation of an incident pulse; this interference has been called disorder-induced dephasing [99]. Scattering sources change the in-plane exciton wavevector and induce emission in all the other directions. Thus, what it is measured in the transmission/reflection directions is the (spatially) coherent emission from exciton that have not been scattered.

During the last years several theories based on a microscopic approach for momentum scattering of QW excitons due to the interface roughness have been developed [99, 103, 104]: in these works the exciton center-of-mass motion problem is embedded in a disordered potential and solved by numerical integration. Also, semiclassical models accounting for the effect of the inhomogeneous broadening on excitons in multiple [12, 95, 105] and single [95] quantum wells have been proposed.

In the framework of the polariton picture, a theory for the exciton radiative lifetime in the presence of the homogeneous broadening has been formulated in Refs. [73, 74]. In this work, a thermal distribution for exciton states is assumed and, when the homogeneous broadening γ_h is much bigger than the kinetic energy $E_1 = (\hbar^2 k_0^2)/(2M_x)$ of excitons which decay radiatively, only states within γ_h contribute to the thermally-averaged radiative decay rate; when $\gamma_h \ll E_1$, the effect of the homogenous broadening is not important, and the result of Eq. (2.46) is recovered.

In the next Chapter the effect of the homogeneous broadening on the "bulk photons - QW exciton" interaction is investigated. In the model proposed, it is assumed that all the exciton states are equally populated and the homogeneous broadening is introduced in the polariton dispersion as an incoherent damping rate γ_x of QW excitons which is due to exciton-phonon and exciton-exciton interactions. In the fourth Chapter, a model dealing with scattering of QW excitons by random impurities

is introduced.

2.6 SUMMARY

In this Chapter the polariton picture resulting from the strong-coupling between QW-excitons and the retarded electromagnetic field has been studied. There is a basic difference between polariton effects in bulk and in confined systems like quantum wells. In fact, due to the breakdown of the translational invariance, exciton-polaritons in quantum wells are classified in radiative and non-radiative (confined) modes. The latter are stationary states and represent the analogue of bulk polaritons in quantum well structures. The main polaritonic effect in quantum wells is actually the radiative lifetime, i.e. the imaginary part of the self-energy arising in the radiative region; the intrinsic radiative lifetime of free excitons is thus explained as due to the coupling between a discrete exciton state and a continuum of bulk photons states. Such intrinsic recombination mechanism (as compared to polariton thermalization and escape in bulk crystals) is most likely one of the main reasons for the increased efficiency of free-exciton luminescence in quantum well structures as compared to bulk.

While providing a full analysis of the confined polariton modes, the standard approach based on the nonlocal susceptibility and the standard perturbation theory lacks a complete and coherent description of the radiative polariton states: within this approach the radiative lifetime broadening (for T-modes) $\Gamma_{\rm T}(k_{\|})$ shows an unphysical divergence when $k_{\|} \to k_0 = k_0(\omega_0)$, i.e. at the crossover between the exciton resonance and the photon dispersion and, at the same point, the radiative shift Δ_T to the exciton energy shows a strong discontinuity. A complete and non-perturbative description of both polariton modes is provided by the dispersion relation obtained after the diagonalization of a second-quantized Hamiltonian describing QW-excitons, bulk photons and their mutual interaction: the radiative width $\Gamma_{\rm T} = \Gamma_{\rm T}(k_{\|})$, corresponding to the imaginary part of the complex solution of the dispersion relation, does not diverge, but reaches its maximum value $\Gamma_{\rm T}^{\rm max}$ at $k_{\|} = k_0$ and then decreases to zero for $k_{\|} > k_0$; the radiative shift $\Delta_{\rm T} = \Delta_{\rm T}(k_{\|})$, related to the real part of the complex solution, does not show any discontinuity at $k_{\|} = k_0$ and even persists beyond the photon dispersion. A new energy parameter, $(\Gamma_0^2\omega_0)^{1/3}$ arises, that scales the energy corrections at $k_{\|} \simeq k_0$. In high quality quantum wells the radiative corrections $\Gamma_{\rm T}^{\rm max}$ and $\Delta_{\rm T}^{\rm max}$ can be observed experimentally.

The origin of the divergence of radiative states at $k_{||} = k_0$ has also been clarified: it can be traced back to the van Hove singularity present at that point in the joint density of states for the optical decay of the QW exciton. By introducing a small and coherent damping rate due to optical decay itself the divergence is *washed out* and a "self-consistent" perturbation theory, whose results qualitatively agree with the exact solutions of the polariton dispersion relation, has been formulated.

The ideal QW-picture is modified when effects due to thermalization, homogeneous and inhomogeneous broadening and disorder are explicitly taken into account. To some extent, this is the topic of the next Chapter.

3 Strong-weak coupling transition for QW-polaritons

In the previous Chapter the QW-polariton problem has been studied in the so called strong coupling limit, i.e. when no decoherence of the "bulk photons - QW exciton" coupling occurs. The aim of this Chapter is to study how an incoherent amount of damping γ_x affects the well-developed dispersion of both QW-polariton confined and radiative modes.

In the mean-field theory proposed here (i) the conservation of the in-plane exciton wavevector $\mathbf{k}_{||}$ is preserved and (ii) the damping rate $\gamma_x = 1/T_2$, which refers to the homogeneous broadening and stems from the exciton-phonon and exciton-exciton interactions, does not affect the orthogonality of the radiative and confined modes. It will be shown that, with increasing γ_x, both modes undergo a *phase* transition: from a strong coupling regime (where $\gamma_x = 0$) to a weak coupling one, so that the transition is attributed to a topological change of the polariton dispersion curves when the damping reaches a critical value γ_x^{tr}.

Section 3.1 deals with the analysis of the QW-polariton confined modes. Two solutions of the dispersion relation (2.36) for a non-zero damping γ_x are studied: quasi-particle solutions analyzed in the 3D space $\{k_{||}, \mathrm{Im}(\omega), \mathrm{Re}(\omega)\}$ and harmonic-forced solutions in the $\{\omega, \mathrm{Im}(k_{||}), \mathrm{Re}(k_{||})\}$ space. In both cases, with increasing γ_x, a new damping-induced (anomalous) branch relevant to the confined QW-polariton modes emerges and evolves and the crossover from the strong to the weak coupling regime is

thus attributed to the intersection of the two dispersion branches. All the characteristic points (in terms of wavevectors, frequencies and damping values) relevant to the transition, e.g. marginal points for the appearance and termination of the anomalous branch and transition points for the intersection between the two branches, are expressed in terms of the QW parameters (oscillator strength, dielectric background constant) and quantified for the realistic case of GaAs quantum well. The anomalous branch can be thought as new damping-induced channel for the optical decay of exciton states.

In Section 3.2 the question about the *real* existence of the damping-induced polariton branch is addressed. An expression for the photonic component (as signature of brightness) of the confined QW-polariton modes, is thus derived. It is shown that the anomalous polariton mode becomes optically active in the close proximity of $k_{\|} = k_0$.

Section 3.3 is devoted to the analysis of the strong-weak coupling transition for the radiative states. In this case the damping does not induce any additional radiative branch and a transition between the two regimes is explained in terms of the qualitative changes of the shape of the radiative corrections dispersions, $\Gamma_T = \Gamma_T(k_{\|})$ and $\Delta_T = \Delta_T(k_{\|})$, which occur for increasing γ_x.

3.1 ANALYSIS OF CONFINED QW POLARITON STATES

In order to study how the effective strength of exciton-photon coupling relaxes with increasing damping, the dispersion Eq. (2.36) is analyzed and solved with a nonzero excitonic damping γ_x.

Following the terminology developed by Tait [39] for bulk polaritons, two cases should be distinguished: the quasi-particle solution $\omega = \omega(k_{\|})$ (where the wavevector $k_{\|}$ is real), and the harmonic-forced solution $k_{\|} = k_{\|}(\omega)$ (where frequency ω is real). While the first geometry deals with photoluminescence (PL) experiments, the second one is relevant to optical reflectivity experiments.

THE QUASI-PARTICLE SOLUTION FOR QW POLARITONS

For confined QW polaritons (non-radiative states), the true solutions $\omega = \omega(k_{\|})$ of Eq. (2.36) have to satisfy the same conditions given for the strong-coupling case:

$$\begin{aligned} \mathrm{Re}[\kappa] &\equiv \mathrm{Re}\big[\sqrt{k_{\|}^2 - k_0^2(\omega)}\big] \geq 0\,, \\ \mathrm{Im}[\omega] &\leq 0\,. \end{aligned} \tag{3.1}$$

For small γ_{x}, there is only one dispersion branch (which will be referred to as the normal QW-polariton) which is relevant to confined QW polaritons, $\omega = \omega_1(k_{\|})$ (see the r.h.s. solid line n in Fig. 3.1), as shown in the previous Chapter (see Section 2.4) and detailed in Refs. [65, 66, 68, 76] for $\gamma_{\mathrm{x}} = 0$.

However, when the damping γ_{x} reaches a critical value $\gamma_{\mathrm{c}}^{(1)}$ a new (anomalous), second dispersion branch $\omega = \omega_2(k_{\|})$ relevant to the confined QW polaritons, emerges and develops with increasing $\gamma_{\mathrm{x}} \geq \gamma_{\mathrm{c}}^{(1)}$ (see the l.h.s. lines a in Fig. 3.1). The critical rate $\gamma_{\mathrm{c}}^{(1)}$ of incoherent scattering is given by

$$\gamma_{\mathrm{c}}^{(1)} = R_{\mathrm{QW}}\,\frac{\sqrt{\varepsilon_{\mathrm{b}}}}{\hbar c} = \Gamma_0\,, \tag{3.2}$$

i.e. is exactly equal to the intrinsic radiative Γ_{T} width of QW excitons with $\mathbf{k}_{\|} = 0$. This second dispersion branch starts at point A_{i}, which is characterized by

$$\begin{aligned} k_{\|} = k_{\|}^{\mathrm{i}} &= 0\,, \\ \mathrm{Re}[\omega_2(k_{\|}{=}0)] &= \sqrt{\omega_0^2 - \Gamma_0^2} \simeq \omega_0\,, \\ \mathrm{Im}[\omega_2(k_{\|}{=}0)] &= 0\,, \end{aligned} \tag{3.3}$$

and terminates at point A_{f}, which is given by

$$\begin{aligned} k_{\|} = k_{\|}^{\mathrm{f}}(\gamma_{\mathrm{x}} \geq \gamma_{\mathrm{c}}^{(1)}{=}\Gamma_0) &= \omega_0\frac{\sqrt{\varepsilon_{\mathrm{b}}}}{\hbar c}\sqrt{1 - \frac{\varepsilon_{\mathrm{b}} R_{\mathrm{QW}}^2}{\gamma_{\mathrm{x}}^2\hbar^2 c^2}} = k_0(\omega_0)\sqrt{1 - \left(\frac{\Gamma_0}{\gamma_{\mathrm{x}}}\right)^2}\,, \\ \mathrm{Re}[\omega_2(k_{\|}{=}k_{\|}^{\mathrm{f}})] &= \sqrt{\omega_{\mathbf{k}_{\|}}^{\mathrm{x}} - \gamma_{\mathrm{x}}^2} \simeq \omega_0 \\ \mathrm{Im}[\omega_2(k_{\|}{=}k_{\|}^{\mathrm{f}})] &= 0 \\ \mathrm{Re}[\kappa(k_{\|} = k_{\|}^{\mathrm{f}})] &= 0\,. \end{aligned} \tag{3.4}$$

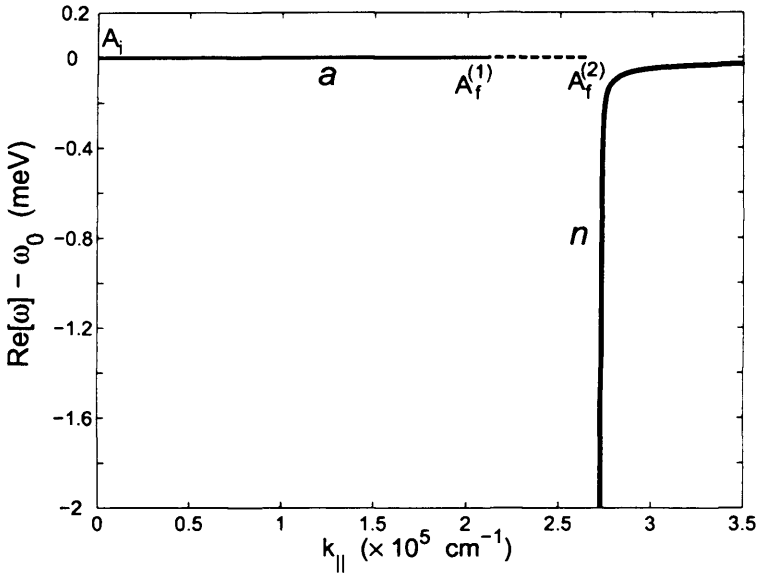

Figure 3.1: The quasi-particle dispersion branches of QW polaritons, $\mathrm{Re}[\omega] = \mathrm{Re}[\omega(k_{\|})]$, evaluated with Eq. (2.36). The solid curve n shows the normal QW polariton dispersion branch calculated for $\gamma_x = 0$. The solid (dashed) curve a refers to the anomalous, γ_x-induced QW polariton dispersion branch calculated for $\gamma_x = 70\,\mu$eV and $\gamma_x = 200\,\mu$ eV. The critical damping $\gamma_c^{(1)} = \Gamma_0 = 45.5\,\mu$eV. The parameters ω_0, R_{QW}, ε_b are the ones used in the previous Chapter to simulate a realistic GaAs QW when $\gamma_x = 0$.

At the marginal points A_i and A_f (see Fig. 3.1), which are characterized by $\mathrm{Im}[\omega_2] = 0$, the anomalous, damping-induced dispersion branch $\omega = \omega_2(k_{\|})$ appears from and leaves for the unphysical part of 3D space $\{k_{\|}, \mathrm{Im}[\omega], \mathrm{Re}[\omega]\}$. This last point is clearly understood after inspection of the dispersion relation Eq. (2.36): this non-linear relation can easily be transformed to a cubic equation, generally with complex coefficients, for $\omega^2 = \omega^2(k_{\|})$. In the strong coupling limit, $\gamma_x = 0$, the coefficients are all real and one of the roots of this equation, the one characterized by $\mathrm{Im}[\omega^2] = 0$, corresponds to the confined QW polaritons, while the second and third root are complex conjugated. Among the latter two solutions, one of the roots satisfies the selection criteria for radiative polaritons, as discussed in Section 3.3, giving rise to the radiative state, and the other one is unphysical.

For $\gamma_x \geq \gamma_c^{(1)} = \Gamma_0$, the unphysical branch changes so that it has a sector where the criteria for the confined QW polaritons (3.1) are satisfied. Similarly to the radiative states which can exist beyond the photon cone, the appearance of the second dispersion branch of QW polaritons within the photon cone is due to relaxation of

the energy conservation δ-function by the damping rate γ_x. Since $\mathrm{Re}[\omega_2] \simeq \omega_0$ (see Fig. 3.1), the anomalous dispersion branch can be interpreted in terms of a new, damping-induced optical decay channel of the exciton states that opens up and develops with increasing $\gamma_x \geq \gamma_c^{(1)}$. In this case, a QW exciton with momentum $k_\parallel < k_0$, i.e. within the photon cone, can directly emit an interface photon of the evanescent light field.

It is worth to notice that the damping-induced dispersion branches are known in plasma physics [106] and in the physics of the surface electromagnetic waves [107, 108]. Hence, the novel damping-induced polariton branch is a not completely unexpected result. Furthermore, a similar strong-weak coupling transition occurs in semiconductor photonic dots [109]; in this case, the transition is triggered by the parameters of the dot and the surrounding medium.

With increasing $\gamma_x \geq \gamma_c^{(1)}$, the two dispersion curves, $\omega_1 = \omega_1(k_\parallel)$ and $\omega_2 = \omega_2(k_\parallel)$, move in 3D space $\{k_\parallel, \mathrm{Im}[\omega], \mathrm{Re}[\omega]\}$ towards each other (see Figs. 3.2, 3.3 and 3.4). The intersection of the dispersion curves, which occurs for $\gamma_x = \gamma_x^{tr} = \gamma_c^{(2)}$, can be interpreted as a transition from a *strong* ($\gamma_x \leq \gamma_c^{(2)}$) to a *weak* ($\gamma_x \geq \gamma_c^{(2)}$) coupling limit of QW exciton – photon interaction.

According to the dispersion Eq. (2.36), there is only one intersection point [see Figs. 3.2(b), 3.3(e) and 3.4(h)], which is given by the conditions

$$\begin{aligned} \mathrm{Re}[\omega_1(k_\parallel, \gamma_x)] &= \mathrm{Re}[\omega_2(k_\parallel, \gamma_x)] , \\ \mathrm{Im}[\omega_1(k_\parallel, \gamma_x)] &= \mathrm{Im}[\omega_2(k_\parallel, \gamma_x)] . \end{aligned} \tag{3.5}$$

The conditions (3.5) define (see Appendix C) the following transition parameters:

$$\begin{aligned} \gamma_x^{tr} &= \gamma_c^{(2)} = \frac{3\sqrt{3}}{2} \left(\frac{\omega_0 R_{QW}^2 \varepsilon_b}{4c^2\hbar^2} \right)^{1/3} = \frac{3\sqrt{3}}{2\sqrt[3]{4}} \left(\Gamma_0^2 \omega_0 \right)^{1/3} \simeq 1.64 \left(\Gamma_0^2 \omega_0 \right)^{1/3} , \\ k_\parallel^{tr} &= k_0(\omega_0) \left[1 - \frac{1}{\sqrt{3}} \frac{\gamma_c^{(2)}}{\omega_0} \right] = k_0 - \frac{3}{2\sqrt[3]{4}} \frac{\sqrt{\varepsilon_b}}{\hbar c} \left(\Gamma_0^2 \omega_0 \right)^{1/3} . \end{aligned} \tag{3.6}$$

The transition point is characterized (see Appendix C) by the complex polariton

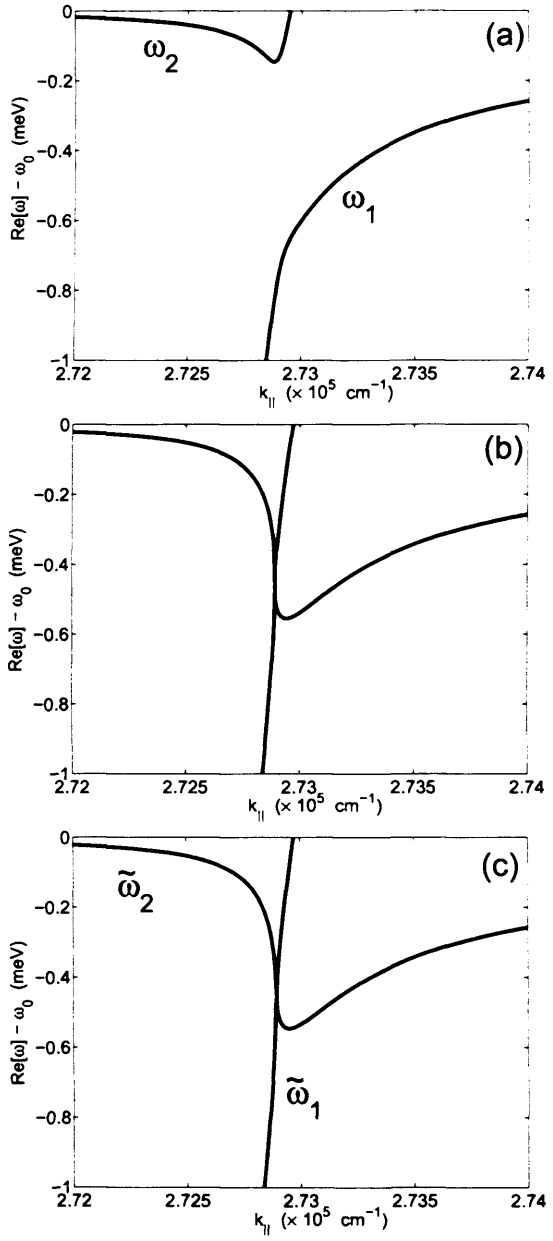

Figure 3.2: The damping-induced transition between the strong and weak coupling limits for quasi-particle confined QW polaritons. Evolution of the real part of the solution of the dispersion Eq. (2.36) $\omega = \omega(k_{||})$ parametrically dependent upon real $k_{||}$. For $R_{QW} = 0.025\,\mathrm{eV}^2\text{Å}$, the transition damping rate is given by $\gamma_x^{tr} = \gamma_c^{(2)} \simeq 2.39\,\mathrm{meV}$, according to Eqs. (3.6). (a): The strong coupling regime, $\gamma_x = 2.20\,\mathrm{meV} < \gamma_c^{(2)}$. (b): The transition point, $\gamma_x = \gamma_x^{tr} = \gamma_c^{(2)}$. (c): The weak coupling regime, $\gamma_x = 2.44\,\mathrm{meV} > \gamma_c^{(2)}$.

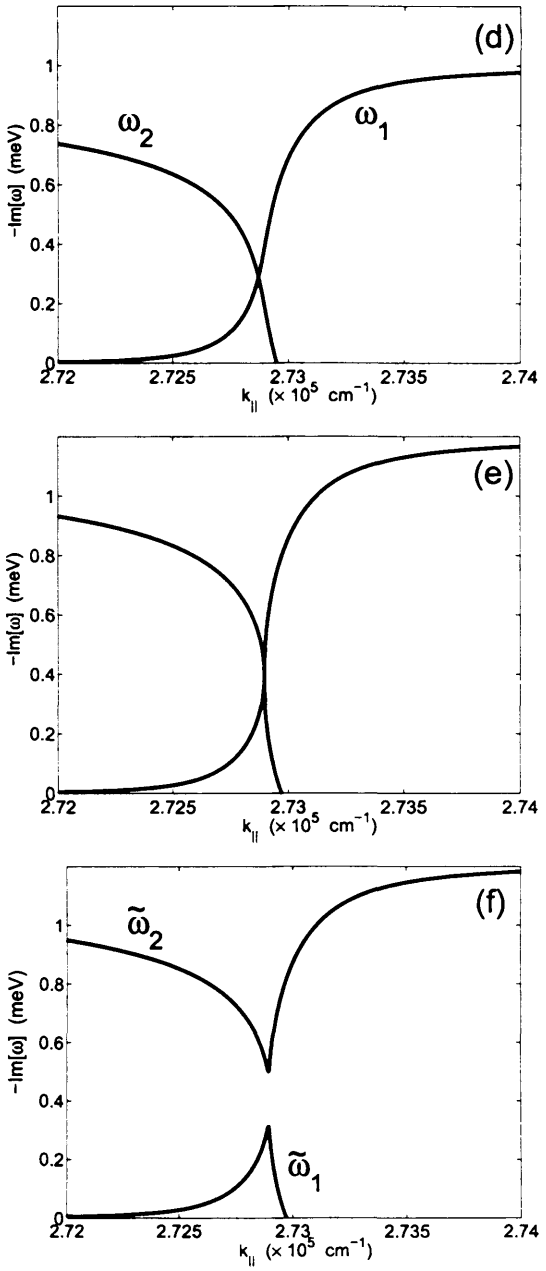

Figure 3.3: The damping-induced transition between the strong and weak coupling limits for quasi-particle confined QW polaritons. Evolution of the imaginary part of the solution of the dispersion Eq. (2.36) $\omega = \omega(k_{||})$ parametrically dependent upon real $k_{||}$. (d): The strong coupling regime, $\gamma_x = 2.20\,\text{meV} < \gamma_c^{(2)}$. (e): The transition point, $\gamma_x = \gamma_x^{tr} = \gamma_c^{(2)}$. (f): The weak coupling regime, $\gamma_x = 2.44\,\text{meV} > \gamma_c^{(2)}$.

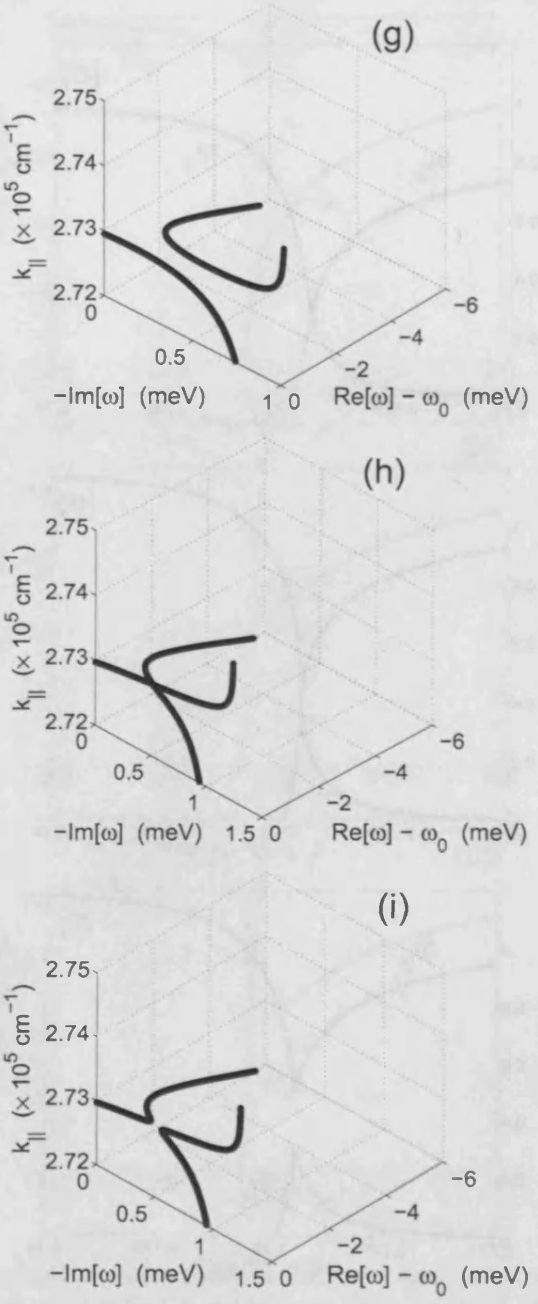

Figure 3.4: The damping-induced transition between the strong and weak coupling limits for quasi-particle confined QW polaritons. Evolution of the polariton branches in the 3D space $\{\mathrm{Re}[\omega(k_\parallel)], \mathrm{Im}[\omega(k_\parallel)], k_\parallel\}$. (g): The strong coupling regime, $\gamma_x = 2.20\,\mathrm{meV} < \gamma_c^{(2)}$. (h): The transition point, $\gamma_x = \gamma_x^{tr} = \gamma_c^{(2)}$. (i): The weak coupling regime, $\gamma_x = 2.44\,\mathrm{meV} > \gamma_c^{(2)}$.

frequency $\omega(k_{\|}^{\rm tr}) = \omega_1(k_{\|}^{\rm tr}) = \omega_2(k_{\|}^{\rm tr})$ given by

$$\begin{aligned} \Delta_{\rm T}^{\rm tr} &= {\rm Re}[\omega(k_{\|}^{\rm tr})] - \omega_0 = -\frac{1}{\sqrt[3]{4}} \left(\Gamma_0^2 \omega_0\right)^{1/3}, \\ \Gamma_{\rm T}^{\rm tr} &= -2\,{\rm Im}[\omega(k_{\|}^{\rm tr})] = \frac{2}{3}\gamma_{\rm c}^{(2)} = \frac{\sqrt{3}}{\sqrt[3]{4}} \left(\Gamma_0^2 \omega_0\right)^{1/3}. \end{aligned} \tag{3.7}$$

For the parameters used in our numerical evaluations, $\gamma_{\rm x}^{\rm tr} = \gamma_{\rm c}^{(2)} \simeq 2.39\,{\rm meV}$, $\Delta_{\rm T}^{\rm tr} \simeq -0.92\,{\rm meV}$, and $\Gamma_{\rm T}^{\rm tr} \simeq 1.59\,{\rm meV}$.

At the intersection point between two dispersion curves, when $\gamma_{\rm x} = \gamma_{\rm x}^{\rm tr}$, the interconnection between the dispersion branches changes from "anti-crossing" (strong coupling regime) to "crossing" (weak coupling regime). As a result, topologically new dispersion branches, $\tilde{\omega}_1(k_{\|})$ and $\tilde{\omega}_2(k_{\|})$, arise for $\gamma_{\rm x} > \gamma_{\rm x}^{\rm tr}$ [see Figs. 3.2(c) and 3.2(f)]. For example, for $\gamma_{\rm x} = 0$ the only QW polariton dispersion branch $\omega_1 = \omega_1(k_{\|})$ can be interpreted in terms of photon-like [$k_{\|} \lesssim k_0 = k_0(\omega_0)$] and exciton-like ($k_{\|} \gtrsim k_0$) parts ["anti-crossing" of the exciton and photon dispersions, see Fig. 3.2(a)]. In contrast, for $\gamma_{\rm x} \gtrsim \gamma_{\rm x}^{\rm tr}$, i.e. after the transition, the new dispersion branch $\tilde{\omega}_1(\mathbf{k}_{\|})$, which starts at $k_{\|} = 0$ with $\tilde{\omega}_1 = 0$ and terminates at $k_{\|} = k_{\|}^{\rm f}(\gamma_{\rm x}) \simeq k_0(\omega_0)$ [for $\gamma_{\rm x} \gg \gamma_{\rm c}^{(2)} = \gamma_{\rm x}^{\rm tr}$, Eq. (3.4) yields $k_{\|}^{\rm f} \to k_0(\omega_0)$] with $\tilde{\omega}_1 \simeq \omega_0$, can be visualized as a purely photon-like branch ["crossing" of the exciton and photon dispersions, see Fig. 3.2(c)]. In a similar way, the entire $\tilde{\omega}_2$-branch can be interpreted in terms of the exciton dispersion.

As already mentioned, the new damping-induced branch $\omega_2(k_{\|})$ is relevant to the confined QW-polariton modes. This is understood in terms of the criteria given in Eq. (3.1) and it is confirmed by the analysis of the light profile $\propto e^{-[\kappa]|z|}$ of the new branch. Figures 3.5 and 3.6 show the light profiles of both anomalous and normal confined QW polariton branches: before the transition ($\gamma_{\rm x} < \gamma_{\rm x}^{\rm tr}$), the damping-induced branch can be described in terms of a plane wave characterized by a slowly decaying envelope light field along the QW growth direction (see the solid line in Fig. 3.5). At the transition point ($\gamma_{\rm x} = \gamma_{\rm x}^{\rm tr}$), the new branch $\omega_2(k_{\|})$ is also confined and its light profile almost overlaps with the normal one $\omega_1(k_{\|})$ (see the dashed and solid lines in Fig. 3.6). Before the transition point, the damping-induced polariton mode can thus be observed by detecting its long-tail evanescent field.

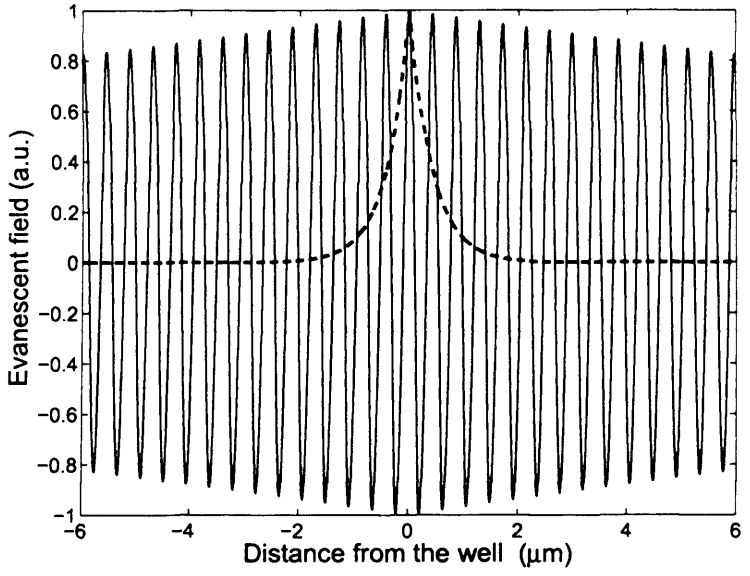

Figure 3.5: The light field profile of the QW-polariton modes at γ_x=2 meV. The dashed line refers to the normal fully confined QW-polariton mode $\omega_1(k_{||})$: the solid line refers to the damping-induced branch.

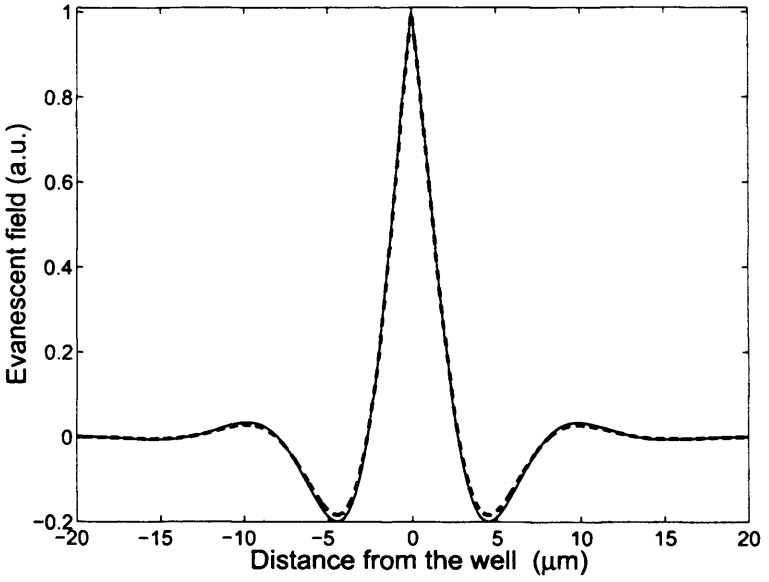

Figure 3.6: The light field profile of the confined QW-polariton modes at $\gamma_x = \gamma_x^{tr}$. Both normal and anomalous branches are fully confined at the strong-weak coupling transition.

The harmonic-forced solution for QW polaritons

For quasi-2D confined QW polaritons, the harmonic-forced solutions $k_{\|} = k_{\|}(\omega)$ of Eq. (2.36) should satisfy the following conditions:

$$\begin{aligned} \mathrm{Re}[\kappa] &\geq 0\,, \\ \mathrm{Im}[k_{\|}] &\geq 0\,. \end{aligned} \tag{3.8}$$

The second condition holds since the effective absorption coefficient (always positive) is given by $2\mathrm{Im}[k_{\|}]$.

In comparison with the quasi-particle solutions, an additional dimensionless parameter $\nu_{\mathrm{x}} = (\hbar\omega_0\varepsilon_{\mathrm{b}})/(M_{\mathrm{x}}c^2)$ is relevant to this class of solutions. The parameter ν_{x} explicitly depends on the translational mass of QW excitons, so that $\nu_{\mathrm{x}} \to 0$ for $M_{\mathrm{x}} \to \infty$. For the control parameters relevant to GaAs QWs used in this work, one estimates $\nu_{\mathrm{x}} \simeq (1.2 - 1.3) \times 10^{-4}$.

Similarly to the quasi-particle solutions, a new dispersion branch $k_{\|}^{(2)} = k_{\|}^{(2)}(\omega)$ emerges with increasing $\gamma_{\mathrm{x}} \geq \tilde{\gamma}_{\mathrm{c}}^{(1)}$. In this case, however, the critical damping $\tilde{\gamma}_{\mathrm{c}}^{(1)} = 0$, and the anomalous dispersion branch starts to develop at a point characterized by

$$\begin{aligned} k_{\|}^{\mathrm{i}} &= 0\,, \\ \omega^{\mathrm{i}} &= 0\,. \end{aligned} \tag{3.9}$$

For a given incoherent scattering rate $\gamma_{\mathrm{x}} > 0$, the terminal point A_{f}, where the γ_{x}-induced branch leaves for the unphysical part of 3D space $\{\mathrm{Im}[k_{\|}], \mathrm{Re}[k_{\|}], \omega\}$ (see Figs. 3.7 and 3.9), is characterized by the frequency

$$\omega = \omega^{\mathrm{f}}(\gamma_{\mathrm{x}}) = \frac{\omega_0}{\left[1 - \nu_{\mathrm{x}} + \nu_{\mathrm{x}}(\Gamma_0/\gamma_{\mathrm{x}})^2\right]^{1/2}}\,. \tag{3.10}$$

Equation (3.10), which is valid for $\nu_{\mathrm{x}} \ll 1$, indeed shows that $\tilde{\gamma}_{\mathrm{c}}^{(1)} = 0$ and $\omega^{\mathrm{f}} \to 0$ for $\gamma_{\mathrm{x}} \to 0$. For $\gamma_{\mathrm{x}} \gtrsim \Gamma_0$, when the frequency ω^{f} approaches ω_0 (see Fig. 3.7), Eq. (3.10) reduces to

$$\omega = \omega^{\mathrm{f}}(\gamma_{\mathrm{x}} \gtrsim \Gamma_0) = \omega_0\left[1 + \frac{\nu_{\mathrm{x}}}{2}\left[1 - \left(\frac{\Gamma_0}{\gamma_{\mathrm{x}}}\right)^2\right]\right]\,. \tag{3.11}$$

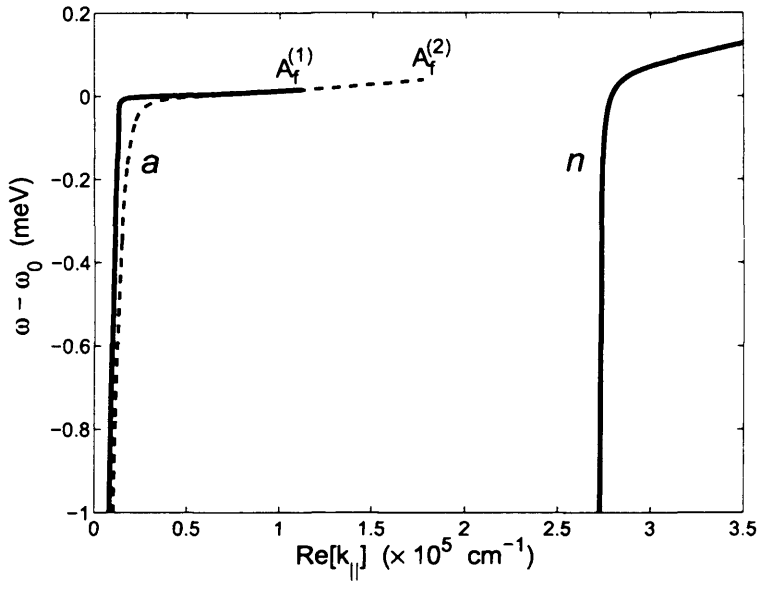

Figure 3.7: The harmonic-forced dispersion branches of confined QW polaritons, $\mathrm{Re}[k_{\|}] = \mathrm{Re}[k_{\|}(\omega)]$. The solid line n refers to the normal QW polariton dispersion branch calculated with Eq. (2.36) for $\gamma_x = 0$. The solid (dashed) line a is the anomalous, damping-induced dispersion branch of QW polaritons evaluated for $\gamma_x = 50\,\mu$eV ($\gamma_x = 60\,\mu$eV). The in-plane translational mass of QW excitons is given by $M_x = 0.3\,m_0$, where m_0 is the free electron mass.

For the terminal point A_f of the anomalous dispersion branch, which is characterized by $k_{\|}^{f} = \{\mathrm{Re}[k_{\|}(\omega^f)], \mathrm{Im}[k_{\|}(\omega^f)]\}$, one has

$$\begin{aligned} \mathrm{Im}[k_{\|}(\omega^f)] &= 0, \\ \mathrm{Re}[\kappa] &= 0. \end{aligned} \tag{3.12}$$

and Eq. (3.11) yields

$$\mathrm{Re}[k_{\|}^{(2)}(\omega^f)] = k_0\left[1 - \left(\frac{\Gamma_0}{\gamma_x}\right)^2\right]. \tag{3.13}$$

Similarly to the case of the quasi-particle solutions, the transition between the strong and weak coupling regimes of the QW exciton – photon interaction is attributed to the intersection of the two dispersion curves, $k_{\|}^{(1)}(\omega)$ and $k_{\|}^{(2)}(\omega)$, in 3D space $\{\mathrm{Im}(k_{\|}), \mathrm{Re}(k_{\|}), \omega\}$ (see Figs. 3.8 and 3.9). Thus, the topologically new dispersion branches $\tilde{k}_{\|}^{(1)}(\omega)$ and $\tilde{k}_{\|}^{(2)}(\omega)$ arise from the old ones (see Fig. 3.9), $k_{\|}^{(1)}(\omega)$ and $k_{\|}^{(2)}(\omega)$, for a damping γ_x increasing above the critical value $\gamma_x^{tr} = \tilde{\gamma}_c^{(2)}$.

The transition point is given by

$$\gamma_{\mathrm{x}}^{\mathrm{tr}} = \tilde{\gamma}_{\mathrm{c}}^{(2)} = \frac{3\sqrt{3}}{2}\left(\frac{\omega_0^2 R_{\mathrm{QW}}^2 \varepsilon_{\mathrm{b}}^2}{c^4\hbar^2 M_{\mathrm{x}}}\right)^{1/3} = \sqrt[3]{4}\,\nu_{\mathrm{x}}^{1/3}\gamma_{\mathrm{c}}^{(2)}\,, \tag{3.14}$$

$$\omega^{\mathrm{tr}} = \omega_0\left[1 + \frac{\omega_0\varepsilon_{\mathrm{b}}}{2c^2 M_{\mathrm{x}}} - \frac{2^{1/3}}{2\sqrt{3}}\frac{\tilde{\gamma}_{\mathrm{c}}^{(2)}}{\omega_0}\right]. \tag{3.15}$$

In contrast with the quasi-particle solution, for the harmonic-forced one, the transition point is thus very sensitive to the in-plane translational mass M_{x} of QW excitons: $\gamma_{\mathrm{x}}^{\mathrm{tr}} \propto M_{\mathrm{x}}^{-1/3}$, according to Eq. (3.14).

In particular, when $M_{\mathrm{x}} \to \infty$ and therefore the spatial dispersion due to excitons is removed, one has $\gamma_{\mathrm{x}}^{\mathrm{tr}} = 0$. In this case, the integrated absorption associated with the exciton-like branch, $\tilde{k}_{\parallel}^{(2)} = \tilde{k}_{\parallel}^{(2)}(\omega)$, is constant and independent of the damping rate γ_{x}:

$$\int \mathrm{Im}[\tilde{k}_{\parallel}^{(2)}(\omega)]\mathrm{d}\omega = \text{constant} \propto R_{\mathrm{QW}}\,. \tag{3.16}$$

This sum rule on the absorption coefficient is known for bulk [53] and QW excitons [95].

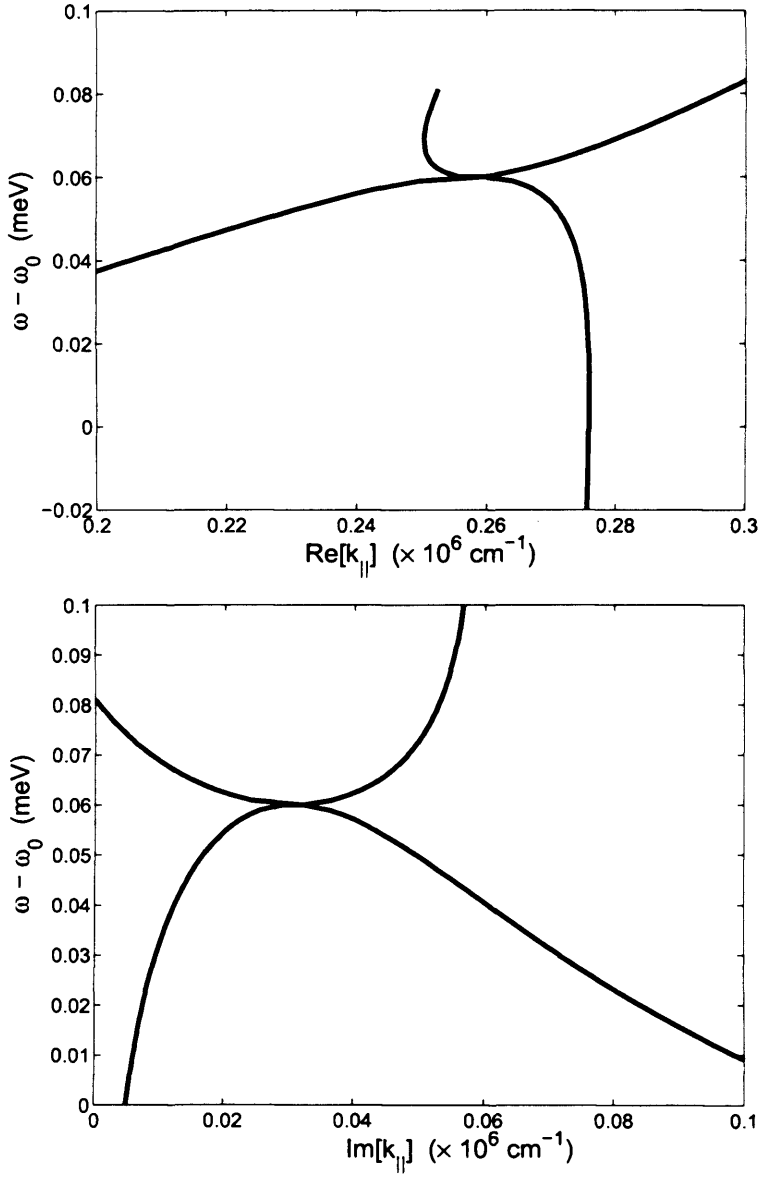

Figure 3.8: The γ_x-induced transition point between the strong and weak coupling limits for harmonic-forced confined QW polaritons. For $R_{QW} = 0.025\,\mathrm{eV}^2\,\mathring{A}$ and $M_x = 0.3\,m_0$, the critical value of the damping rate is given by $\tilde{\gamma}_c^{(2)} = 119.8\,\mu\mathrm{eV}$, according to Eq. (3.14). Top: the transition point projected in the space $\{\mathrm{Re}[k_{\|}], \omega\}$. Down: the transition point projected in the space $\{\mathrm{Im}[k_{\|}], \omega\}$.

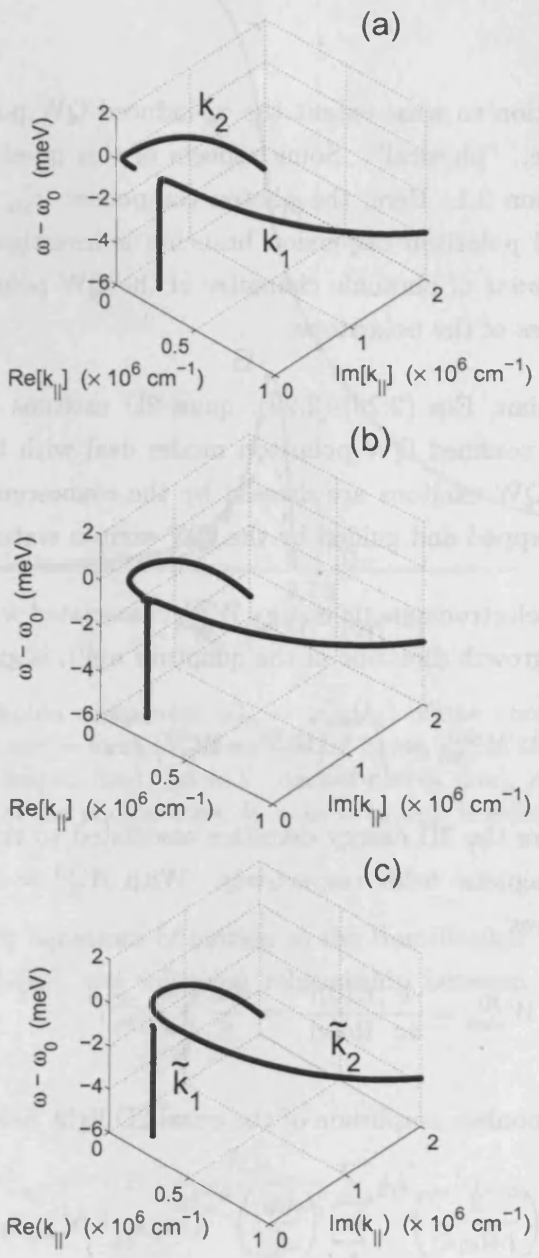

Figure 3.9: The γ_x-induced transition between the strong and weak coupling limits for harmonic-forced confined QW polaritons visualized in the 3-D space $\{\mathrm{Re}[k_\parallel], \mathrm{Im}[k_\parallel], \omega\}$. (a) The strong coupling regime, $\gamma_x < \tilde{\gamma}_c^{(2)}$, (b) the transition point, $\gamma_x = \tilde{\gamma}_c^{(2)}$, and (c) the weak coupling regime, $\gamma_x > \tilde{\gamma}_c^{(2)}$.

3.2 BRIGHTNESS OF THE DAMPING-INDUCED QW POLARITONS

One can naturally question to what extent the γ_x-induced QW polariton dispersion branch is observable, i.e. "physical". Some aspects of this question have been already discussed in Section 3.1. Here, the photon component φ_{2D}^{γ} along the normal and anomalous confined polariton dispersion branches is investigated. The photon component, i.e. the *amount* of photonic character of the QW polariton branch, is a measure of the brightness of the polaritons.

In the initial Hamiltonian, Eqs. (2.28)-(2.29), quasi-2D excitons couple with bulk photons. However, the confined QW polariton modes deal with the quasi-2D light field: in this case the QW excitons are dressed by the evanescent electromagnetic field which in turn is trapped and guided by the QW exciton states themselves.

The area-density of the electromagnetic energy W_{phot}^{2D}, associated with the evanescent light field (along the z-growth direction of the quantum well), is given by

$$W_{\text{phot}}^{2D} = \int_{-\infty}^{+\infty} \left(W_{\text{E}}^{3D} + W_{\text{H}}^{3D}\right) dz \,. \tag{3.17}$$

where W_{E}^{3D} and W_{H}^{3D} are the 3D energy densities associated to the bulk photons of the the electric and magnetic fields respectively. With $W_{\text{E}}^{3D} = W_{\text{H}}^{3D}$ and $E(z) = E(0)e^{-\text{Re}[\kappa]|z|}$, one receives

$$W_{\text{phot}}^{2D} = \frac{1}{4\pi} \frac{|E(0)|^2}{\text{Re}[\kappa]} = \frac{\hbar\omega}{S} \sum_{\mathbf{k}_\parallel} |e_{\mathbf{k}_\parallel}^{2D}|^2 \,, \tag{3.18}$$

where $e_{\mathbf{k}_\parallel}^{2D}$ is the dimensionless amplitude of the quasi-2D light field defined as

$$e_{\mathbf{k}_\parallel}^{2D} \stackrel{\text{def}}{=} i \left(\frac{2}{L\text{Re}[\kappa]}\right)^{1/2} \sum_{k_z} \left(\frac{\omega_0}{\omega_{\mathbf{k}_\parallel}^{\gamma}}\right)^{1/2} \left(\alpha_{\mathbf{k}_\parallel, k_z} + \alpha_{-\mathbf{k}_\parallel, -k_z}^{\dagger}\right) . \tag{3.19}$$

Hence, the amplitude $e_{\mathbf{k}_\parallel}^{2D}$ can also be interpreted as a combination of the creation ($\alpha_{\mathbf{k}}^{\dagger}$) and annihilation ($\alpha_{\mathbf{k}}$) operators of the quasi-2D photons. In a similar way, the dimensionless amplitude of the quasi-2D excitonic polarization is given by

$$x_{\mathbf{k}_\parallel}^{2D} \stackrel{\text{def}}{=} b_{\mathbf{k}_\parallel} - b_{-\mathbf{k}_\parallel}^{\dagger} . \tag{3.20}$$

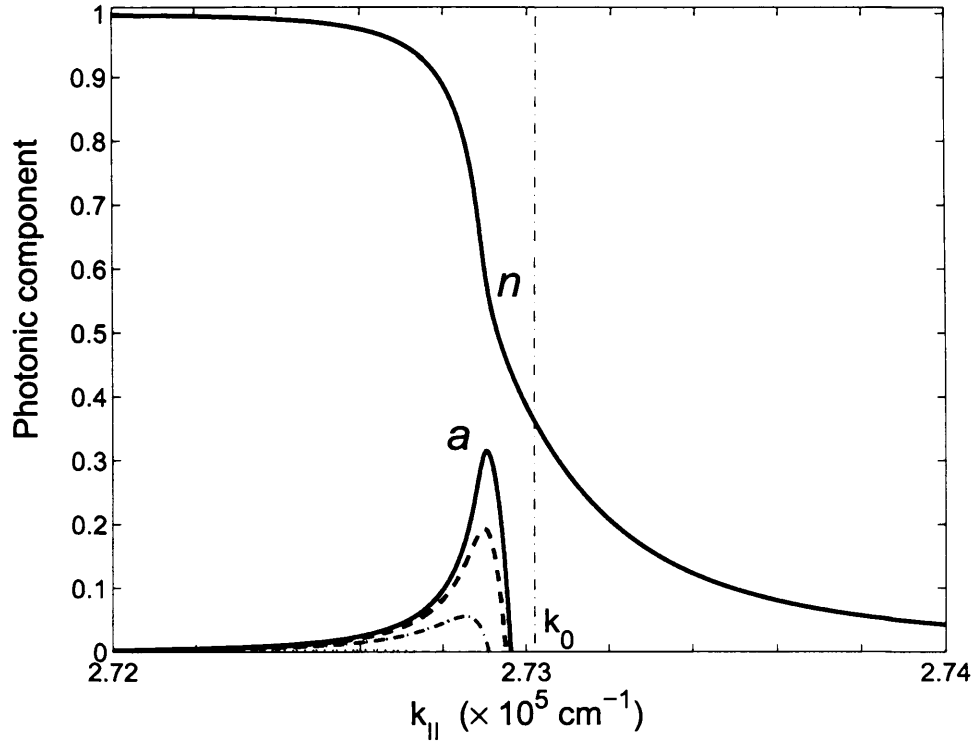

Figure 3.10: The photon component $\varphi^{\gamma}_{2D} = \varphi^{\gamma}_{2D}(k_{\|})$ of the normal and anomalous, damping-induced branches for $\gamma_x = 2.2\,\text{meV}$ (solid lines), and of the anomalous branch for $\gamma_x = 2.0\,\text{meV}$ (dashed line), 1.6 meV (dashed-dotted line), and 1.0 meV (dotted line). The position of the photon cone, $k_{\|} = k_0 = k_0(\omega_0)$, is indicated by the vertical dash-dotted line.

Applying Heinsenberg equations of motion to the Hamiltonian (2.28)-(2.29) [see Appendix A, Eq. (A.9)-(b)], the following relationship between $e^{2D}_{\mathbf{k}_{\|}}$ and $x^{2D}_{\mathbf{k}_{\|}}$ is then obtained:

$$\begin{aligned} b_{\mathbf{k}_{\|}} - b^{\dagger}_{-\mathbf{k}_{\|}} &= -2i \frac{\hbar\omega_0}{\hbar^2\omega^2 - \hbar^2\omega_0^2} \sum_{p_z} C_{\mathbf{k}_{\|},p_z}(\alpha_{\mathbf{k}_{\|},p_z} + \alpha^{\dagger}_{-\mathbf{k}_{\|},-p_z}) \\ &\Leftrightarrow \\ [\omega^2 - (\omega^{x}_{\mathbf{k}_{\|}})^2] x^{2D}_{\mathbf{k}_{\|}} &= \frac{\omega_0}{\hbar}\left(R_{QW}\mathrm{Re}[\kappa]\right)^{1/2} e^{2D}_{\mathbf{k}_{\|}} . \end{aligned} \tag{3.21}$$

The photon $\varphi^{\gamma}_{2D}(k_{\|})$ and exciton $\varphi^{x}_{2D}(k_{\|})$ components of quantum well polaritons are defined as the relative intensities of the light and polarization fields respectively and

are given by

$$\begin{aligned} \varphi_{2D}^{\gamma}(k_{\|}) &= \frac{|\tilde{e}_{\mathbf{k}_{\|}}^{2D}|^2}{|\tilde{e}_{\mathbf{k}_{\|}}^{2D}|^2 + |\tilde{x}_{\mathbf{k}_{\|}}^{2D}|^2}, \\ \varphi_{2D}^{x}(k_{\|}) &= 1 - \varphi_{2D}^{\gamma} = \frac{|\tilde{x}_{\mathbf{k}_{\|}}^{2D}|^2}{|\tilde{e}_{\mathbf{k}_{\|}}^{2D}|^2 + |\tilde{x}_{\mathbf{k}_{\|}}^{2D}|^2}. \end{aligned} \tag{3.22}$$

Here, $\tilde{e}_{\mathbf{k}_{\|}}^{2D}$ and $\tilde{x}_{\mathbf{k}_{\|}}^{2D}$ correspond to the phase-synchronous components of the electric and polarization fields which contribute to the total energy stored in the quasi-2D system.

Thus, by using Eq. (3.21) in Eqs. (3.22), the final expression for the photon component $\varphi_{2D}^{\gamma}(k_{\|})$ reads:

$$\varphi_{2D}^{\gamma}(k_{\|}) = \frac{\hbar^2 \left(\mathrm{Re}[\omega^2 - (\omega_{\mathbf{k}_{\|}}^{x})^2]\right)^2}{\omega_0^2 R_{QW} \mathrm{Re}[\kappa] + \hbar^2 \left(\mathrm{Re}[\omega^2 - (\omega_{\mathbf{k}_{\|}}^{x})^2]\right)^2}. \tag{3.23}$$

For $\gamma_x = 0$, Eq. (3.23) reduces to the known expression for the photon component along the normal confined polariton branch [37, 60, 76].

The photon component φ_{2D}^{γ} along the anomalous (a) and normal (n) QW polariton dispersion branches, calculated with Eq. (3.23) for the quasi-particle solution of the dispersion Eq. (2.36), is plotted in Fig. 3.10 for various damping rates $\gamma_x > \gamma_c^{(1)}$. It is clearly seen that, with increasing γ_x, the damping-induced QW polariton states become bright, i.e. optically-active, only in the close vicinity of $k_{\|} = k_0$ and can thus be observed experimentally.

At the crossover point $k_{\|} = k_{\|}^{tr}$ of the dispersion branches, which occurs for $\gamma_x = \gamma_x^{tr} = \gamma_c^{(2)}$ [see Eqs. (3.6)], the brightness of the anomalous and normal confined QW polariton states become equal to each other. A similar behaviour of the photon component φ_{2D}^{γ} of the QW polariton states takes place for the harmonic-forced solution $k_{\|} = k_{\|}(\omega)$ of Eq. (2.36).

3.3 THE RADIATIVE STATES OF QW POLARITONS IN THE PRESENCE OF DAMPING

The damping-induced transition between the strong and weak coupling regimes of the QW-exciton – photon interaction can also be traced for the radiative states. The modifications which occur in the radiative width $\Gamma_T = \Gamma_T(k_\parallel)$ and in the Lamb shift $\Delta_T = \Delta_T(k_\parallel)$ with increasing γ_x are shown in Figs. 3.11(a)-(b).

In this case the radiative corrections are defined as

$$\begin{aligned} \Gamma_T &= -2\mathrm{Im}[\omega] - \gamma_x \\ \Delta_T &= \mathrm{Re}[\omega] - \omega_0 \,, \end{aligned} \tag{3.24}$$

where ω is the solution of Eq. (2.36) that satisfies the following conditions:

$$\begin{aligned} \mathrm{Re}[\kappa] &\equiv \mathrm{Re}\left[\sqrt{k_\parallel^2 - k_0^2(\omega)}\right] \leq 0 \,, \\ \mathrm{Im}[\omega] &\leq 0 \,. \end{aligned} \tag{3.25}$$

The solid lines in Figs. 3.11(a)-(b) (see also the solid line in Fig. 2.4 and the upper solid line in Fig. 2.5) refer to the completely coherent case, i.e. to the strong coupling limit with $\gamma_x = 0$, when the low-energy exciton state with $k_\parallel \leq k_\parallel^{(B)}$ is dressed by outgoing bulk photons and interpreted as the radiative QW polariton. In this case, the point B (see Figs. 2.4, 2.5 and 3.11) is the terminal point of the dispersion of the radiative states.

For an arbitrary small $\gamma_x > 0$ the dispersion of radiative polaritons persists beyond the point B, where the dispersion splits into two sub-branches, as a γ_x-induced tail of the radiative states at $k_\parallel \geq k_\parallel^{(B)}$. In this case, the upper dispersion sub-branch beyond the bifurcation point B becomes unphysical, i.e. completely disappears, while the damping-induced radiative tail is associated with the lower dispersion sub-branch [see Figs. 3.11(a)-(b)]. The optical width Γ_T of the γ_x-induced radiative states at $k_\parallel \geq k_\parallel^{(B)}$ is approximated by the following expression:

$$\Gamma_T(k_\parallel > k_\parallel^{(B)}) = \Gamma_0 \left(\frac{\gamma_x}{2\omega_0}\right)\left(\frac{k_0^2}{k_\parallel^2 - k_0^2}\right)^{3/2}, \tag{3.26}$$

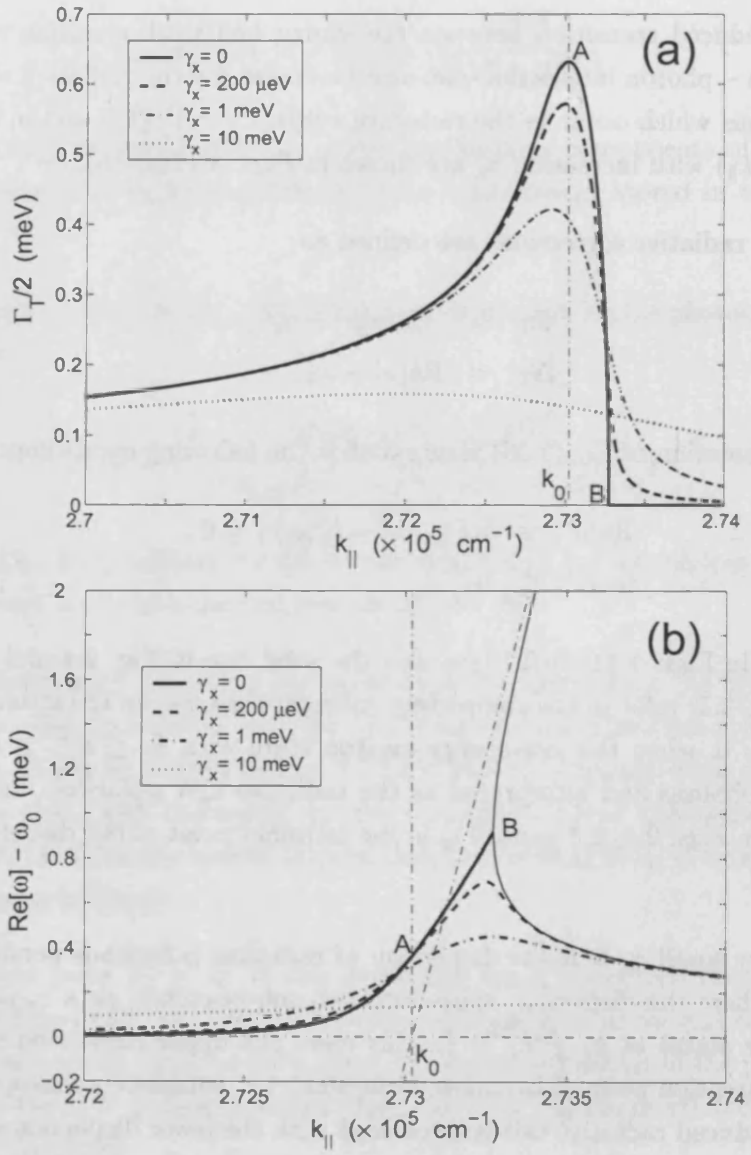

Figure 3.11: (a): the radiative half-width $\Gamma_T/2 = -\mathrm{Im}(\omega) - \gamma_x/2$ for different values of the damping rate. (b): the related corrections Lamb shifts $\Delta_T = \mathrm{Re}[\omega] - \omega_0$.

provided that $(\hbar c/\sqrt{\varepsilon_b})\sqrt{k_{||}^2 - k_0^2} \gg \gamma_x$. Equation (3.26) clearly shows the damping-induced nature of the radiative tail: $\Gamma_T\left(k_{||} > k_{||}^{(B)}\right)$ is proportional to the incoherent damping rate γ_x and therefore vanishes when $\gamma_x \to 0$. A similar γ_x-induced tail of the radiative states has also been numerically found for quasi-one-dimensional plasmon-polaritons [110].

As shown in Figs. 3.11(a)-(b), in the vicinity of the point $k_{||} = k_0$ the radiative corrections Γ_T and Δ_T effectively decrease with increasing γ_x.

At the same time, there is no damping-induced anomalous branch for the radiative states of QW excitons. Therefore, in this case, the transition between strong and weak coupling regimes of exciton-photon interaction can only be approximately quantified in terms of the γ_x-induced qualitative changes of the shape of the radiative corrections, $\Gamma_T = \Gamma_T(k_{||})$ and $\Delta_T = \Delta_T(k_{||})$, at $k_{||} \simeq k_0$ [see, e.g. the solid against dotted lines in Figs. 3.11(a)-(b)]. The drastic, qualitative changes occur when the damping rate γ_x becomes comparable with the maximum radiative corrections, $\Gamma_T^A \propto \left(\Gamma_0^2\omega_0\right)^{1/3}$ given by Eq. (2.37) and $\Delta_T^B \propto \left(\Gamma_0^2\omega_0\right)^{1/3}$ given by Eq. (2.39).

In order to attribute the transition to the critical damping $\gamma_x^{tr} = \gamma_x^{(2)} \propto \left(\Gamma_0^2\omega_0\right)^{1/3}$ defined by Eq. (3.6) for confined QW polaritons, the following criterion for the transition point has been chosen:

$$\gamma_x^{tr} = \gamma_c^{(2)} = \frac{3}{\sqrt[3]{4}}\,\Gamma_T^A \simeq 1.89\,\Gamma_T^A\,. \tag{3.27}$$

In this case, the transition occurs synchronously for both conjugated states, i.e. confined and radiative polariton modes.

3.4 ROBUSTNESS AGAINST THE INHOMOGENEOUS BROADENING

Another natural question is whether an inhomogeneous distribution of exciton energies, i.e. the inhomogeneous broadening, can effectively *screen* the incoherent damping γ_x and thus suppress the damping-induced strong-weak coupling transition.

In order to solve this problem, it is supposed that, due to the inhomogeneous broadening, the exciton resonant frequency ω_0 is described by a Lorentzian distribution. The

propagator for optically non-interacting excitons $G^{(0)}_{\mathbf{k}_\parallel}$ [see Eq. (2.33)] is thus replaced by the following function

$$\tilde{G}^{(0)}_{\mathbf{k}_\parallel} = \frac{1}{\pi}\int_{-\infty}^{+\infty} \frac{2\omega^{\mathrm{x}}_{\mathbf{k}_\parallel}}{\omega^2 - \tilde{\omega}_0^2} \frac{\gamma_{\mathrm{inh}}/2}{\gamma^2_{\mathrm{inh}}/4 + (\tilde{\omega}_0 - \omega_0)^2} \mathrm{d}\tilde{\omega}_0 \,. \tag{3.28}$$

where γ_{inh} is the inhomogeneous broadening. By analytical integration of Eq. (3.28), and for $\gamma \ll \omega_0$ (which is a reasonable assumption), one finds

$$\tilde{G}^{(0)}_{\mathbf{k}_\parallel} = \frac{2\omega^{\mathrm{x}}_{\mathbf{k}_\parallel}}{\omega^2 - (\omega^{\mathrm{x}}_{\mathbf{k}_\parallel} + i\gamma_{\mathrm{inh}}/2)^2} = \frac{2\omega^{\mathrm{x}}_{\mathbf{k}_\parallel}}{\omega^2 - [\omega^{\mathrm{x}}_{\mathbf{k}_\parallel} - i(\gamma_{\mathrm{x}}/2 - \gamma_{\mathrm{inh}}/2)]^2} \,. \tag{3.29}$$

if the incoherent damping rate γ_{x} is also included in the exciton propagator. In good quality samples it can be assumed that $\gamma_{\mathrm{inh}} \ll \gamma_{\mathrm{x}}$. Hence, the QW-polariton dispersion, i.e. the poles of Eq. (3.29), and the resulting strong-weak coupling transition are not affected by the inhomogeneous broadening.

3.5 SUMMARY

In this Chapter a mean field theory for the role of the homogeneous broadening on the "bulk photons - QW exciton" interaction which gives rise to the QW-polariton picture has been proposed. In this model, the in-plane exciton wavevector $\mathbf{k}_\parallel$ is conserved and the homogenous broadening, due to exciton-phonon and exciton-exciton interactions, has been introduced in terms of an incoherent damping rate $\gamma_{\mathrm{x}} = 1/T_2$ for the exciton states.

By analyzing the QW-polariton dispersion with a non-zero γ_{x}, it has been shown that an increasing amount of incoherent damping does not affect the orthogonality between the radiative and confined polariton modes, i.e. the two states do not mix, but induces a phase transition (for both modes) from a strong coupling regime (when $\gamma_{\mathrm{x}} = 0$) to a weak coupling one. The crossover between the two regimes is attributed to a topological change of the polariton dispersion curves which occurs when the damping reaches a critical value $\gamma_{\mathrm{x}} = \gamma^{\mathrm{tr}}_{\mathrm{x}}$.

In the case of confined QW polariton modes, a novel result has been found: when γ_{x} is above a critical threshold value, a new damping-induced (anomalous) branch of confined QW-polariton modes emerges and evolves for increasing values; the transition from the strong to the weak coupling regime is thus attributed to the intersection

between the normal and the anomalous confined branches. Very interestingly, all the characteristic points of the transition are scaled by the same *control parameter* $(\Gamma_0\omega_0^2)^{1/3}$. The analysis of the light-field profile and the photon component suggest that the γ_x-induced branch can be observed in high quality quantum wells.

The radiative states are also affected by the incoherent damping and a strong-weak coupling transition can be attributed to the drastic qualitative changes of the shape of both radiative shift and width.

Finally, it has been proved that the whole picture is *robust* against the inhomogeneous broadening.

4 Quantum well Polaritons in the presence of impurities

In the previous Chapter it has been shown that an incoherent damping rate for QW exciton states strongly modifies the dispersion of both radiative and confined modes, but does not affect their orthogonality, i.e. the two states do not mix. Here, a microscopic model dealing with scattering of QW excitons by random impurities is proposed. The work is still in progress, but preliminary results suggest that effects related to disorder like random impurities and width fluctuations, can indeed lead to finite radiative lifetimes of confined polariton states by scattering of the exciton wavevector. Hence, confined and radiative modes are no more *orthogonal* states.

The breaking of the in-plane translation symmetry - the exciton center-of-mass wavevector is no longer a good quantum number - induced by disorder has been widely investigated both theoretically and experimentally (see for example Refs. [85, 97, 111–113]), but mainly in connection with the notion of secondary emission: when a sample is excited with an electromagnetic plane wave, there is not only transmission and reflection (specular optics), but also (i) coherent emission in other directions due the elastic scattering of excitons into different center-of-mass directions and (ii) emission over different angles due to inelastic processes which redistribute excitons over different momenta.

In the model presented here, random impurities are distributed in a sample of area S and modelled in terms of delta-like scattering potential $U(\mathbf{r}-\mathbf{r}_j)$ for QW excitons, which change the in-plane exciton wavevector in both direction and modulus. In the

occupation number representation the scattering of an exciton from an initial state $|\mathbf{k}_\parallel\rangle$ to a state $|\mathbf{p}_\parallel\rangle$ due to the delta-like contact potential is given by:

$$H^j_{\rm dis} = \sum_{\mathbf{p}_\parallel,\mathbf{k}_\parallel} \langle \mathbf{p}_\parallel | U | \mathbf{k}_\parallel \rangle b^\dagger_{\mathbf{p}_\parallel} b_{\mathbf{k}_\parallel} = \sum_{\mathbf{p}_\parallel \mathbf{k}_\parallel} \frac{M}{\sqrt{S}} b^\dagger_{\mathbf{p}_\parallel} b_{\mathbf{k}_\parallel} e^{i(\mathbf{p}_\parallel - \mathbf{k}_\parallel)\cdot\vec{r}_j} \,. \tag{4.1}$$

where $\vec{r}_j$ is the in-plane coordinate of the j-impurity in a sample of area S, M is the matrix element of the scattering process, here assumed constant and a plane-wave basis $\{e^{i\mathbf{k}_\parallel\cdot\vec{r}_\parallel}\}$ has been used.

The total Hamiltonian describing optically dressed QW-excitons and exciton-scattering induced by N random impurities is thus given by

$$\begin{aligned} H &= \sum_{\mathbf{p}} \hbar\omega^\gamma_{\mathbf{p}} \alpha^\dagger_{\mathbf{p}} \alpha_{\mathbf{p}} + \sum_{\mathbf{p}_\parallel} \hbar\omega^x_{\mathbf{p}_\parallel} b^\dagger_{\mathbf{p}_\parallel} b_{\mathbf{p}_\parallel} + \sum_{\mathbf{p}_\parallel, p_z} i\frac{\Omega_c}{2} \left(\alpha_{\mathbf{p}_\parallel, p_z} b^\dagger_{\mathbf{p}_\parallel} - b_{\mathbf{p}_\parallel} \alpha^\dagger_{\mathbf{p}_\parallel, p_z} \right) \\ &+ \sum_{\mathbf{p}_\parallel,\mathbf{k}_\parallel} \sum_{j=1}^{N} \frac{M}{\sqrt{S}} b^\dagger_{\mathbf{p}_\parallel} b_{\mathbf{k}_\parallel} e^{i(\mathbf{p}_\parallel - \mathbf{k}_\parallel)\mathbf{r}_j} \,, \end{aligned} \tag{4.2}$$

where, in the first line, the unperturbed QW-polariton Hamiltonian has been written in the resonant approximation and the effective exciton-photon coupling Ω_c is given by:

$$\Omega_c = \sqrt{\frac{2R_{\rm QW}\omega_0}{L\omega^\gamma_{\mathbf{k}}}} \,. \tag{4.3}$$

Applying Heisenberg equations of motion to the Hamiltonian (4.2) yields:

$$(\omega - \omega_0 + \frac{\alpha\omega_0}{\sqrt{k^2_\parallel - k^2_0(\omega)}}) b_{\mathbf{k}_\parallel} - \frac{M}{\sqrt{S}} \sum_{\mathbf{p}_\parallel} \sum_{j=1}^{N} e^{i(\mathbf{p}_\parallel - \mathbf{k}_\parallel)\vec{r}_j} b_{\mathbf{p}_\parallel} = 0 \tag{4.4}$$

If scattering process by impurities are disregarded, Eq. (4.4) describes the standard QW-polariton problem (in the resonant approximation). In this case, the dispersions of the radiative shift $\Delta = \Delta_{\rm T}(k_\parallel)$ and the radiative linewidth $\Gamma_{\rm T} = \Gamma_{\rm T}(k_\parallel)$ have already been analyzed and shown in the second Chapter (see Figs 2.4 and 2.5). Figure 4.1 shows the same solutions, $\omega = \omega(k_\parallel) = {\rm Re}[\omega] + i{\rm Im}[\omega] = {\rm Re}[\omega] - i\Gamma_{\rm T}/2$.

projected in the complex plane $\{\mathrm{Re}[\omega], \mathrm{Im}[\omega]\}$ for a given set of in-plane wavevectors $k_\parallel$. By visualizing the solutions in the complex plane, the difference between radiative and confined polariton modes naturally arises: confined modes, characterized by an infinite lifetime $\tau = 1/\Gamma_T$ and therefore by an imaginary part $\mathrm{Im}[\omega]$ of the complex solutions equal to zero, correspond to the red points lying on the real axis of the complex plane; radiative modes have a finite lifetime and their dispersion is shown by the blue points which describe both radiative shifts and radiative widths.

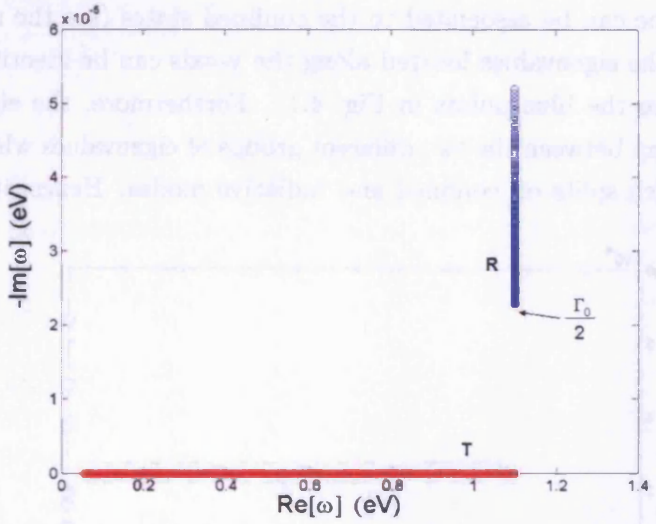

Figure 4.1: Solutions of the polariton dispersion projected in the complex plane $\{\mathrm{Re}[\omega], \mathrm{Im}[\omega]\}$. The red branch corresponds to the confined (trapped) modes; the almost vertical blue branch describes the radiative modes characterized by small radiative shifts and finite radiative widths. The intrinsic half-radiative width $\Gamma_T(k_\parallel = k_0)/2 = -\mathrm{Im}[\omega(k_\parallel = k_0)]$ is also shown. The calculations refer to $\hbar\omega_0 = 1.1$ eV.

If scattering induces a radiative lifetime for the confined modes, the corresponding solutions will be *lifted up* from the real axis of the complex plane by a non-zero imaginary part since $\Gamma_T/2 = -\mathrm{Im}[\omega]$.

In order to observe such "gap-filling" effect, i.e. the mixing of radiative and non-radiative modes, one needs to find the true eigenstates of the Hamiltonian "unperturbed polariton + scattering terms", i.e. to solve the set of equations (4.4) for a given set of $\{\mathbf{k}_\parallel\}$ wavevectors and for all the scattered wavevectors $\mathbf{p}_\parallel \neq \mathbf{k}_\parallel$. Hence, a discretization for the in-plane wavevector space is needed. However, from the numerical (and computational) point of view this problem is very complicated.

Alternatively, one can find the true eigenstates in a statistical fashion. This procedure is still under investigation. Nevertheless, some interesting results have already been obtained. The analysis starts from the following observation: when in the set of equations (4.4) the disorder term is disregarded, the eigenspectrum evaluated for a given $\tilde{\omega}$ - $\tilde{\omega}$ is now a fixed parameter for the system (4.4) - reveals the same *dynamics* of the true solutions of the polariton dispersion. Figure 4.2 shows the complex eigenvalues λ of (4.4) evaluated with the same set of wavevectors used to find the true polariton solutions $\omega = \omega(k_{\|})$ depicted in Fig. 4.1. The eigenvalues located on the real axis of the complex plane can be associated to the confined states (see the red points in Fig. 4.1), whereas the eigenvalues located along the y-axis can be identified with the radiative modes (see the blue points in Fig. 4.1). Furthermore, the eigenspectrum exhibits a *pseudo* gap between the two different groups of eigenvalues which is similar to the real gap which splits off confined and radiative modes. Hence, it is expected

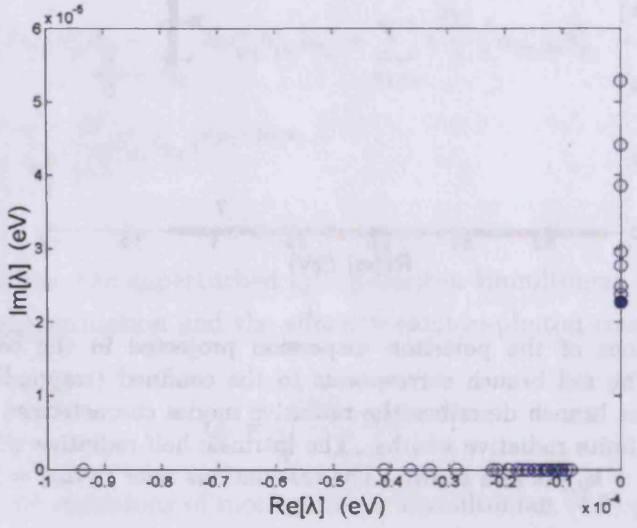

Figure 4.2: Eigenspectrum of the system (4.4) evaluated for a frequency $\tilde{\omega} = \omega_0$

that the evolution of the true eigenstates in the complex plane $\{\mathrm{Re}[\omega], \mathrm{Im}[\omega]\}$ has a counterpart in the eigenspectrum. When the real gap between radiative and confined modes will close up, so it will the pseudo gap of the eigenspectrum.

The effective strength of the disorder-process can be expressed in terms of the parameter $(N|M|^2)/S$ and its intensity must be compared to the effective exciton-photon coupling given[1] by $R_{\mathrm{QW}}k_0$. A regime of a weak disorder is defined by $(N|M|^2)/S \ll R_{\mathrm{QW}}k_0$.

[1]This choice is not unique.

Figure 4.3 shows the eigenspectra of the system (4.4) evaluated for $\tilde{\omega} = \omega_0$ (for a 225 values set of $\{\mathbf{k}_\parallel\}$ wavevectors), after 100 different random arrangements of 100 impurities in a sample of $1\mu m^2$ for three increasing values of the disorder strength. It can be clearly seen that for increasing disorder the pseudo-gap starts the close up. It is worth to stress that this result should be interpreted only as a signature of the mixing between confined and radiative polariton states. Further investigations are needed in order to correctly relate the eigenspectrum to the true eigenstates of the *disordered* Hamiltonian and are still in progress.

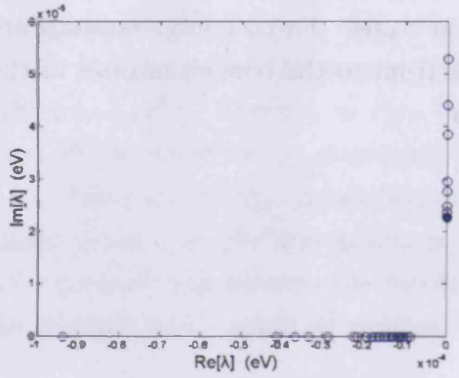

(a) Eigenspectrum without disorder.

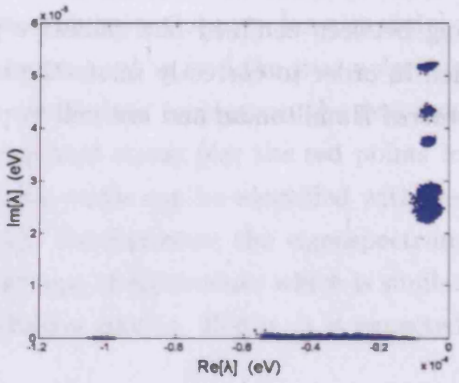

(b) $\frac{N|M|^2}{S} = 10^{-13}$ eV^2

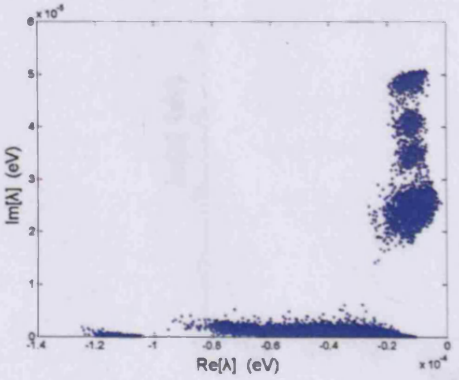

(c) $\frac{N|M|^2}{S} = 2 \times 10^{-12}$ eV^2

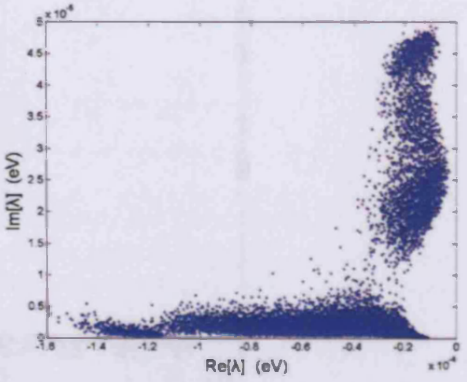

(d) $\frac{N|M|^2}{S} = 5 \times 10^{-12}$ eV^2

Figure 4.3: Evolution of the eigenspectra of the Hamiltonian (4.2) for (a) no scattering terms included and (b),(c),(d) with an increasing strength of the scattering process. The eigenvalues have been calculated for $\tilde{\omega} = \omega_0$, $R_{\mathrm{QW}} k_0 = 10^{-4}$ eV^2.

5 CONCLUSIONS

In this thesis the properties of exciton-polaritons in quantum wells were theoretically investigated. The main aim of this research work was two-fold:

- To provide a complete and definitive picture for the polariton effect in quantum wells in the so called *strong coupling limit*, i.e. when no decoherence of the "QW exciton - photon" coupling occurs.
- To investigate the modifications which occur in the polariton picture when an incoherent damping-rate for QW exciton states is taken into account.

The first task has been explored in the second Chapter. The main polariton effect in quantum wells is the intrinsic decay mechanism for radiative excitons due to coupling of a discrete exciton state with a continuum of bulk photon states, i.e. the *radiative* polariton modes. The other states resulting from the exciton-photon interaction cannot couple to incident light propagating along the QW growth direction and are called *non-radiative* (or confined) polaritons and, in this sense, they stand as the analog of the (stationary) bulk polaritons. QW-polaritons are classified in terms of $L-$, $Z-$ and $T-$ modes according to the orientation of the polarization vector with respect to the in-plane exciton wavevector $\mathbf{k}_{\|}$; this work has been focused on the $T-$ modes, i.e. transverse QW excitons interacting with the in-plane TE-polarized light field, since they represent the most interesting case for GaAs QWs which have been chosen here for numerically modeling. Both polariton modes are described by the dispersions of the radiative shift $\Delta_{\mathrm{T}} = \Delta_{\mathrm{T}}(k_{\|})$ (the correction to the exciton energy induced by the interaction with the electromagnetic field) and of the radiative lifetime $\Gamma_{\mathrm{T}} = \Gamma_{\mathrm{T}}(k_{\|})$,

this latter being zero for the non-radiative trapped polaritons characterized by an *infinite* decay time $\tau = 1/\Gamma_T$.

In the standard approach the radiative width $\Gamma_T = \Gamma_T(k_\parallel)$ is calculated by Fermi's Golden Rule and yields an unphysical divergence at the crossover $k_\parallel = k_0 [= k_0(\omega_0)]$ between the excitonic resonance and photon dispersion. As a consequence, the dispersion of the radiative shift discontinuously terminates at the same point. It has been proved that such anomalies in the dispersion of the radiative states disappear if one analyzes the exciton-photon coupling non perturbatively. This has been done by using a microscopic approach: a second quantized form of the Hamiltonian describing the system "QW exciton - bulk photons" and their interaction (with both resonant and non resonant terms) has been set up. By applying the diagrammatic technique or by the straightforward diagonalization of the Hamiltonian, a dispersion relation $\omega = \omega(k_\parallel) [= (\Delta_T(k_\parallel) + \omega_0) - i\Gamma_T(k_\parallel)/2]$ describing both conjugate states has been derived. The radiative width, found solving numerically the dispersion relation, does not diverge at point $k_\parallel = k_0$, but rather attains its maximum value Γ_T^{max}. Also, the related radiative shift $\Delta_T(k_\parallel)$ is no more discontinuous at $k_\parallel = k_0$ and reaches its maximum value Δ_T^{max} beyond the photon cone, at the point where $\Gamma_T = 0$ drops to zero.

Furthermore, the origin of the divergence which arises within the perturbative approach has been clarified as due to a 1D van Hove singularity which occurs at $k_\parallel = k_0$ in the joint density of states (JDS) for the optical decay of QW-excitons. It has been shown that the divergence can be removed if one introduces a scattering rate for QW excitons in the JDS. Moreover, in the completely coherent interaction of QW excitons with bulk photons, the radiative width $\Gamma_T(k_\parallel)$ calculated with the JDS qualitatively agree with the exact solutions of the dispersion relation. In this case the divergence is relaxed and removed by the very optical decay of QW excitons into the bulk photon modes.

The radiative corrections Δ_T^{max} and Γ_T^{max} can be experimentally observed in high-quality GaAs quantum wells even with a relatively small oscillator strength of QW excitons: for the parameters used in the numerical evaluation, for example, one estimates that the shift -half-width ratio $2\Delta_T^{max}/\Gamma_T^{max} \simeq 1.5$ and thus the maximum shift cannot be completely screened by the maximum radiative width.

In the third Chapter, the effects of an incoherent damping rate γ_x for the exciton states on the well developed QW polariton pictures have been studied. In the model here

proposed, the wavevector conservation is preserved and the damping rate $\gamma_x = 1/T_2$ which corresponds to the homogeneous broadening, originates from exciton-phonon and exciton-exciton interactions. In order to study the relaxation of the effective strength of the exciton-photon coupling with increasing damping, the dispersion relation derived by the diagonalization of the Hamiltonian has been solved with a nonzero excitonic damping γ_x. It has been shown that an increasing damping does not affect the orthogonality between the radiative and non-radiative polariton modes, i.e. the two states do not mix, but induces a *phase transition* (for both modes) from a strong coupling regime (when $\gamma_x = 0$) to a weak coupling one. The crossover between the two regimes is attributed to a topological change of the polariton dispersion curves which occurs when the damping reaches a critical value $\gamma_x = \gamma_x^{tr}$.

For the non-radiative QW-polariton modes, two solutions (related to two different experimental geometries) have been studied: the quasi-particle solutions analyzed in the 3D space $\{\omega, \mathrm{Im}(k_\parallel), \mathrm{Re}(k_\parallel)\}$ and the harmonic-forced solutions in the $\{k_\parallel, \mathrm{Im}(\omega), \mathrm{Re}(\omega)\}$ space. In both cases a novel polariton effect has been found: for increasing damping values, a new γ_x-induced polariton branch (called anomalous) relevant to the confined modes emerges and evolves; the strong-weak coupling transition is thus attributed to the intersection between the normal and anomalous polariton branches. The appearance of a second dispersion branch of confined QW polaritons is explained as due to the relaxation of the energy conservation δ-function by the damping rate γ_x.

The quasi particle solution is particularly interesting: in this case the dispersion of the anomalous branch, which lies within the photon cone, is very close to the exciton resonance and can thus be thought as a new optical decay channel of the exciton states that opens up and develops with increasing damping. In the overdamped ($\gamma_x > \gamma_x^{tr}$) regime, the polariton effect, i.e. a coherent superposition of the exciton and photon states, is completely lost, since the anomalous branch can be interpreted in terms of an excitonic dispersion, while the normal (old) polariton mode is almost photon-like. The analysis of the photon component shows that the damping-induced branch indeed can be observed.

For what concerns the radiative states, the incoherent damping rate does not induce any anomalous radiative branch. In this case the transition between strong and weak coupling regimes has been approximately quantified in terms of the damping-induced qualitative changes in the shape of the radiative corrections $\Delta_T(k_\parallel)$ and

$\Gamma_T(k_\parallel)$; drastic, qualitative changes have been shown to take place when the damping rate γ_x becomes comparable with the maximum radiative corrections Δ_T^{max} and Γ_T^{max}.

The overall picture of the strong-weak coupling transition is robust against the effect of the inhomogeneous broadening.

In the last Chapter a microscopic theory for momentum scattering of exciton states by impurities has been presented. The model proposed has been formulated in terms of a quadratic Hamiltonian for interacting QW excitons, bulk photons and localised impurities. Preliminary results suggest that with increasing disorder, the radiative and confined polariton modes start to mix.

A Diagonalization of the "QW-exciton - bulk photon" Hamiltonian

The starting point is the Hamiltonian density for the interaction between the 2-dimensional excitons and the light field, which is given by:

$$\mathcal{H} = 2\pi v^2 \vec{\rho}_{\mathbf{A}}^2 + \frac{1}{8\pi}(\nabla \times \mathbf{A})^2 + \frac{L}{2\tilde{\beta}}\mathbf{P}^2 + \frac{\omega_0^2 \tilde{\beta}}{2}\delta(z)\left(\vec{\rho}_{\mathbf{P}} - \frac{1}{c}\mathbf{A}^2\right)^2 , \tag{A.1}$$

where $\mathbf{P}$ and $\mathbf{A}$ are the polarization density and the potential vector field, respectively ($\vec{\rho}_{\mathbf{A}}$, $\vec{\rho}_{\mathbf{P}}$ are the corresponding conjugate momenta), $\tilde{\beta}$ is the two-dimensional polarizability, L is the quantization length, ω_0 is the exciton resonance frequency and $v = c/\sqrt{\bar{\varepsilon}_b}$. A second-quantization form for $\mathbf{A}$ and $\mathbf{P}$ is given by:

$$\begin{aligned} \mathbf{P} &= \sum_{\mathbf{k}_\parallel} \frac{1}{L}\left(\frac{\hbar\tilde{\beta}\omega_0}{2S}\right)^{1/2} e^{i\mathbf{k}_\parallel\cdot\mathbf{r}_\parallel}(b_{\mathbf{k}_\parallel} + b^\dagger_{-\mathbf{k}_\parallel}) , \\ \mathbf{A} &= \sum_{k} \left(\frac{2\pi\hbar v}{V|\mathbf{k}|}\right)^{1/2} \hat{\epsilon}_k e^{i\mathbf{k}\cdot\mathbf{r}}(\alpha_{\mathbf{k}} - \alpha^\dagger_{-\mathbf{k}}) , \end{aligned} \tag{A.2}$$

where $V = SL$ is the quantization volume, $\alpha_{\mathbf{k}}$, $b_{\mathbf{k}_\parallel}$ are the boson operators for bulk photons and quasi-2D excitons, respectively; $\mathbf{k} = \{\mathbf{k}_\parallel, k_z\}$ and the in plane wavevector $\mathbf{k}_\parallel$ is the good quantum number (translational invariance).

The Hamiltonian H is obtained by integrating the density $\mathcal{H}$ over the volume V. The final result is the following:

$$H = H_\gamma + H_x + H_i^{\mathrm{I}} + H_i^{\mathrm{II}} , \tag{A.3}$$

with

$$\begin{aligned} H_\gamma &= \sum_{\mathbf{k}} \hbar\omega^\gamma_{\mathbf{k}} \alpha^\dagger_{\mathbf{k}} \alpha_{\mathbf{k}} \,. \\ H_x &= \sum_{\mathbf{k}_\parallel} \hbar\omega^{\mathrm{x}}_{\mathbf{k}_\parallel} b^\dagger_{\mathbf{k}_\parallel} b_{\mathbf{k}_\parallel} \,, \\ H^{\mathrm{I}}_i &= i \sum_{\mathbf{k}_\parallel} \sum_{k_z} C_{\mathbf{k}_\parallel, k_z} (\alpha_{\mathbf{k}_\parallel, k_z} + \alpha^\dagger_{-\mathbf{k}_\parallel, -k_z})(b_{-\mathbf{k}_\parallel} - b^\dagger_{\mathbf{k}_\parallel}) \,. \\ H^{\mathrm{II}}_i &= \frac{1}{\hbar\omega^{\mathrm{x}}_{\mathbf{k}_\parallel}} \sum_{\mathbf{k}_\parallel} \sum_{k_z, k'_z} C_{\mathbf{k}_\parallel, k_z} C_{\mathbf{k}_\parallel, k'_z} (\alpha_{\mathbf{k}_\parallel, k_z} + \alpha^\dagger_{-\mathbf{k}_\parallel, -k_z})(\alpha_{-\mathbf{k}_\parallel, -k'_z} + \alpha^\dagger_{\mathbf{k}_\parallel, k'_z}) \,, \end{aligned} \tag{A.4}$$

where $\omega^\gamma_{\mathbf{k}}$, $\omega^{\mathrm{x}}_{\mathbf{k}_\parallel}$ are the photon and exciton dispersions, respectively. The coupling constant $C_{\mathbf{k}_\parallel, k_z}$ (having the dimensions of an energy) is expressed in terms of the dimensional oscillator strength per QW unit area R_{QW} and the quantization length L as

$$C_{\mathbf{k}_\parallel, k_z} = \sqrt{\frac{R_{\mathrm{QW}}\omega_0}{2L\omega^\gamma_{\mathbf{k}}}} \,. \tag{A.5}$$

Heisenberg's equations of motion

$$i\hbar \frac{\partial}{\partial t} \hat{A} = [\hat{A}, H] \,, \tag{A.6}$$

where $\hat{A} = \hat{A}(0)e^{-i\omega t}$ is a generic boson operator, are applied to the operators $\alpha_{\mathbf{k}}, \alpha^\dagger_{\mathbf{k}}, b_{\mathbf{k}_\parallel}, b^\dagger_{\mathbf{k}_\parallel}$. By using the standard commutation rules for boson operators, i.e. $[\hat{A}_\lambda, \hat{A}^\dagger_{\lambda'}] = \delta_{\lambda,\lambda'}$, one gets:

$$\begin{cases} \hbar\omega\alpha_{\mathbf{k}} = & \hbar\omega^\gamma_{\mathbf{k}} \alpha_{\mathbf{k}} + iC_{k_\parallel, k_z}(b_{\mathbf{k}_\parallel} - b^\dagger_{-\mathbf{k}_\parallel}) + 2\dfrac{C_{\mathbf{k}_\parallel, k_z}}{\hbar\omega_0} \displaystyle\sum_{p_z} C_{\mathbf{k}_\parallel, p_z}(\alpha_{\mathbf{k}_\parallel, p_z} + \alpha^\dagger_{-\mathbf{k}_\parallel, -p_z}) \,, \\ \hbar\omega\alpha^\dagger_{-\mathbf{k}} = & -\hbar\omega^\gamma_{\mathbf{k}} \alpha^\dagger_{-\mathbf{k}} + iC_{k_\parallel, k_z}(b^\dagger_{-\mathbf{k}_\parallel} - b_{\mathbf{k}_\parallel}) - 2\dfrac{C_{\mathbf{k}_\parallel, k_z}}{\hbar\omega_0} \displaystyle\sum_{p_z} C_{\mathbf{k}_\parallel, p_z}(\alpha_{\mathbf{k}_\parallel, p_z} + \alpha^\dagger_{-\mathbf{k}_\parallel, -p_z}) \,. \\ \hbar\omega b_{\mathbf{k}_\parallel} = & \hbar\omega_0 b_{\mathbf{k}_\parallel} - i \displaystyle\sum_{p_z} C_{\mathbf{k}_\parallel, p_z}(\alpha_{\mathbf{k}_\parallel, p_z} + \alpha^\dagger_{-\mathbf{k}_\parallel, -p_z}) \,, \\ \hbar\omega b^\dagger_{-\mathbf{k}_\parallel} = & -\hbar\omega_0 b^\dagger_{-\mathbf{k}_\parallel} - i \displaystyle\sum_{p_z} C_{\mathbf{k}_\parallel, p_z}(\alpha_{\mathbf{k}_\parallel, p_z} + \alpha^\dagger_{-\mathbf{k}_\parallel, -p_z}) \,. \end{cases} \tag{A.7}$$

Applying two times the Heisenberg's equation to the operators $\alpha_{\mathbf{k}}$ and $b_{\mathbf{k}_\parallel}$ yields:

$$\begin{aligned} -\hbar^2 \frac{\partial^2}{\partial t^2} \alpha_{\mathbf{k}} &= \Big[[\alpha_{\mathbf{k}}, H], H \Big], \\ -\hbar^2 \frac{\partial^2}{\partial t^2} b_{\mathbf{k}_\parallel} &= \Big[\Big[b_{\mathbf{k}_\parallel}, H \Big], H \Big]. \end{aligned} \tag{A.8}$$

Using the results provided by Eqs. (A.7) and adding to each equation of the set (A.8) its complex conjugate, the following set of coupled equations is obtained:

$$\begin{cases} \alpha_{\mathbf{k}} + \alpha^\dagger_{-\mathbf{k}} = 2i \dfrac{\hbar \omega^\gamma_{\mathbf{k}} C_{\mathbf{k}_\parallel, k_z} \hbar^2 \omega^2}{\hbar^2 \omega_0^2 \left[\hbar^2 \omega^2 - \hbar^2 (\omega^\gamma_{\mathbf{k}})^2 \right]} (b_{\mathbf{k}_\parallel} - b^\dagger_{-\mathbf{k}_\parallel}), & \text{(a)} \\ b_{\mathbf{k}_\parallel} - b^\dagger_{-\mathbf{k}_\parallel} = -2i \dfrac{\hbar \omega_0}{\hbar^2 \omega^2 - \hbar^2 \omega_0^2} \displaystyle\sum_{p_z} C_{\mathbf{k}_\parallel, p_z} (\alpha_{\mathbf{k}_\parallel, p_z} + \alpha^\dagger_{-\mathbf{k}_\parallel, -p_z}). & \text{(b)} \end{cases} \tag{A.9}$$

Coupling of the above two equations yields:

$$\alpha_{\mathbf{k}_\parallel, p_z} + \alpha^\dagger_{-\mathbf{k}_\parallel, -p_z} = \frac{4 \hbar \omega_0 \hbar \omega^\gamma_{\mathbf{k}} C_{\mathbf{k}_\parallel, k_z} \hbar^2 \omega^2}{\hbar^2 \omega_0^2 [\hbar^2 \omega^2 - \hbar^2 (\omega^\gamma_{\mathbf{k}})^2]} \sum_{p_z} C_{\mathbf{k}_\parallel, p_z} (\alpha_{\mathbf{k}_\parallel, p_z} + \alpha^\dagger_{-\mathbf{k}_\parallel, -p_z}). \tag{A.10}$$

Multiplying each side by $C_{\mathbf{k}_\parallel, k_z}$ and summing over k_z one gets the following dispersion relation

$$\omega^2 - \omega_0^2 = \frac{4\omega^2}{\hbar^2 \omega_0} \sum_{k_z} \frac{\left| C_{\mathbf{k}_\parallel, k_z} \right|^2 \omega^\gamma_{\mathbf{k}}}{\omega^2 - (\omega^\gamma_{\mathbf{k}})^2}. \tag{A.11}$$

By replacing the sum over k_z with the integral, $\displaystyle\sum_{k_z} \rightarrow (L/2\pi) \int \mathrm{d}k_z$ and using the definition (A.5) for $C_{\mathbf{k}_\parallel, k_z}$, Eq. (A.11) reads

$$\omega^2 - \omega_0^2 = -\frac{R_{\mathrm{QW}} \varepsilon_{\mathrm{b}} \omega^2}{c^2 \hbar^2 \pi} \int_{-\infty}^{\infty} \frac{\mathrm{d}k_z}{k_z^2 + k_\parallel^2 - k_0(\omega)^2}. \tag{A.12}$$

After analytical solution of the integral [114], the final form of the dispersion relation

is then obtained:

$$\omega^2 - \omega_0^2 + \frac{\varepsilon_b R_{QW} \omega^2}{c^2 \hbar^2 \sqrt{k_\parallel^2 - k_0^2(\omega)}} = 0 . \tag{A.13}$$

B SELF-CONSISTENT PERTURBATION THEORY OF THE JOINT DENSITY OF STATES

The starting point is the joint density of states (JDS)

$$\rho(\mathbf{k}_{\|}, \omega = \omega^{\mathrm{x}}_{\mathbf{k}_{\|}}) \propto \frac{1}{\pi} \int_{-\infty}^{+\infty} dk_z \frac{\gamma}{\gamma^2 + \left(\omega^{\mathrm{x}}_{\mathbf{k}_{\|}} - \omega^{\gamma}_{\mathbf{k}}\right)^2} . \tag{B.1}$$

With new variables

$$k_z = k_{\|} \tan\varphi \,, \varphi \in [-\pi/2, \pi/2] \,, \tag{B.2}$$

$$\delta = \frac{ck_{\|}}{\sqrt{\varepsilon_{\mathrm{b}}}\omega_0} = \frac{k_{\|}}{k_0(\omega_0)} \equiv \cos\varphi_0 \,, \varphi_0 \in [-\pi/2, \pi/2] \;\; (k_{\|} \leqslant k_0) \,, \tag{B.3}$$

$$\tilde{\delta} = \sqrt{1-\delta^2} \equiv \sin\varphi_0 \,, \tag{B.4}$$

$$\tilde{\gamma} = \frac{\gamma}{\omega_0} \ll 1 \,, \tag{B.5}$$

the JDS can be written as

$$\rho \propto \frac{1}{\pi} \int_{-\pi/2}^{\pi/2} \frac{k_{\|}}{\omega_0} \frac{\tilde{\gamma}\mathrm{d}\varphi}{\tilde{\gamma}^2 \cos\varphi^2 + [\cos\varphi - \delta]^2} \overset{\tilde{\gamma}\to 0}{\simeq}$$

$$\frac{2}{\pi} \int_{-\varphi_0}^{\pi/2-\varphi_0} \frac{k_{\|}}{\omega_0} \frac{\tilde{\gamma}\mathrm{d}x}{x^2 \left[\tilde{\delta} + \frac{\delta}{2}x\right]^2 + \delta^2\tilde{\gamma}^2} \,, \tag{B.6}$$

where $x = \varphi - \varphi_0$.

By expansion of the new variables x and δ in the close proximity of the *dangerous*

point $k_\parallel = k_0$, Eq. (B.6) is approximated by the following expression

$$\rho \propto \frac{k_\parallel}{\pi\omega_0} 2 \int_{-\varphi_0}^{\pi/2-\varphi_0} \frac{\tilde{\gamma} \mathrm{d}x}{\frac{1}{4}(x+\tilde{\delta})^4 - \frac{1}{2}\tilde{\delta}^2(x+\tilde{\delta})^2 + \tilde{\delta}^4/4 + \delta^2\tilde{\gamma}^2} . \tag{B.7}$$

By introduction of the new variable $u = x + \tilde{\delta}$, the integral at the r.h.s. of Eq. (B.7) becomes

$$\mathrm{I} = \int_{-\varphi_0+\sin\varphi_0}^{\pi/2-\varphi_0+\sin\varphi_0} \frac{\tilde{\gamma}\mathrm{d}u}{u^4/4 - \frac{1}{2}\tilde{\delta}^2 u^2 + \tilde{\delta}^4/4 + \delta^2\tilde{\gamma}^2} \simeq \frac{\pi\sqrt{2}}{\sqrt{4\delta^2\tilde{\gamma}^2 + \tilde{\delta}^4}\sqrt{\sqrt{4\delta^2\tilde{\gamma}^2 + \tilde{\delta}^4} - \tilde{\delta}^2}} . \tag{B.8}$$

By replacing the result (B.8) in Eq. (B.7), the final expression for the JDS in the original variables is then obtained:

$$\rho = \frac{k_\parallel\sqrt{2}}{\pi\omega_0} \frac{\tilde{\gamma}k_0^3}{\sqrt{(k_0^2-k_\parallel^2)^2 + 4\tilde{\gamma}^2k_\parallel^2k_0^2}\left[\sqrt{(k_0^2-k_\parallel^2)^2 + 4\tilde{\gamma}^2k_\parallel^2k_0^2} - k_0^2 + k_\parallel^2\right]^{1/2}} . \tag{B.9}$$

The radiative decay rate $\Gamma_\mathrm{T}(\mathbf{k}_\parallel)$ is then obtained by using the density of states given above within the Golden Rule:

$$\Gamma_\mathrm{T} = \Gamma_0 \frac{k_\parallel k_0^2\tilde{\gamma}\sqrt{2}}{\sqrt{(k_0^2-k_\parallel^2)^2 + 4\tilde{\gamma}^2k_\parallel^2k_0^2}\left[\sqrt{(k_0^2-k_\parallel^2)^2 + 4\tilde{\gamma}^2k_\parallel^2k_0^2} - k_0^2 + k_\parallel^2\right]^{1/2}} . \tag{B.10}$$

In the limit $k_0 - k_\parallel \gg \tilde{\gamma}k_0$, i.e. *far* from the $k_\parallel = k_0$ point, the JDS is approximated by the following expression:

$$\rho = \frac{\varepsilon_\mathrm{b}\omega_0}{\pi c^2} \frac{1}{\sqrt{k_0^2 - k_\parallel^2}} , \tag{B.11}$$

and the result for Γ_T provided by the standard perturbation theory [see Eq. (2.25)] is recovered:

$$\Gamma_\mathrm{T} \simeq \Gamma_0 \frac{k_0}{\sqrt{k_0^2 - k_\parallel^2}} . \tag{B.12}$$

In the opposite limit $k_\parallel \to k_0^-$:

$$\Gamma_\mathrm{T} = \frac{\Gamma_0}{2\sqrt{\tilde{\gamma}}} . \tag{B.13}$$

The JDS (B.9) has been derived for $k_{\|} \lesssim k_0$, but it is possible to show that the same expression is valid also for a narrow band $k_{\|} \gtrsim k_0$, i.e. even beyond the critical point k_0. In this case, the new variables to work with are: $\delta = k_{\|}/k_0 \equiv \cosh\varphi_0$ ($\gtrsim 1$) and $\tilde{\delta} \equiv \sinh\varphi_0 = \sqrt{\delta^2 - 1}$. Hence, Eqs. (B.9) and (B.10) characterize $\Gamma_T(k_{\|})$ in the narrow region $|k_{\|} - k_0| \lesssim k_0$.

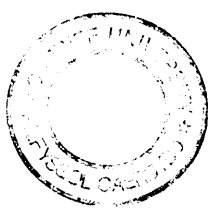

C Derivation of the characteristic parameters

In this Appendix, the characteristic parameters of the strong-weak coupling transition and of the strong-coupling regime are analytically derived.

The starting point is the dispersion relation

$$\omega^2 - (\omega^{\mathrm{x}}_{\boldsymbol{k}_\parallel})^2 + \frac{\varepsilon_{\mathrm{b}} R_{\mathrm{QW}} \omega^2}{c^2\hbar^2\sqrt{k_\parallel^2 - k_0^2(\omega)}} = 0\,. \tag{C.1}$$

Equation (C.1) can be transformed in the following cubic equation in $x = \omega^2$:

$$x^3 - A\,x^2 + B\,x - C = 0\,, \tag{C.2}$$

The coefficients (generally complex), related to the quantum well parameters, are:

$$\begin{aligned} A &= \beta + 2\alpha_0 - \delta \\ B &= 2\alpha_0\beta + \alpha_0^2 \\ C &= \alpha_0^2\beta \\ \alpha_0 &= \omega_0^2 \\ \beta &= (\omega^{\mathrm{x}}_{\boldsymbol{k}_\parallel})^2 = \frac{\hbar^2c^2}{\varepsilon_{\mathrm{b}}}k_\parallel^2 \\ \delta &= \frac{R_{\mathrm{QW}}^2\varepsilon_{\mathrm{b}}}{c^2\hbar^2}\,. \end{aligned} \tag{C.3}$$

Analysis of the transition point

At the transition point the damping-induced and the standard QW-polariton branches intersect and this means that Eq. (C.2) is characterized by a double-degenerate complex root. In terms of the coefficients A, B and C of the cubic equation, this condition is expressed by the following equation:

$$\begin{aligned} 4A^3C - 18ABC - A^2B^2 + 27C^2 + 4B^3 &= 0 \\ &\Longleftrightarrow \\ 4\beta\delta^2 - \delta[20\alpha\beta + 8\beta^2 - \alpha^2] - 4(\alpha - \beta)^3 &= 0\,. \end{aligned} \tag{C.4}$$

To find the critical damping γ_x^{tr} inducing the transition, one makes the following substitution in Eq. (C.4):

$$\omega^x_{\mathbf{k}_\parallel} \rightarrow \omega^x_{\mathbf{k}_\parallel} - i\gamma_x/2 \sim \omega_0 - i\gamma_x/2 \;\Rightarrow\; \alpha_0 \rightarrow \alpha_0 - i\tilde{\gamma}_x \;:\; \tilde{\gamma}_x = \omega_0\gamma_x\,. \tag{C.5}$$

A set of two coupled equations is thus obtained:

$$\begin{aligned} \tilde{\gamma}_x^2 &= \delta(5\beta - \alpha_0/2) + 3(\alpha_0 - \beta)^2 \\ 32(\alpha_0 &- \beta)^3 - 71\delta\beta^2 + 52\alpha_0\delta\beta - 8\alpha_0^2\delta + \alpha_0\delta^2/2 - \beta\delta^2 = 0\,. \end{aligned} \tag{C.6}$$

By solving *perturbatively* the system (C.6) [disregarding terms proportional to δ^d with $\delta > 1$ (δ being the smallest parameter)], the following expression for the critical damping γ_x^{tr} is found:

$$\gamma_x^{tr} = \frac{3\sqrt{3}}{2}\left(\frac{\omega_0 R_{QW}^2 \varepsilon_b}{4c^2\hbar^2}\right)^{1/3} = \frac{3\sqrt{3}}{2\sqrt[3]{4}}\left(\Gamma_0^2\omega_0\right)^{1/3}. \tag{C.7}$$

The wavevector $k_\parallel = k_\parallel^{tr}$ where the transition takes place is found by the substitution of Eq. (C.7) in Eq. (C.6) and it is given by:

$$k_\parallel^{tr} = k_0(\omega_0)\left[1 - \frac{1}{\sqrt{3}}\frac{\gamma_x^{tr}}{\omega_0}\right]. \tag{C.8}$$

In order to find the radiative width Γ_T^{tr} and the radiative shift Δ_T^{tr} at the transition point specified by $(k_\parallel^{tr}, \gamma_x^{tr})$, one needs to replace the coefficients (C.3) of the cubic

equation (C.2) according to

$$\omega^{x}_{\mathbf{k}_\parallel} \to \omega^{x}_{\mathbf{k}_\parallel} - i\gamma_x^{tr}/2 \sim \omega_0 - i\gamma_x^{tr}/2 \;\Rightarrow\; \alpha_0 \;\to\; \alpha_0 - i\tilde{\gamma}_x^{tr}\;;\; \tilde{\gamma}_x^{tr} = \omega_0\gamma_x^{tr}\,, \quad \text{(C.9)}$$

$$\beta \;\to\; \beta^{tr} \;=\; \frac{\hbar^2c^2}{\varepsilon_b}\,(k_\parallel^{tr})^2\,. \quad \text{(C.10)}$$

With these substitutions Eq. (C.2) reads:

$$x^3 - \tilde{A}x^2 + \tilde{B}x + \tilde{C} = 0\,, \quad \text{(C.11)}$$

where

$$\begin{aligned}
\tilde{A} = \tilde{A}_1 + i\tilde{A}_2 &= \beta^{tr} + 2\alpha_0 - \delta - 2i\tilde{\gamma}_x^{tr} \\
\tilde{B} = \tilde{B}_1 + i\tilde{B}_2 &= \alpha_0^2 + 2\alpha_0\beta^{tr} - (\tilde{\gamma}_x^{tr})^2 - 2i\beta^{tr}\tilde{\gamma}_x^{tr} - 2i\alpha_0\tilde{\gamma}_x^{tr}\,, \\
\tilde{C} = \tilde{C}_1 + i\tilde{C}_2 &= -\alpha_0^2(\beta^{tr})^2 + (\tilde{\gamma}_x^{tr})^2\beta^{tr} + 2i\alpha_0\beta^{tr}\tilde{\gamma}_x^{tr}\,.
\end{aligned} \quad \text{(C.12)}$$

Equation (C.11) must be compared with the following cubic equation:

$$(x-a)^2(x-b) = 0 \;\Leftrightarrow\; x^3 - x^2(2a+b) + x(a^2+2ab) - a^2b = 0\,, \quad \text{(C.13)}$$

where a is the double degenerate root corresponding to the solution $\omega = \omega_{tr}$ of the dispersion relation (C.1) at the transition point, i.e. when for $\gamma_x = \tilde{\gamma}_x^{tr}$ the two branches $\omega = \omega_1(k_\parallel)$ and $\omega = \omega_2(k_\parallel)$ intersect $[\omega_1(k_\parallel) = \omega_2(k_\parallel) =: \omega_{tr}]$ at $k_\parallel = k_\parallel^{tr}$: $a = (\omega_{tr})^2 = (\mathrm{Re}[\omega_{tr}] - i\,\mathrm{Im}[\omega_{tr}])^2 \simeq \mathrm{Re}[\omega_{tr}]^2 - 2i\mathrm{Re}[\omega_{tr}]\mathrm{Im}[\omega_{tr}] = a_r + i\,a_i$. $b = b_r + ib_i$ is the other solution of the cubic equation (related to the radiative states). By matching the coefficients of the two cubic equation (and after some algebraic manipulation) the following set of two coupled equations for a_r and a_i is then obtained:

$$\begin{aligned}
3a_i^2 - 3a_r^2 - 2\tilde{A}_2a_i + 2a_r\tilde{A}_1 - \tilde{B}_1 &= 0\,, \\
2\tilde{A}_2a_r + 2\tilde{A}_1a_i - 6a_ra_i - \tilde{B}_2 &= 0\,.
\end{aligned} \quad \text{(C.14)}$$

Its solutions are:

$$\begin{aligned}
a_r &= \frac{\tilde{A}_1 - \sqrt{\tilde{A}_1^2 - 3\tilde{B}_1}}{3} \;\Rightarrow\; \Delta_T^{tr} = \mathrm{Re}[\omega_{tr}] - \omega_0 = \sqrt{a_r} - \omega_0 \simeq \frac{2\tilde{\gamma}_x^{tr}}{3\sqrt{3}} = -\frac{1}{\sqrt[3]{4}}\left(\Gamma_0^2\omega_0\right)^{1/3}, \\
a_i &= \frac{\tilde{B}_2 - 2\tilde{A}_2a_r}{2\tilde{A}_1 - 6a_r} \;\Rightarrow\; \Gamma_T^{tr} = 2\mathrm{Im}[\omega_{tr}] = \frac{a_i}{-2\mathrm{Re}[\omega_{tr}]} \simeq \frac{\tilde{\gamma}_x^{tr}}{3} = \frac{\sqrt{3}}{\sqrt[3]{4}}\left(\Gamma_0^2\omega_0\right)^{1/3}.
\end{aligned} \quad \text{(C.15)}$$

Characterization of the maximum radiative width Γ_T^A

To find the maximum value of the radiative width Γ_T^A occurring at the wavevector $k_{||} = k_0 = k_0(\omega_0)$ and the corresponding radiative shift $\Delta_T^A = \omega^A - \omega_0$, it is necessary to start from Eq. (C.2). In this case, one needs to find the real and imaginary parts of the complex root $\omega^2 = (\mathrm{Re}[w] - i\,\mathrm{Im}[\omega])^2 \simeq \mathrm{Re}[\omega]^2 - 2i\mathrm{Re}[\omega]\mathrm{Im}[\omega] = x_r - i\,x_i$ which satisfies Eq. (C.2) at the point $k_{||} = k_0 \Rightarrow \beta = (\hbar^2 c^2/\varepsilon_b)k_0^2 = \beta_0$.
By imposing these condition, the following set of two equations for the variable $z = x_r - \alpha_0$ is obtained:

$$\begin{aligned} 3z^2 &= x_i^2 - 2\delta\alpha_0 \\ -z^3 &+ x_i^2 z + 2x_i^2 z = \delta\alpha_0^2 . \end{aligned} \tag{C.16}$$

Coupling of Eqs. (C.16) yields the following cubic equation in the dimensionless variables $\tilde{z} = z/\alpha_0$, $\tilde{\delta} = \delta/\alpha_0$:

$$8\tilde{z}^3 + 6\tilde{\delta}\tilde{z} - \tilde{\delta} = 0 . \tag{C.17}$$

Solution of (C.17) (with $\tilde{\delta}$ as the smallest parameter) yields:

$$z = \frac{1}{2}\alpha_0^{2/3}\delta^{1/3} \qquad \Gamma_T^A = 2\mathrm{Im}[\omega] = \frac{x_i}{\sqrt{x_r}} = \frac{\sqrt{3}}{2}\sqrt[3]{\frac{\omega_0 R_{QW}^2 \varepsilon_b}{c^2\hbar^2}} , \tag{C.18}$$

$$\Rightarrow$$

$$x_i = \frac{\sqrt{3}}{2}\alpha_0^{2/3}\delta^{1/3} \qquad \Delta_T^A = \mathrm{Re}[\omega] - \omega_0 = \sqrt{x_r} = \sqrt{z + \alpha_0} - \omega_0 = \frac{1}{4}\sqrt[3]{\frac{\omega_0 R_{QW}^2 \varepsilon_b}{c^2\hbar^2}} .$$

Characterization of the maximum radiative shift $\Delta_T^B = \Delta_T^B(k_{||}^B)$

The solution of the dispersion relation (C.1) at the bifurcation point B (see Fig. 2.5) corresponds to a double degenerate real root since $\Gamma_T^B = \Gamma_T(k_{||} = k_{||}^B) = 0$ (see Fig. 2.4). The other solution is also real and correspond to the confined polariton mode (described by real frequencies, the imaginary part being zero since the radiative lifetime goes to infinite for trapped states) at $k_{||} = k_{||}^B$. In terms of the (real) coefficients α,β and δ of the cubic equation (C.2), this condition is again expressed by Eq. (C.4). In this case one needs to solve only the following equation in the dimensionless variables $\tilde{\delta} = \delta/\alpha_0$ and $\tilde{\beta} = \beta/\alpha_0$:

$$\tilde{\beta}\tilde{\delta}^2 - \tilde{\delta}(5\tilde{\beta} + 2\tilde{\beta}^2 - 1/4) - (1 - \tilde{\beta})^3 = 0 . \tag{C.19}$$

The following expression for the wavevector at point B is obtained:

$$\tilde{\beta} = 1 + \frac{3}{\sqrt[3]{4}}\sqrt[3]{\tilde{\delta}} \;\Rightarrow\; k_{\|} = k_{\|}^{\mathrm{B}} = k_0(\omega_0)\left[1 + \frac{3}{2}\left(\frac{\Gamma_0}{2\omega_0}\right)^{2/3}\right]. \tag{C.20}$$

In order to find the maximum shift $\Delta_{\mathrm{T}}^{\mathrm{B}}$ which occurs at $k_{\|} = k_{\|}^{\mathrm{B}}$, one needs to repeat the derivation used to find the transition radiative shift $\Delta_{\mathrm{T}}^{\mathrm{tr}}$, since, also in this case one solution is double degenerate. In this case, the procedure is more simple since all the roots of the cubic equation are real and it yields:

$$\Delta_{\mathrm{T}}^{\mathrm{B}}(k_{\|} = k_{\|}^{\mathrm{B}}) = \frac{1}{\sqrt[3]{4}}\sqrt[3]{\Gamma_0^2\omega_0}\,. \tag{C.21}$$

The same procedure is applied in order to derive the characteristic parameters of the harmonic-forced solution.

REFERENCES

[1] C. F. Klingshirn. *Semiconductor Optics* (Springer-Verlag, Berlin, 1995).

[2] R. S. Knox. Theory of Excitons. In *Solid State Physics*, suppl. **5** (edited by F. Seitz and D. Turnbull, Academic Press, New York, 1963).

[3] F. Bassani and G. Pastori Parravicini. *Electronic States and Optical Transitions in Solids* (Pergamon Press, Oxford, 1975).

[4] L. C. Andreani. Optical transitions, excitons, and polaritons in bulk and low-dimensional semiconductor structures. In *Confined Electrons and Photons - New Physics and Devices* (edited by E. Burstein and C. Weisbuch, Plenum Press, New York, 1995), p. 57.

[5] G. Bastard. *Wave Mechanics Applied to Semiconductor Heterostructures* (Les Editions de Physique, Paris, 1989).

[6] J. H. Davies. *The Physics of Low-Dimensional Semiconductors* (Cambridge University Press, Cambridge, 1998).

[7] R. C. Miller, D. A. Kleinman, W. T. Tsang, and A. C. Gossard. Observation of the excited level of excitons in GaAs quantum wells. *Phys. Rev. B*, **24**, 1134 (1981).

[8] G. Bastard, E. E. Mendez, L. L. Chang, and L. Esaki. Exciton binding energy in quantum wells. *Phys. Rev. B*, **26**, 1974 (1982).

[9] R. L. Greene, K. K. Bajaj, and D. E. Phelps. Energy levels of Wannier excitons in GaAs-$Ga_{1-x}Al_xAs$ quantum-well structures. *Phys. Rev. B*, **29**, 1807 (1984).

[10] L. V. Kulik, V. D. Kulakovskii, M. Bayer, A. Forchel, N. A. Gippius, and S. G. Tikhodeev. Dielectric enhancement of excitons in near-surface quantum wells. *Phys. Rev. B*, **54**, R2335 (1996).

[11] L. C. Andreani. Exciton-polaritons in confined systems. In *Proceedings of the Internation School of Physics "Enrico Fermi"* (edited by B. Deveaud, A. Quattropani and P. Schwendimann, IOS Press, Amsterdam, 2003), p. 105.

[12] Y. Merle d'Aubigné, H. Mariette, N. Magnea, H. Tuffigo, R. T. Cox, G. Lentz, Le Si Dang, J. -L. Pautrat, and A. Wasiela. Optical properties of $CdTe/Cd_{1-x}Zn_xTe$ quantum wells and superlattices. *J. Crystal Growth*, **101**, 650 (1990).

[13] L. C. Andreani, A. D'Andrea, and R. Del Sole. Excitons in confined systems: from quantum well to bulk behaviour. *Phys. Lett. A*, **168**, 451 (1992).

[14] R. C. Iotti and L. C. Andreani. Crossover from strong to weak confinement for excitons in shallow or narrow quantum wells. *Phys. Rev. B*, **56**, 3922 (1997).

[15] K. Huang. On the interaction between the radiation field and ionic crystals. *Proc. R. Soc. London, Ser. A*, **208**, 352 (1951).

[16] M. Born and K. Huang. *Dynamical theory of crystal lattices* (Clarendon Press, Oxford, 1954).

[17] U. Fano. Atomic theory of electromagnetic interactions in dense materials. *Phys. Rev.*, **103**, 1202 (1956).

[18] J. J. Hopfield. Theory of the contribution of excitons to the complex dielectric constant of crystals. *Phys. Rev.*, **112**, 1555 (1958).

[19] V. M. Agranovich. Dispersion of electromagnetic waves in crystals. *J. Exp. Theor. Phys.*, **37**, 430 (1959) [*Sov. Phys. JETP*, **37**, 307 (1960)].

[20] P. Y. Yu and M. Cardona *Fundamentals of Semiconductors* (Springer-Verlag, Berlin, 1996).

[21] E. Burstein and F. De Martini. Polaritons. In *Proceedings of the First Taormina Conference on the Structure of the Matter* (Pergamon, New York, 1974).

[22] D. L. Mills and E. Burstein. Polaritons: the electromagnetic modes of media. *Rep. Prog. Phys.*, **37**, 817 (1974).

[23] C. Weisbuch and R. G. Ulbrich. Resonant light scattering mediated by excitonic polaritons in semiconductors. In *Light Scattering in Solids III. Topics in Applied Physics*, **51** (edited by M. Cardona and G. Günderodt, Springer, Berlin, 1982), p. 207.

[24] S. I. Pekar. *Crystal Optics and Additional Light Waves* (Benjamin-Cummings, Menlo Park, California, 1983).

[25] B. Hönerlage, R. Lévy, J. B. Grun, C. Klingshirn, and K. Bohnert. The dispersion of excitons, polaritons and biexcitons in direct-gap semiconductors. *Phys. Rep.*, **124**, 161 (1985).

[26] F. Bassani and L. C. Andreani. Exciton-polariton states in insulators and semiconductors. In *Excited-State Spectroscopy in Solids* (edited by U. Grassano and N. Terzi, Academic Press, Amsterdam, 1987), p. 1.

[27] P. Halevi. Exciton-polaritons and optical properties of direct-gap semiconductors. In *Spatial Dispersion in Solids and Plasmas* (edited by P. Halevi, Elsevier, 1992), p. 340; R. Fuchs and P. Halevi. Basic concepts and formalism of spatial dispersion. *ibid.*, p. 2.

[28] A. Christ, S. G. Tikhodeev, N. A. Gippius, J. Kuhl, and H. Giessen. Waveguide-plasmon polaritons: strong coupling of photonic and electronic resonances in a metallic photonic crystal slab. *Phys. Rev. Lett.*, **91**, 183901 (2003).

[29] S. I. Pekar. Theory of electromagnetic waves in a crystal in which excitons are produced. *J. Exp. Theor. Phys.*, **33**, 1022 (1957) [*Sov. Phys. JETP*, **6**, 785 (1958)].

[30] J. J. Hopfield and D.Thomas. Theoretical and experimental effects of spatial dispersion on the optical properties of crystals. *Phys. Rev.*, **132**, 563 (1963).

[31] V. M. Agranovich and V. L. Ginzburg. *Spatial Dispersion in Crystal Optics and the Theory of Excitons* (Interscience Publ. , London, 1966).

[32] K. Henneberger. Additional boundary conditions: an historical mistake. *Phys. Rev. Lett.*, **80**, 2889 (1998).

[33] D. F. Nelson and B. Chen. Comment on "Additional boundary conditions: an historical mistake". *Phys. Rev. Lett.*, **83**, 1263 (1999); R. Zeyher. Comment on "Additional boundary conditions: an historical mistake". *Phys. Rev. Lett.*, **83**, 1264 (1999); K. Henneberger. Henneberger replies. *Phys. Rev. Lett.*, **83**, 1265 (1999).

[34] A. Davydov. *Théorie du solide* (Editions Mir, Moscou, 1980).

[35] F. Bassani, F. Ruggiero, and A. Quattropani. Microscopic quantum theory of exciton polaritons with spatial dispersion. *Nuovo Cimento D*, **7**, 700 (1986).

[36] M. Combescot and O. Betbeder-Matibet. The exciton-polariton: microscopic derivation of the phenomenological theory. *Solid State Commun.*, **80**, 1011 (1991).

[37] A. L. Ivanov, H. Haug, and L. V. Keldysh. Optics of excitonic molecules in semiconductors and semiconductors microstructures. *Phys. Reports*, **296**, 237 (1998).

[38] D. Fröhlich., E. Mohler, and P. Wiesner. Observation of exciton polariton dispersion in CuCl. *Phys. Rev. Lett.*, **26**, 554 (1971).

[39] W. C. Tait. Quantum theory of basic light-matter interaction. *Phys. Rev. B*, **5**, 648 (1972).

[40] J. J. Hopfield. Resonant scattering of polaritons as composite particles. *Phys. Rev.*, **182**, 945 (1969).

[41] R. Ulbrich and C. Weisbuch. Resonant Brillouin Scattering of excitonic polaritons in Gallium Arsenide. *Phys. Rev. Lett.*, **38**, 865 (1977).

[42] V. A. Kisilev, B. S. Razbirin, and I. N. Uraltsev. Additional waves and Fabry-Perot interference of photoexcitons (polaritons) in thin II-VI crystals. *Phys. Stat. Solidi (b)*, **72**, 161 (1975).

[43] D. D. Sell., S. E. Stokovski, R. Dingle, and J. V. DiLorenzo. Polariton reflectance and photoluminescence in high-purity GaAs. *Phys. Rev. B*, **7**, 4568 (1973).

[44] R. G. Ulbrich and G. W. Fehrenbach. Polariton wave packet propagation in the exciton resonance of a semiconductor. *Phys. Rev. Lett.*, **43**, 963 (1979).

[45] H. Sumi. On the exciton luminescence at low temperatures: importance of the polariton viewpoint. *J. Phys. Soc. Jpn.*, **41**, 526 (1976).

[46] C. Weisbuch and R. G. Ulbrich. Resonant polariton fluorescence in Gallium Arsenide. *Phys. Rev. Lett.*, **39**, 654 (1977).

[47] J. Voigt. Additional waves and Fabry-Perot interference of photoexcitons (polaritons) in thin II-VI crystals. *Phys. Stat. Solidi (b)*, **64**, 549 (1974).

[48] F. I. Kreingol'd and V. L. Makarov. Investigation of the role of damping in absorption of light by excitons. *ZhETF Pis. Red.*, **20**, 441 (1974) [*JETP Lett.*, **20**, 201 (1974)].

[49] F. I. Kreingol'd and V. L. Makarov. Investigation of the role of damping in absorption of light by excitons. *Fiz. Tverd. Tela*, **17**, 472 (1975) [*Sov. Phys. Solid State*, **17**, 297 (1975)].

[50] A. Bosacchi, B. Bosacchi, and S. Franchi. Polariton effects in the exciton absorption of GaSe. *Phys. Rev. Lett.*, **36**, 1086 (1976).

[51] B. Sermage and M. Voos. Reabsorption of the excitonic luminescence in direct band gap semiconductors. *Phys. Rev. B*, **15**, 3935 (1977).

[52] V. A. Kosobukin, R. P. Seisyan, and S. A. Vaganov. Exciton-polariton light absorption in bulk GaAs and semiconductor superlattices. *Semicond. Sci. Technol.*, **8**, 1235 (1993).

[53] R. Loudon. The propagation of electromagnetic energy through an absorbing dielectric. *J. Phys. A*, **3**, 233 (1970).

[54] Y. Toyozawa. On the dynamical behavior of an exciton. *Prog. Theor. Phys. Suppl.*, **12**, 111 (1959).

[55] C. Benoit a la Guillaume, A. Bonnot, and J. M. Debever. Luminescence from Polaritons. *Phys. Rev. Lett.*, **24**, 1235 (1970).

[56] U. Heim and P. Wiesner. Direct Evidence for a Bottleneck of Exciton-Polariton Relaxation in CdS. *Phys. Rev. Lett.*, **30**, 1205 (1973).

[57] B. Gil, S. Clur, and O. Briot. The exciton-polariton effect on the photoluminescence of GaN on sapphire. *Solid State Commun.*, **104**, 267 (1997).

[58] W. J. Rappel, L. F. Feiner, and M. F. H. Schuurmans. Exciton-polariton picture of the free-exciton lifetime in GaAs . *Phys. Rev. B*, **38**, 7874 (1988).

[59] V. M. Agranovich and O. A. Dubovskii. Effect of retarded interaction on the exciton spectrum in one-dimensional and two-dimensional crystals. *Zh. Eksp. Teor. Fiz. Pisma* , **3**, 345 (1966) [*JETP Lett.*, **3**, 223 (1966)].

[60] A. L. Ivanov, H. Wang, J. Shah, T. C. Damen, L. V. Keldysh, H. Haug, and L. N. Pfeiffer. Coherent transient in photoluminescence of excitonic molecules in GaAs quantum wells. *Phys. Rev. B*, **56**, 3941 (1997).

[61] A. L. Ivanov, P. Borri, W. Langbein, and U. Woggon. Radiative corrections to the excitonic molecule state in GaAs microcavities. *Phys. Rev. B*, **69**, 075312 (2004).

[62] R. Kubo. Statistical-Mechanical Theory of Irreversible Processes. I. General Theory and Simple Applications to Magnetic and Conduction Problems. *J. Phys. Soc. Jpn.*, **12**, 570 (1957).

[63] D. A. Dahl and L. J. Sham. Electrodynamics of quasi-two-dimensional electrons. *Phys. Rev. B*, **16**, 651 (1977).

[64] K. Cho. *Optical response of nanostructures: Microscopic Nonlocal theory* (Springer-Verlag, Berlin, 2003).

[65] F. Tassone, F.Bassani, and L. C. Andreani. Resonant and surface polaritons in quantum wells. *Nuovo Cimento D*, **12**, 1673 (1990).

[66] M. Nakayama. Theory of the excitonic polariton of the quantum well. *Solid State Commun.*, **55**, 1053 (1985).

[67] M. Nakayama and M. Matsuura. Theory of the quantum well excitonic polariton: effect of the valence subband splitting. *Surf. Sci.*, **170**, 641 (1986).

[68] L. C. Andreani and F.Bassani. Exchange interaction and polariton effects in quantum-well excitons. *Phys. Rev. B*, **41**, 7536 (1990).

[69] J. E. Inglesfield. A method of embedding. *J. Phys. C*, **14**, 3795 (1981).

[70] S. Crampin, M. Nekovee, and J. E. Inglesfield. Embedding method for confined quantum systems. *Phys. Rev. B*, **51**, 7318 (1995).

[71] E. Hanamura. Rapid radiative decay and enhanced optical nonlinearity of excitons in a quantum well. *Phys. Rev. B*, **38**, 1228 (1988).

[72] L. C. Andreani, F. Tassone, and F.Bassani. Radiative lifetime of free excitons in quantum wells. *Solid State Commun.*, **77**, 641 (1990).

[73] D. S. Citrin. Homogeneous-linewidth effects on radiative lifetimes of excitons in quantum wells. *Solid State Commun.*, **84**, 281 (1992).

[74] D. S. Citrin. Radiative lifetimes of excitons in quantum wells: Localization and phase-coherence effects. *Phys. Rev. B*, **47**, 3832 (1993).

[75] L. C. Andreani and A. Pasquarello. Accurate theory of excitons in GaAs-$Ga_{1-x}Al_xAs$ quantum wells. *Phys. Rev. B*, **42**, 8928 (1990).

[76] M. Orrit, C. Aslangul, and P. Kottis. Quantum-mechanical-model calculations of radiative properties of a molecular crystal. I. Polaritons and abnormal decays of excitons in one- and two-dimensional systems. *Phys. Rev. B*, **25**, 7263 (1982).

[77] S. Jorda, U. Rossler, and D. Broido. Fine structure of excitons and polariton dispersion in quantum wells. *Phys. Rev. B*, **48**, 1669 (1993).

[78] S. Jorda. Quantum theory of the interaction of quantum-well excitons with electromagnetic waveguide modes. *Phys. Rev. B*, **50**, 2283 (1994).

[79] G. D. Mahan. *Many-Particle Physics* (Kluwer Academic / Plenum Publishers, New York, 2000).

[80] L. D. Landau and E. M. Lifshitz. *Quantum Mechanics, Course of Theoretical Physics, Volume III* § 128 (Pergamon Press, Oxford, 1981).

[81] F. Tassone, F. Bassani, and L. C. Andreani. Quantum-well reflectivity and exciton-polariton dispersion. *Phys. Rev. B*, **45**, 6023 (1992).

[82] V. V. Popov, T. V. Teperik, N. J. M. Horing, and T. Yu. Bagaeva. Inhomogeneous radiative decay of polariton modes in a two-dimensional excitonic system. *Solid State Commun.*, **127**, 589 (2003).

[83] B. Deveaud, F. Clérot, N. Roy, K. Satzke, B. Sermage, and D. S. Katzer. Enhanced radiative recombination of free excitons in GaAs quantum wells. *Phys. Rev. Lett.*, **67**, 2355 (1991).

[84] A. Vinattieri, J. Shah, T. C. Damen, D. S. Kim, L. N. Pfeiffer, M. Z. Maialle, and L. J. Sham. Exciton dynamics in GaAs quantum wells under resonant excitation. *Phys. Rev. B*, **50**, 10868 (1994).

[85] H. Wang, J. Shah, T. C. Damen, and L. N. Pfeiffer. Spontaneous Emission of Excitons in GaAs Quantum Wells: The Role of Momentum Scattering. *Phys. Rev. Lett.*, **74**, 3065 (1995).

[86] P. Vledder, A. V. Akimov, J. I. Dijkhuis, J. Kusano, Y. Aoyagi, and T. Sugano. Transport of superradiant excitons in GaAs single quantum wells. *Phys. Rev. B*, **56**, 15282 (1997).

[87] V. Srinivas, Y. J. Chen, and E. C. Wood. Reflectivity of two-dimensional polaritons in GaAs quantum wells. *Phys. Rev. B*, **48**, 12300 (1993).

[88] J. Hegarty, L. Goldner, and M. D. Sturge. Localized and delocalized two-dimensional excitons in GaAs-AlGaAs multiple-quantum-well structures. *Phys. Rev. B*, **30**, 7346 (1984).

[89] L. Schulteis, J. Kuhl, A. Honold, and C. W. Tu. Picosecond Phase Coherence and Orientational Relaxation of Excitons in GaAs. *Phys. Rev. Lett.*, **57**, 1797 (1986).

[90] B. Sermage, B.Deveaud, K. Satzke., F. Clérot, C. Dumas, N. Roy, D. S. Katzer, F. Mollot, R. Planel, M. Berz, and J. L. Oudar. Radiative recombination of free excitons in GaAs quantum wells. *Superl. Microstr.* **13**, 271 (1993).

[91] J. Feldmann, G. Peter, E. O. Göbel, P. Dawson, K. Moore, C. Foxon, and R.J. Elliot. Linewidth dependence of radiative exciton lifetimes in quantum wells. *Phys. Rev. Lett.*, **59**, 2337 (1987).

[92] J. Martinez-Pastor, A. Vinattieri, L. Carraresi, M. Colocci, Ph. Roussignol, and G. Weimann. Temperature dependence of exciton lifetimes in $GaAs/Al_xGa_{1-x}As$ single quantum wells. *Phys. Rev. B*, **47**, 10456 (1993).

[93] A. L. Ivanov, P. B. Littlewood, and H. Haug. Bose-Einstein statistics in thermalization and photoluminescence of quantum-well excitons. *Phys. Rev. B*, **59**, 5032 (1999).

[94] J. Humlicek, E. Schmidt, L. Bocanek, R. Svehla, and K. Ploog. Exciton line shapes of GaAs/AlAs multiple quantum wells. *Phys. Rev. B*, **48**, 5241 (1993).

[95] L. C. Andreani, G. Panzarini, A. V. Kavokin, and M. R. Vladimirova. Effect of inhomogeneous broadening on optical properties of excitons in quantum wells. *Phys. Rev. B*, **57**, 4670 (1998).

[96] Al. L. Efros, C. Wetzel, and J. M. Worlock. Effect of a random adiabatic potential on the optical properties of two-dimensional excitons. *Phys. Rev. B*, **52**, 8384 (1995).

[97] H. Stolz, D. Schwarze, W. von der Osten, and G. Weimann. Transient resonance Rayleigh scattering from electronic states in disordered systems: Excitons in $GaAs/Al_xGa_{1-x}As$ multiple-quantum-well structures. *Phys. Rev. B*, **47**, 9669 (1993).

[98] V. I. Belitsky, A. Cantarero, S. T. Pavlov, M. Gurioli, F. Bogani, A. Vinattieri, and M. Colocci. Elastic light scattering from semiconductor structures: Localized versus propagating intermediate electronic excitations. *Phys. Rev. B*, **52**, 16665 (1995).

[99] R. Zimmermann. Theory of Dephasing in Semiconductor Optics. *Phys. Stat. Solidi (b)*, **173**, 129 (1992).

[100] D. S. Citrin. Time-domain theory of resonant Rayleigh scattering by quantum wells: Early-time evolution. *Phys. Rev. B*, **54**, 14572 (1996).

[101] S. Haacke, R. A. Taylor, R. Zimmermann, I. Bar-Joseph, and B. Deveaud. Resonant Femtosecond Emission from Quantum Well Excitons: The Role of Rayleigh Scattering and Luminescence. *Phys. Rev. Lett.*, **78**, 2228 (1997).

[102] M. Gurioli, F. Bogani, S. Ceccherini, and M. Colocci. Coherent vs incoherent emission from semiconductor structures after resonant femtosecond rxcitation. *Phys. Rev. Lett.*, **78**, 3205 (1997).

[103] S. Glutsch and F. Bechstedt. Theory of asymmetric broadening and shift of excitons in quantum structures with rough interfaces. *Phys. Rev. B*, **50**, 7733 (1994).

[104] S. Glutsch, D. S. Chemla, and F. Bechstedt. Numerical calculation of the optical absorption in semiconductor quantum structures. *Phys. Rev. B*, **54**, 11592 (1996).

[105] D. S. Citrin. Exciton polaritons in double versus single quantum wells: Mechanism for increased luminescence linewidths in double quantum wells. *Phys. Rev. B*, **49**, 1943 (1994).

[106] Yu. M. Aliev, H. Schlüter, and A. Shivarova. *Guided-Wave-Produced Plasmas* (Springe-Verlag, Berlin, 2000), Chap. 3.

[107] P. Halevi. *Electromagnetic Surface Modes* (Wiley, Chichester, 1982).

[108] P. Halevi. Electromagnetic wave propagation at the interface between two conductors. *Phys. Rev. B*, **12**, 4032 (1975).

[109] N. I. Nikolaev, A. Smith, and A. L. Ivanov. Polariton optics of semiconductor photonic dots: weak and strong coupling limits. *J. Phys.: Cond. Matt.*, **16**, S3703 (2004).

[110] D. S. Citrin and T. D. Backes. Plasmon-polariton transport in hybrid semiconductor-metal-nanoparticle structures with gain. *phys. stat. sol. (b)*, **243**, 2349 (2006).

[111] R. Zimmermann and E. Runge. Optical lineshape and radiative lifetime of excitons in quantum structures with interface roughness. In *Proc. 22nd Int. Conf. on the Physics of Semiconductors, Vancouver* (edited by D. J. Lookwood, World Scientific, Singapore, 1994), p. 1424.

[112] R. Zimmermann and E. Runge. Optical properties of localized excitons in nanostructures: Theoretical aspects. In *Advances in Solid State Physics* (edited by B. Kramer, Vieweg, Braunschweig, 1998), p. 251.

[113] R. Zimmermann and E. Runge. Statistical properties of speckle distribution in resonant secondary emission. *Phys. Rev. B*, **61**, 4786 (2000).

[114] I. S. Gradshteyn and I. M. Ryzhik. *Table of Integrals, Series, and Products* (Academic Press Inc.,U.S., 2000).